INSECT TRACE FOSSILS ON DINOSAUR BONES FROM THE UPPER JURASSIC MORRISON FORMATION, NORTHEASTERN WYOMING, AND THEIR USE IN VERTEBRATE TAPHONOMY

by

Kenneth Stephen Bader

B.S., University of Kansas, 2003

Submitted to the Department of Geology and the Faculty of the Graduate School of the University of Kansas in partial fulfillment of the requirements for the degree of Master of Science

Advisory Committee:

_____
Stephen T. Hasiotis, Chairman

_____
Larry D. Martin, Co-Chairman

_____
Robert H. Goldstein

Date defended: _____

The thesis committee for Kenneth S. Bader certifies
that this is the approved version of the following thesis:

INSECT TRACE FOSSILS ON DINOSAUR BONES FROM THE UPPER JURASSIC MORRISON FORMATION, NORTHEASTERN WYOMING, AND THEIR USE IN VERTEBRATE TAPHONOMY

Advisory Committee:

_____
Stephen T. Hasiotis, Chairman

_____
Larry D. Martin, Co-Chairman

_____
Robert H. Goldstein

Date submitted: _____

ABSTRACT

Kenneth S. Bader, M.S.
Department of Geology, May 2008
University of Kansas

The skeletons of a diplodocid and three *Camarasaurus* sauropods, ranging from mostly articulated to disarticulated, were collected from a quarry in the Upper Jurassic Morrison Formation in northeastern Wyoming by the University of Kansas during the 1997, 1998, 2002, and 2004 field seasons. Preparation revealed five types of trace fossils on the bone surfaces—shallow pits; rosettes; hemispherical pits; thin, curvilinear grooves; and U- to V-shaped grooves. These traces were identified through comparison with traces produced on bone and wood by modern organisms. The shallow pits, rosettes, and hemispherical pits are interpreted as pupation chambers constructed by dermestid beetles, or another holometabolous insect with a similar behavior. The morphology of these traces is distinct from traces produced by such other bone-modifying insects as termites and tineid moths. The thin, curvilinear grooves and are interpreted as rhizoetchings that were chemically etched into the bones after burial. The U- to V- shaped grooves are likely bite marks produced by a large theropod or crocodilian while feeding on the sauropod carcasses.

Application of the concepts of forensic entomology and the study of the disarticulation and scattering of vertebrate carcasses after death are used to understand better the taphonomy of the sauropods at the quarry. Necrophagous insects that bore into

bone, such as dermestid beetles, only feed on desiccated carcasses that are subaerially exposed. The sauropods likely died during the dry season, which allowed time for their carcasses to desiccate (~3 weeks) and for the insects to arrive and lay eggs, hatch into necrophagous larvae, feed on the carcasses, and pupate (~4 weeks). Overlapping traces provide evidence that at least two generations of bone modifying insects fed on the carcass of one large *Camarasaurus*. The diplodocid died first—its remains were scattered and subaerially exposed approximately 1–3 years before the other sauropods died at the locality. The large *Camarasaurus* died second and was exposed and fed upon by the first generation of bone-modifying insects. Approximately five weeks after its death, the final two *Camarasaurus* died at the locality and were infested by bone-modifying insects. A second generation of insects colonized the large *Camarasaurus* carcass and all four sauropod carcasses were shallowly buried during a flooding event.

Two new ichnogenera and three ichnospecies are erected for the shallow pits; rosettes, and hemispherical pits on the sauropod bones. *Osteogronos* contains two *ichnospecies*: the shallow pits are named *O. hyposkytos* and the rosettes are named *O. nyssa*. Both ichnospecies are restricted to the Upper Jurassic Morrison Formation in Wyoming and Utah. *Osteokryptos entaphiopoles* is named for the hemispherical pits. Hemispherical pits found on Neogene bones from Africa and North America were originally referred to *Cubiculum ornatus*, however, the morphology of these traces are identical to *Ok. entaphiopoles* and they are transferred to this ichnospecies. [The ichnotaxonomic paper that defines these new ichnotaxa is currently under review; therefore, the names used here are unofficial and are used here informally].

ACKNOWLEDGEMENTS

Everyone at the Division of Vertebrate Paleontology (KUVP)—Larry Martin, Dave Burnham, Desui Miao, John Chorn, Hans Peter Schultze, and the students made the museum my second home. Without help from the volunteers and student hourlies at the KUVP Fossil Preparation Lab, especially Bryan Becker, Todd Bowers, Liz Ebert, John and Lois Eppich, Christine Frese, Scott Hannah, Allan Hemmy, Ali Nabavizadeh, Lou Scott, Lynn Swafford, Patsy Whitney, and Jacqueline Wood, the sauropod skeletons would not have been prepared in time for my thesis. Matt Christopher and the volunteers at Science City prepared the Lyle skeleton in record time. The material they prepared provided crucial information about the interactions between the dinosaur carcasses and necrophagous insects. John Carnell, Matt Christopher, Rod Pellegrini, and Craig Sundell donated photographs of the KU-WY-121 quarry. These pictures were instruments in the construction of the quarry maps.

Larry Martin was the first to notice the traces on the skeletons from KU-WY-121. His courses in vertebrate paleontology led me to reason for myself and question the popular hypothesis about the evolution of birds. As soon as I saw the *Longisquama* specimen, I realized that the popular dinosaur origin of birds was wrong; the "protofeathers" on *Longisquama* were identical to the blood feathers I was familiar with at the Kansas City Zoo. Thank you for supporting me in the Division of Vertebrate Paleontology during by undergraduate and graduate career.

Stephen Hasiotis always remained enthusiastic about my research. His never-ending editing of my thesis and his IchnoBioGeoScience (IBGS) class greatly improved my writing skills.

Many professors, including Ross Black, Paul Enos, Robert Goldstein, Luis Gonzalez, Roger Kaesler, Bruce Lieberman, Edith Taylor, Tom Taylor, and Anthony Walton taught excellent courses in paleontology and geology that often led to opportunities for fieldwork. Dr. Bob's [Goldstein] regional field geology courses allowed me to travel off the map and learn about the geology of regions outside the U.S. These classes helped to keep me in practice at field geology and were often the highlight of my semester. I was not just going on the trips to check out the wildlife—that was just a bonus.

I thank Dave Burnham, who taught me the basics of fossil preparation and more importantly, turned me loose in the lab to improve my molding and casting skills through trial and error, experimentation, and sudden deadlines for projects. Dave—remember that you will never be able to replace me. The wide variety of projects has provided the experience I need to become a successful fossil preparator.

Robert Timm provided access to the University of Kansas dermestid colony and helped me conduct bone-modification experiments within the colony. Bob's knowledge of dermestid behavior led to the discovery of damage to the epiphyses of chicken bones. This form of bone-modification is similar to damage reported from dinosaurs in the Gobi Desert.

Anna Kay Behrensmeyer allowed me to visit her lab at the Smithsonian and examine trace fossils in bone that were produced by termites and tineid moths. In the future I would like to work in with her on a project to describe these traces.

This research was supported by the University of Kansas Department of Geology Summer Research Grant and the University of Kansas Natural History Museum Panorama Grant. I would like to thank my committee members for helping me with the grant proposals. John Babiarz provided access to the KU-WY-121 quarry and specimens in his private collection. John also supplied funding to KUVP that kept me busy molding and casting fossils in the lab.

Thanks to the current and former University of Kansas students, who are my friends and colleagues—Brian Beatty, John Counts, Robert Elder, Katrina Gobetz, Debra Jennings, Kathryn Mickle, Brian Platt, Julie Retrum, John Smith, Celina Suarez, Marina Suarez, Emily Tremain, Dan Williams, and Heather York.

Finally, I thank my family and my girlfriend, Lynn Swafford.

TABLE OF CONTENTS

FIGURES AND TABLES

Figures

Tables

CHAPTER 1. INTRODUCTION

This research focuses on the identification of trace fossils on skeletons and the application of forensic entomology in taphonomic studies. Combining knowledge of the behavior of modern bone-modifying organisms with taphonomic studies provides greater precision for determining the season of death for an ancient vertebrate and the length of time that the carcass was subaerially exposed before final burial. Forensic entomology is the study of necrophagous insects and the changes in the necrophagous insect community as a carcass goes through the stages of decomposition (Payne, 1965). Borings produced by bone-modifying, necrophagous insects on bone are rare in the fossil record and in modern environments (see Chapter 2, Table 2). Three modern taxa are known to regularly modify bone—dermestid beetles (Coleoptera: Dermestidae), tineid moths (Lepidoptera: Tineidae), and termites (Isoptera). Each species produces a unique morphology of boring and has basic biological requirements that restrict their occurrence on carcasses to the dry stage of decomposition. Dermestid beetles and tineid moths are also restricted to subaerially exposed carcasses by their inability to excavate tunnels in sediment.

In this thesis I apply the principles of forensic entomology to study the taphonomic history of sauropod skeletons at the KU-WY-121 quarry in the Upper Jurassic Morrison Formation of northeastern Wyoming. Preparation of these skeletons revealed bite marks from a carnivorous vertebrate, rhizoetchings, and three types of traces identified as insect traces—shallow pits, rosettes, and hemispherical pits. Potential tracemakers are identified, and knowledge of their biology is used to construct a timeline for the death, exposure, and burial of the sauropods (Chapter 2). Three new ichnospecies *Osteogronos hyposkytos*, *O.*

nyssa, and *Osteokryptos entaphiopoles* are described for these traces on bone (Chapter 3). The ichnotaxonomy of insect-bone interactions is revised by restricting *Cubiculum* (Roberts et al., 2007) to distinct traces from the Upper Cretaceous of Madagascar and by identifying a possible tracemaker for *Osteomandibulus*. The ichnotaxonomic chapter that defines these new ichnotaxa is currently under review; therefore, the names used here are unofficial and are used here informally

HISTORY OF EXCAVATION AT KU-WY-121

Active excavation of the KU-WY-121 quarry took place from 1997–1998 and 2002–2007. The quarry is in a layer of gray mudstone that overlies a well-cemented golden sandstone on an east-west trending ridgeline (Fig 1). KU-WY-121 has produced at least seven sauropod skeletons, two ornithischians skeletons, two theropod skeletons, and numerous isolated dinosaur bones, small vertebrates, mollusks, and plants (Table 1).

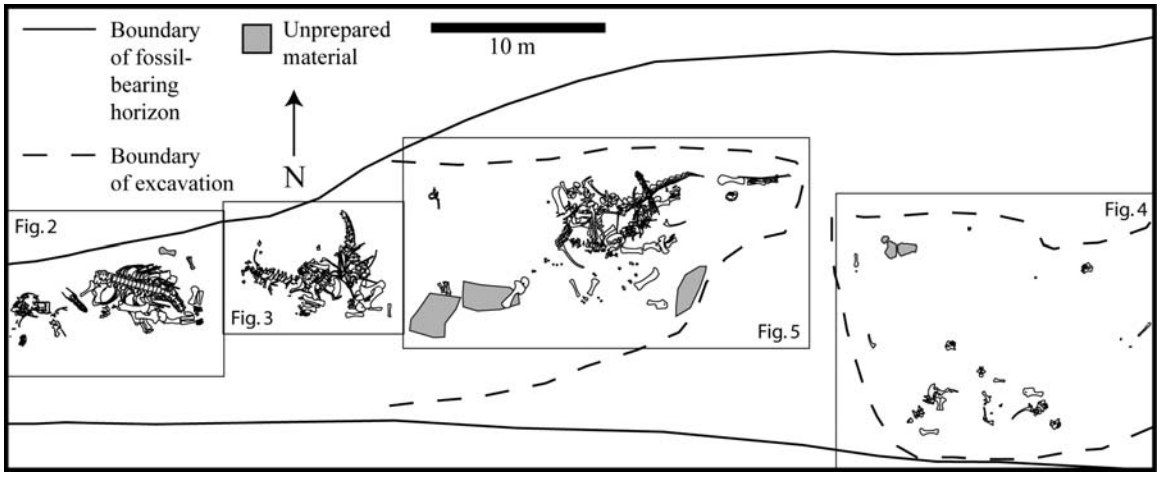

Figure 1. The KU-WY-121 quarry south of Sundance, WY.

Classification	Taxon	Number of Specimens	Repository
Dinosauria: Sauropoda	*Camarasaurus*	6, possibly 7 skeletons plus isolated limb bones from an 8th skeleton	KUVP 129713 "Lyle" KUVP 129714 "Nic Mik" KUVP 129716 "Annabelle" BIOPSI Sub adult (2002) BIOPSI Juvenile (2007)
Dinosauria: Sauropoda	Unidentified new Brachiosaurid	One relatively complete skeleton and the right manus and left pes of a large brachiosaur	KUVP 129724 "Bigfoot" CU Skeleton (2002) BIOPSI "Big Hand"
Dinosauria: Sauropoda	Unidentified Diplodocid, possibly *Barosaurus* or *Diplodocus*	Less than 30% of a skeleton	KUVP 129717 "Elmo"
Dinosauria: Theropoda	Unidentified coelurosaur	Partial skeleton	KUVP 131603
Dinosauria: Theropoda	Unidentified large theropod	Vertebral column and ribs	BIOPSI (2005)
Dinosauria: Theropoda	*Allosaurus*	Numerous teeth and isolated bones	KUVP and BIOPSI
Dinosauria: Theropoda	*Torvosaurus*	Several very large teeth	KUVP and BIOPSI
Dinosauria: Ornithischia	*Dryosaurus altus*	One relatively complete skeleton	BIOPSI
Dinosauria: Ornithischia	*Othneilia*	One partial skeleton and isolated elements	KUVP 129715
Testudines	*Glyptops* sp., possibly *G. plicatalus*	Numerous complete and partial shells and isolated limb bones	KUVP and BIOPSI
Crocodilia	Unidentified Crocodilian	Isolated teeth and possible limb bones	KUVP and BIOPSI
Osteichthys	Unidentified fish	Isolated scales, teeth, and bones	KUVP
Insecta: Coleoptera: Dermestidae (?)	Possible dermestid beetle	Shallow pits, rosettes, and hemispherical pits bored into sauropod bones	KUVP 147901 Shallow pit KUVP 147902 Rosette KUVP 147903 Hemispherical pit
Mollusca: Gastropoda	Unidentified snail	Casts of shells	KUVP
Mollusca: Bivalvia	Unidentified bivalve	Cast of shells	KUVP
Coniferophyta	*Brachyphyllum*	Leaves	KUVP
Coniferophyta	Unidentified conifer	Cones	KUVP

Table 1. Species list for the KU-WY-121 quarry.

The University of Kansas Division of Vertebrate Paleontology (KUVP) started excavating the quarry in 1997. During this year two sauropod skeletons (Fig. 2) were collected: Lyle, an adult *Camarasaurus* (KUVP 129713); Nic Mik, a juvenile *Camarasaurus* (KUVP 129714); and a hypsilophodont, possibly *Othnielia* (KUVP 129715). Another adult *Camarasaurus*, Annabelle (KUVP 129716); a small diplodocid, Elmo (KUVP 129717); the left pes of a large brachiosaur, Bigfoot (KUVP 129724); and the partial skeleton of a coelurosaur (KUVP 131603) were collected the following season (BP Pit, Fig. 3, and Elmo Pit, Fig. 4). Excavation ceased from 1999–2001 while KUVP prepared and mounted Annabelle (KUVP 129716). In 2002, John Babiarz purchased the quarry and the University of Kansas field crew returned to the quarry to help excavate a large, nearly complete brachiosaur (CU Pit, Fig. 5) for a museum in South Korea. A subadult *Camarasaurus* was also found draped over the brachiosaur. In 2003 J. Babiarz expanded the CU Pit and located the arm of the brachiosaur and the skull of the subadult *Camarasaurus* east of the main skeleton and a theropod to the south and west of the main skeleton. KUVP returned to the quarry in 2004 to expand the 1998 Elmo Pit and found additional material from Elmo (KUVP 129717) and a *Dryosaurus altus* skeleton. J. Babiarz returned in 2004–2006 to finish excavating the brachiosaur arm and the theropod. A large brachiosaur manus (Big Hand), possibly belonging to the brachiosaur pes known as Bigfoot, was collected in 2005. In 2007, J. Babiarz returned to the quarry and located another subadult or juvenile *Camarasaurus* between the CU Pit and the Elmo Pit.

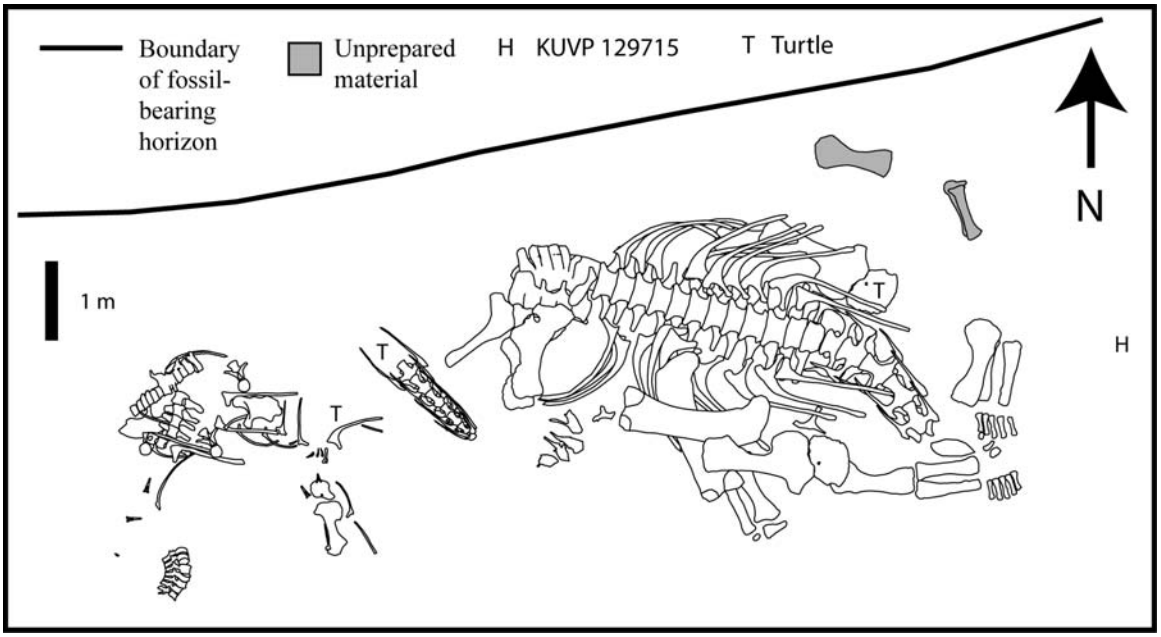

Figure 2. Bone maps for two *Camarasaurus* skeletons (KUVP 129713 on the right and KUVP 129714 on the left) collected in 1997.

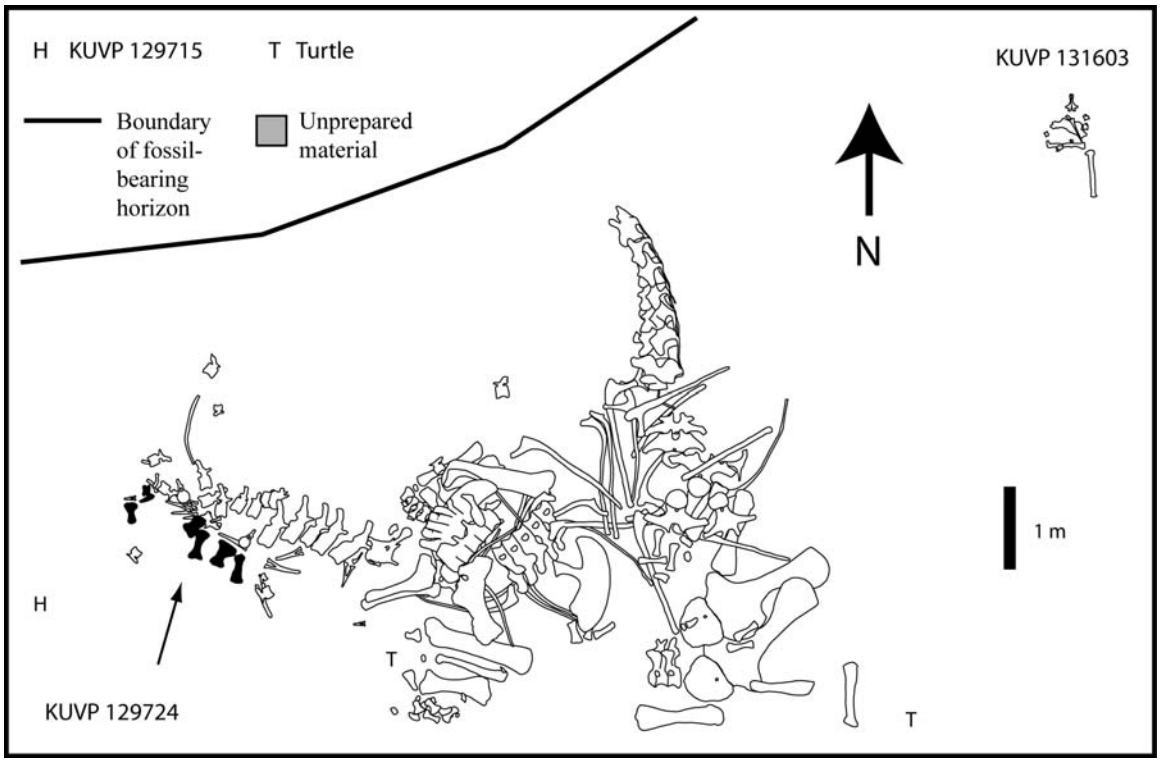

Figure 3. In 1998 the BP Pit was opened east of the previous year's excavation. Bones highlighted in black belong to the brachiosaur pes (KUVP 129724).

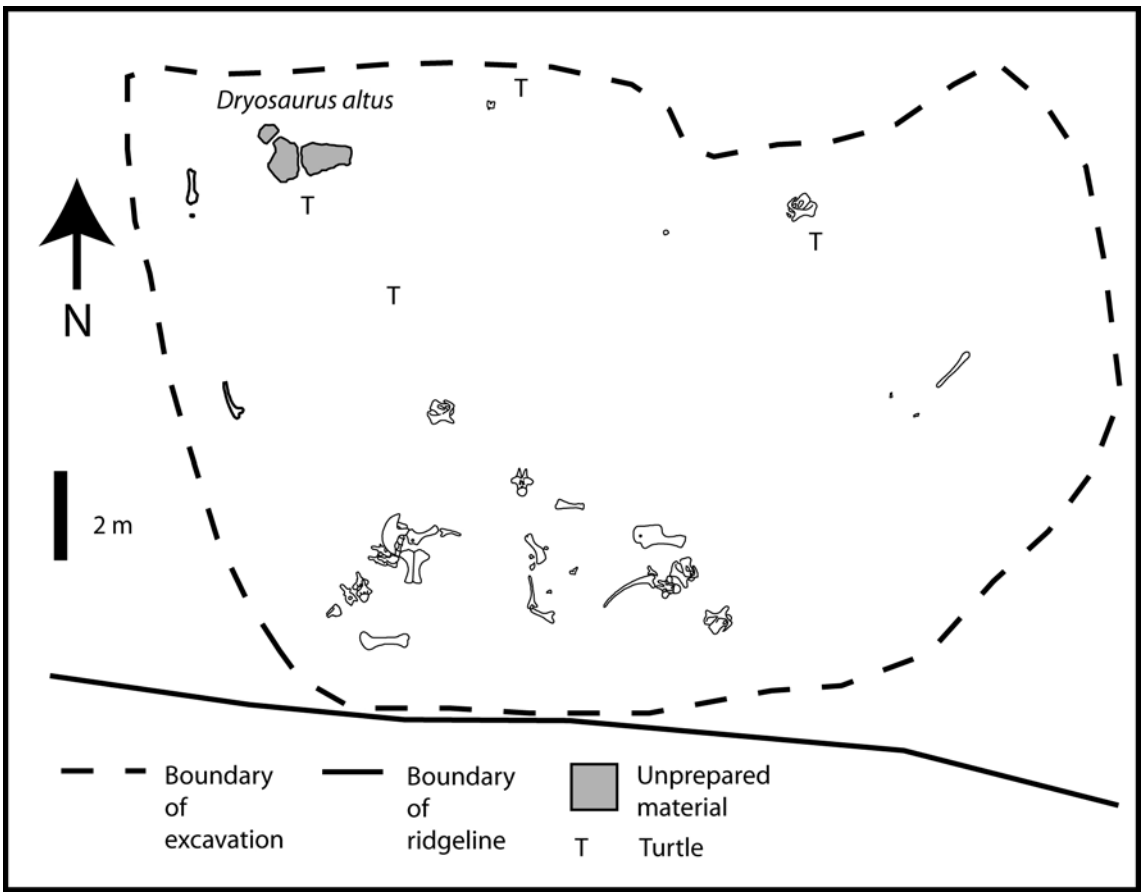

Figure 4. The Elmo Pit (1998 and 2004).

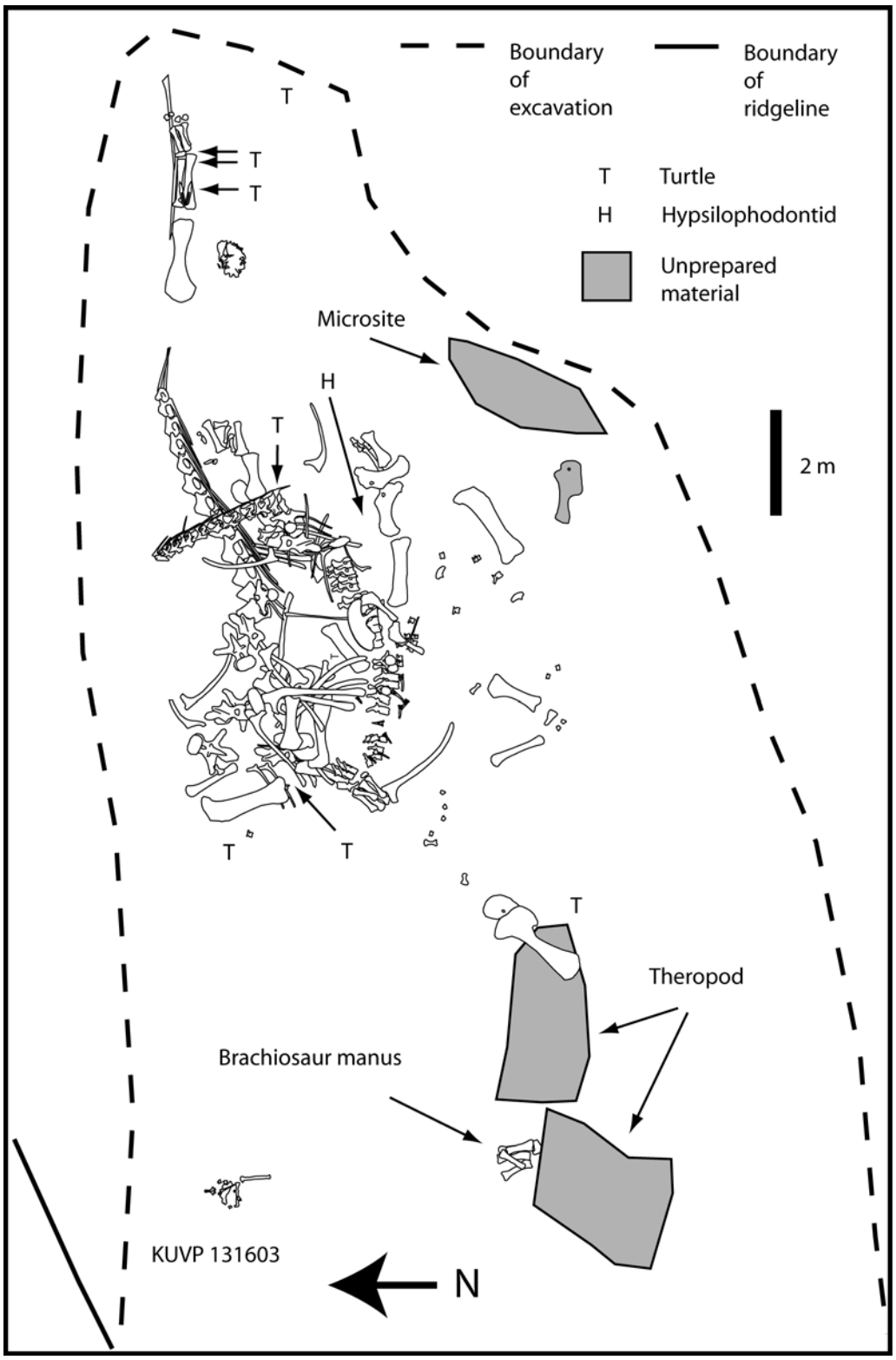

Figure 5. The 2002–2007 CU Pit.

CHAPTER 2. TRACE FOSSILS ON DINOSAUR BONES FROM A QUARRY IN THE UPPER JURASSIC MORRISON FORMATION, NORTHEASTERN WYOMING

Currently in review as:

BADER, K. S., HASIOTIS, S. T., and MARTIN, L. D., Trace fossils on dinosaur bones from a quarry in the Upper Jurassic Morrison Formation, northeastern Wyoming: *PALAIOS*.

ABSTRACT

Trace fossils on sauropod skeletons from a quarry in fluvial deposits of the Morrison Formation, Wyoming, are used to reconstruct the taphonomic history of the quarry. Shallow pits, rosettes, hemispherical pits, thin, curvilinear, branching grooves, and U- to V-shaped linear grooves comprise trace fossils found on sauropod skeletons. These traces were interpreted by comparisons to traces on modern bone. Rosettes are circular rings of modified bone 2.00–6.00 mm in diameter with scalloped walls. Shallow pits are circular to elliptical in plan view, 0.48–6.36 mm in diameter, and < 1.50 mm deep. Rosettes are likely an early stage in the production of shallow pits and are interpreted as pupation chambers constructed in dried flesh and in contact with sauropod bone. Hemispherical pits are 1.98–5.63 mm in diameter, circular with a U-shaped cross section, and interpreted as dermestid pupation chambers completed in sauropod bone. Thin, curvilinear, branching grooves are < 1 mm in diameter, semicircular in cross

section, form irregular dendritic or looping patterns, and are interpreted as root etchings. U- to V-shaped linear grooves are 0.56–9.86 mm in diameter, 0.28–4.69 mm deep, up to 65 mm long, and are interpreted as theropod or crocodilian bite marks. Skeletal articulation and condition and distribution of bone modification traces suggest the skeletons accumulated at this site over no more than 3.5 years, with the bulk of the skeletons contributed during the dry season in the final 3–6 months. Carcasses went through all stages of decomposition including the dry stage, represented by shallow pits, rosettes, and hemispherical pits. Vertebrate scavengers and necrophagous arthropods fed on the carcasses during all decomposition stages prior to burial of the assemblage.

INTRODUCTION

During the summers of 1997, 1998, and 2004, field crews from the University of Kansas Division of Vertebrate Paleontology collected dinosaurs from a site, KU-WY-121, in the Upper Jurassic Morrison Formation south of Sundance, Wyoming **(**Fig. 6–7**)**. The most common dinosaurs found were sauropods: four *Camarasaurus*, two brachiosaurs, and a small diplodocid. Preparation of the skeletons revealed a variety of traces covering the bone surfaces. Our hypothesis is that these traces represent borings that were associated with the decomposition of the dinosaur carcasses before burial, based on their distribution on the skeletons and association with the enclosing matrix. This paper documents trace fossils on sauropods skeletons and uses them to reconstruct the taphonomic history and paleoenvironmental setting of fluvial deposits in the Morrison Formation in northeastern Wyoming. Interpretation of the tracemaking behavior, timing of the emplacement of trace fossils, as well as the tentative identification of the

tracemakers allow us to reconstruct a timeline of the death, decay, and final burial of sauropod skeletons in a mudstone-dominated fluvial deposit.

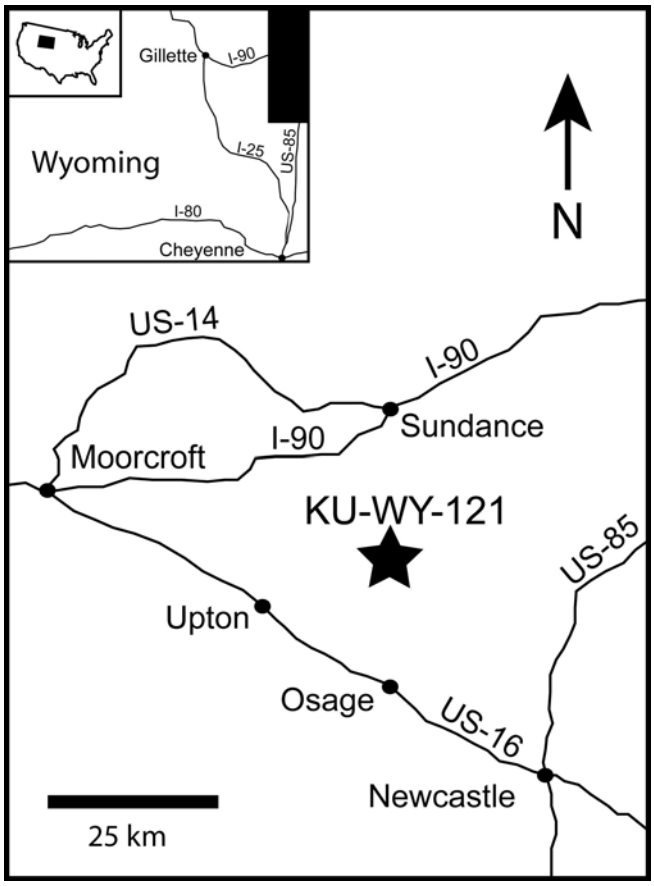

Figure 6. Location of the KU-WY-121 Quarry.

Figure 7 (following page). Quarry map of KU-WY-121 with insets corresponding to bone maps in Figure 9 and position of measured sections. Numbers in bold face correspond to the location of stratigraphic sections in Figure 8.

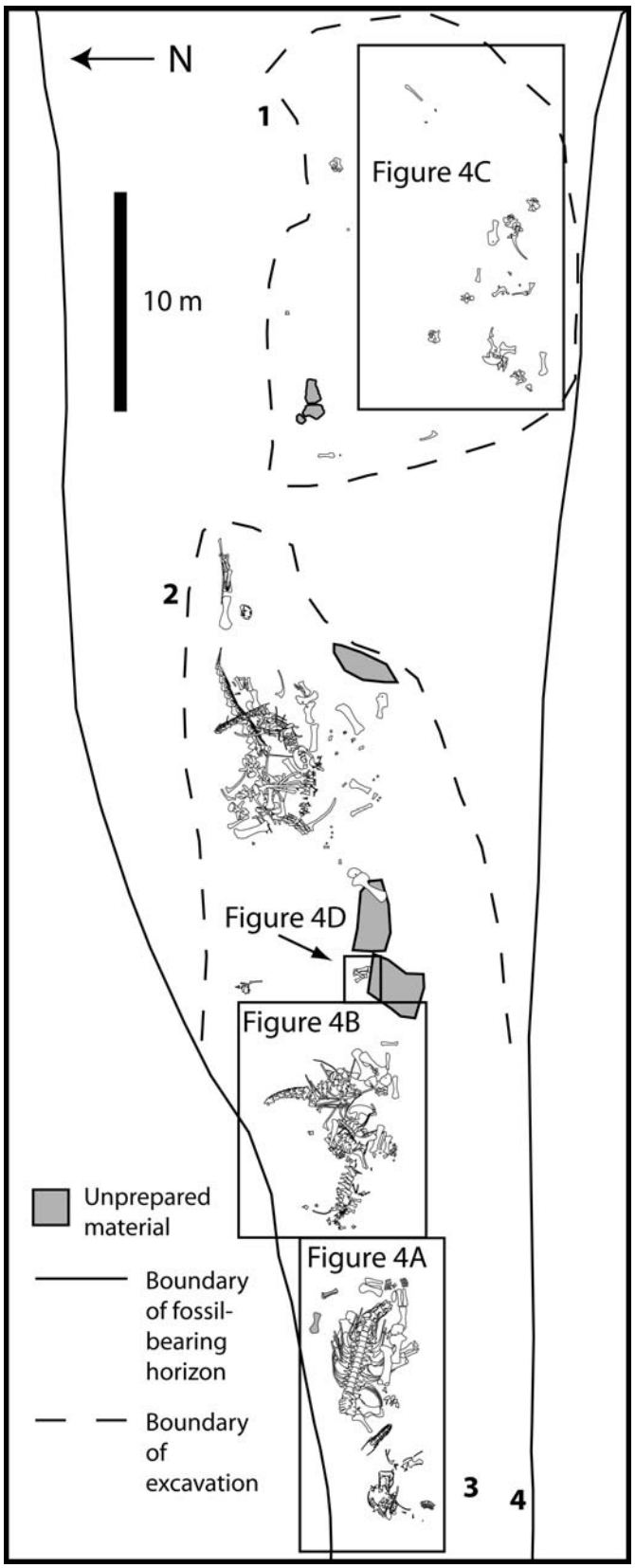
N
1
Figure 4C
10 m
2
Figure 4D
Figure 4B
Figure 4A
Unprepared material
Boundary of fossil-bearing horizon
Boundary of excavation
3
4

Insect traces on bone are relatively rare in present-day and in the fossil record (West and Martin, 2002; West and Hasiotis, 2007). Fossil bone modification by arthropods has been reported from the Late Jurassic, Cretaceous, Paleogene, and Neogene (Table 2). Traces include circular to oval pits, scratches, tunnels, notches, and channels in bone. Identifications for the fossil tracemakers were proposed based on comparisons to traces on bone produced by modern arthropods in taphonomic and forensic studies (Table 3).

Forensic entomology uses the succession of insects and other arthropods to understand the postmortem modification of a carcass and its rate of decay, dependent on temperature, humidity, exposure to sun or wind, scavenging by large vertebrates, and cause of death—for example, drowning or landslide. Martin and West (1995), Hasiotis et al. (1999), and West and Hasiotis (2007) applied the principles developed in forensic entomology to trace fossils found on Pleistocene and Jurassic bones to determine the season of death, the amount of time spent on the surface prior to burial, the organisms responsible for producing trace fossils on bone, and the burial history. The objective of this paper is to apply these same principles to understanding the taphonomy of the KU-WY-121 quarry.

Study	Time Interval	Description	Behavior	Interpretation
Tobien, 1965	Pliocene	Grooves running parallel to bone surface	Pupation	Coleoptera
Tobien, 1965	Pleistocene	Grooves running parallel to bone surface	Pupation	Coleoptera
Kitching, 1980	Plio-Pleistocene	Cylindrical burrows in long bones	Pupation	Coleoptera: Dermestidae
Watson and Abbey, 1986	Pleistocene	Paired scratch marks	Unknown	Isoptera: *Mastotermes*
Jodry and Stanford, 1992	Pleistocene	Enlargement of foramina, excavation of marrow cavities	Unknown	Insects, probably Coleoptera
Rogers, 1992	Late Cretaceous	Perforated bones.	Tunneling in soil	Coleoptera
Martin and West, 1995	Pleistocene	Test-tube shaped borings in horn core.	Pupation	Coleoptera: Dermestidae
Hasiotis et al., 1999	Late Jurassic	Pits in bone surface.	Pupation	Coleoptera: Dermestidae
Paik, 2000	Cretaceous	Perforated bones and bone-chip filled burrows.	Tunneling in soil	Coleoptera
Kaiser, 2000	Plio-Pleistocene	Star-shaped scratches, grooves, and surface erosion	Unknown	Insects, possibly Isoptera
Kaiser and Katterwee, 2001	Plio-Pleistocene	Paired scratch marks	Unknown	Insects, possibly Isoptera
Hasiotis, 2004	Late Jurassic	Curvilinear grooves	Feeding	Bite marks from theropod dinosaurs
Hasiotis, 2004	Late Jurassic	Pits in bone surfaces	Pupation	Coleoptera: Dermestidae
Fejfar and Kaiser, 2005	Oligocene	Star-shaped scratches, grooves, and surface erosion	Unknown	Isoptera
Roberts et al.., 2007	Late Cretaceous	Shallow, oval hollow in bone with numerous scratches	Pupation	Necrophagous Insect
Roberts et al.., 2007	Late Cretaceous	Shallow trail of grooves	Feeding	Necrophagous Insect
Roberts et al.., 2007	Late Cretaceous	Tunnels in bone	Unknown	Necrophagous Insect
West and Hasiotis, 2007	Pleistocene	Oval pits	Pupation	Dermestid beetles
West and Hasiotis, 2007	Pleistocene	Scratches and scallops	Unknown	Insects, possibly Coleoptera
West and Hasiotis, 2007	Pleistocene	Tunnels, notches, channels	Tunneling in soil	Insects, possibly Coleoptera
Kirkland and Bader, 2007	Late Cretaceous	Destruction of condyles on limb bones and associated puparia in surrounding matrix	Feeding	Coleoptera
Kirkland and Bader, 2007	Late Cretaceous	Cylindrical perforations in buried bones	Tunneling in soil	Coleoptera

Table 2. Fossil examples of modified bones.

Tracemaker	Description	Behavior	Reference
Coleoptera: Dermestidae: *Dermestes vulpinus*	Damage to bone, wood, and metal.	Feeding and pupation	Gabel, 1955
Coleoptera: Dermestidae: *Dermestes maculatus*	Damage to bone.	Feeding	Hefti et al., 1980
Coleoptera: Dermestidae: *Dermestes maculatus*	Damage to bones in dermestid colony.	Feeding and pupation	Timm, 1982
Coleoptera: Scarabaeidae: *Anoplognathus*	Damage to buried skeletons.	Unknown	Haglund, 1976
Isoptera	Bone erosion with plugs of stercoral filling openings of a skull	Dwelling	Wood, 1976
Isoptera: Termitidae: *Nasutitermes*	Enlargement of foramina and excavation of marrow cavities under stercoral	Dwelling	Thorne and Kimsey, 1983
Isoptera: *Mastotermes*	Paired scratches on bone surface.	Unknown	Watson and Abbey, 1986
Isoptera: Termitidae: *Nasutitermes*	Destruction of bones underneath stercoral covering.	Dwelling	Wylie et al., 1987
Isoptera	Grooves etched into bone under stercoral.	Unknown	Haynes, 1991
Isoptera	Pits along a stercoral-covered gallery on the underside of bones.	Unknown	Tappen, 1994
Isoptera: *Mastotermes*	Paired scratches on bone surface.	Unknown	Kaiser and Katterwee, 2001
Lepidoptera: Tineidae	Grooves in antelope horn cores.	Dwelling	McCorquodale, 1898
Lepidoptera: Tineidae: *Tinea deperdella*	Etch 2 mm-wide grooves in horn cores.	Dwelling	Behrensmeyer, 1975, 1978
Lepidoptera: Tineidae: *Ceratophaga*	Straight-sided, cylindrical boring in astragulus.	Pupation	Hill, 1987
Lepidoptera	Grooves and chambers on horn core.	Pupation	Gautier, 1993
Insects, likely Isoptera, Coleoptera, or Lepidoptera	Cylindrical holes in bone.	Unknown	Newman, 1993
Insect	Cylindrical pits.	Pupation	Gautier, 1993
Insects, possibly Hymenoptera: Formicidae	Trail on bone surface.	Feeding	Gautier, 1993
Insects, possibly Isoptera	Paired scratches on bone surface.	Unknown	Kaiser and Katterwee, 2001
Nile Crocodile (*Crocodylus niloticus*)	Straight or J-shaped marks with U- to V-shaped cross sections, rounded pits and punctures	Feeding	Njau and Blumenschine, 2006
Roots	Sinuous branching grooves with U-shaped cross section, linear arrangements of pits	Extraction of nutrients	Binford, 1987; Ehrenreich, 1995
Fungi	Tunnels and grooves with U-shaped cross sections 1-100um in diameter	Extraction of Nutrients	Sognnaes, 1955; Hackett, 1981; Piepenbrink, 1986; Davis, 1997

Table 3. Modern examples of bone modification.

GEOLOGIC SETTING

The Upper Jurassic Morrison Formation was deposited in eolian, fluvial, lacustrine, and transitional marine environments following the northern retreat of the Sundance Sea (Peterson, 1994). The formation is found from New Mexico north into Canada and from central Nebraska west to central Utah. Morrison Formation strata range in thickness from 0–150 m at the Front Range of the Rocky Mountains to 0–300 m in the Four Corners (Peterson, 1994). The Late Jurassic climate of the western interior is interpreted as tropical-wet-dry in the southern half of the basin, grading into a Mediterranean climate at the edge of the Sundance Sea (Peterson, 1994; Demko et al., 2004; Hasiotis, 2004). Climates during Morrison deposition likely fluctuated between drier and wetter years.

In the Black Hills of South Dakota and Wyoming the Morrison Formation is 6–60 m thick (Loomis, 1902). The lower beds of the Morrison Formation are composed of yellow sandstone that conformably overlie glauconitic shale of the Upper Jurassic Sundance Formation (Watson 1980). Interbedded layers of variegated mudstone, siltstone, sandstone, and thin limestone characterize the upper part of the Morrison Formation. The Morrison Formation is unconformably overlain by the Lower Cretaceous Lakota Formation (Watson, 1980). Fine- to coarse-grained fluvial sandstone, shale, and coal beds characterize the Lakota Formation. The contact is identified by a change from siltstone and claystone to thick, cross-bedded sandstone (Loomis, 1902).

Dinosaur quarry KU-WY-121 is located on an east–west trending ridge in the Morrison Formation, ~10 m below the lower contact with the Lakota Formation, with a

dip of ~10º to the south (Fig. 8). The remaining portion of the Morrison Formation and the Sundance Formation are covered in the study area. Vertebrate, mollusk, and plant fossils were collected from a finely laminated bed of alternating mudstone and siltstone that fines upward into a gray mudstone. Lenticular beds of sandstone or conglomerate composed of rounded clay pebbles are found at the base of the mudstone. The gray mudstone transitions upwards into a purple mudstone with rhizoliths and carbonate nodules about 96 cm above the base of the unit. Sauropod bones on the eastern side of the quarry are encased commonly in carbonate nodules. The gray mudstone overlies a well-cemented gold sandstone bed. The sandstone is variably thick and pinches out on the southern margin of the ridge. Localized south-facing slopes, depressions, channels, and scours with changes in elevation of less than 2 m are found in the well-cemented sandstone. At the eastern side of the quarry, two parallel channels are incised less than 0.5 m deep into the top of the well-cemented sandstone and trend roughly NW–SE. Asymmetric ripples on the surface of the sandstone are perpendicular to the trend of the channels. The asymmetric ripples dip toward the southeast.

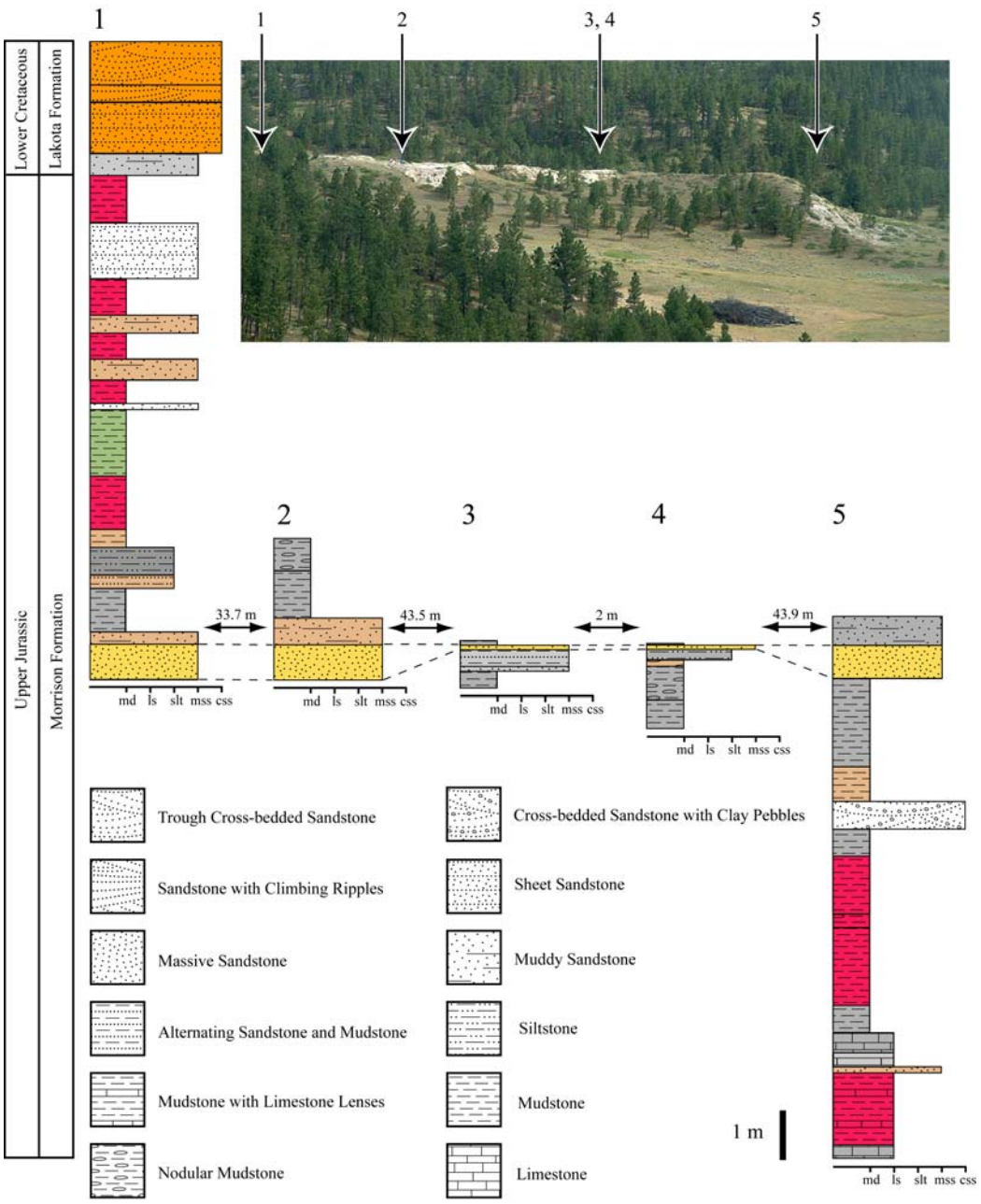

Figure 8. Measured sections at KU-WY-121. Arrows in the measured sections indicate the level of the quarry.

MATERIALS

The nearly complete skeletons of three *Camarasaurus*, a partial diplodocid skeleton, and the left pes and right manus of a brachiosaur were prepared and examined for evidence of bone modification. Three other dinosaurs, a *Camarasaurus*, a brachiosaurid, and a large theropod are not currently available for study (Fig. 5, 7). Partial skeletons of a hypsilophodontid and a coelurosaur, a nearly complete *Dryosaurus*, and numerous turtles, fish, bivalves, gastropods, and teeth from crocodiles, *Allosaurus*, and *Torvosaurus* were also found at KU-WY-121. Most of the sauropod skeletons were found on relatively flat-lying beds; only the juvenile *Camarasaurus* (KUVP 129714) and the two skeletons not available for study—*Camarasaurus* and brachiosaur—were found on sloping beds. Oxidation and modern root-damaged bones were encountered during excavation of the large *Camarasaurus* (KUVP 129713) and the juvenile *Camarasaurus* (KUVP 129714) near the soil surface at the northern margin of the quarry.

The partially disarticulated skeleton of a large *Camarasaurus* (KUVP 129713; Fig 9A) was upside-down, lying on its back. The posterior cervical vertebrae, dorsal vertebrae, and pelvis are articulated. The anterior cervical vertebrae are articulated and were found along with the closely associated skull near to the pubis. The teeth were found ~8 m to the southwest of the rest of the skeleton. The tail probably eroded off the northern edge of the hill. The forelimbs, scapulae, and coracoids are articulated into right and left halves. The femora were found crossing over one another. The left tibia, fibula, and astragulus are articulated, lay underneath the femora, and are surrounded by scattered metatarsals.

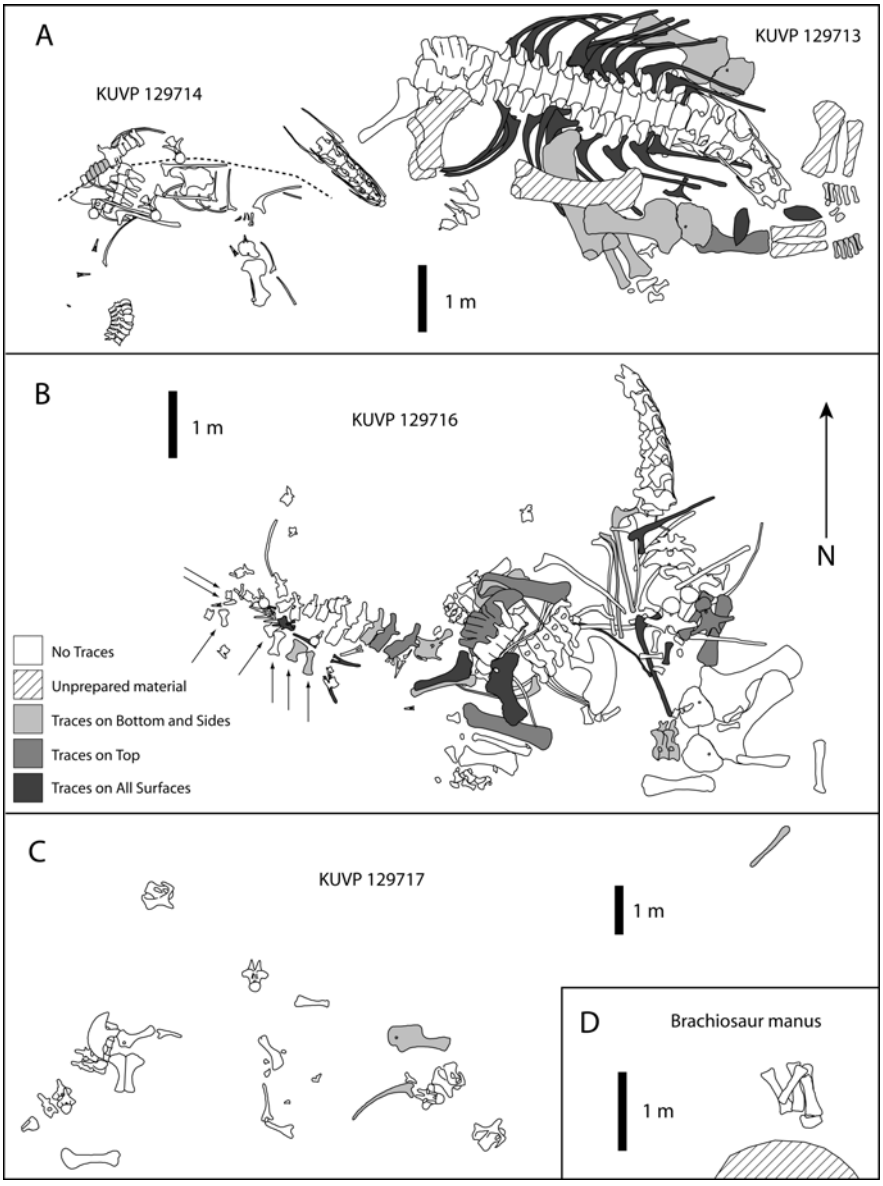

Figure 9. KU-WY-121 Bone maps; shading indicates shallow pits, rosettes, and hemispherical pits. A) Adult *Camarasaurus* (KUVP 129713) on right and juvenile *Camarasaurus* (KUVP 129714) on left at the margin of a slope (dashed line). B) Adult Camarasaurus (KUVP 129716) with a brachiosaur pes (129724), indicated with arrows. C) Diplodocid skeleton (KUVP 129717). D) Brachiosaur manus.

The partially articulated skeleton of a juvenile *Camarasaurus* (KUVP 129714; Fig. 9A) lies on the margin of a small slope with less than 1 m of relief in the sandstone. Bones at the base of the slope are well preserved, whereas those at the top are highly weathered. Unlike the other skeletons in KU-WY-121, the enclosing matrix is predominately poorly cemented, fine-grained sandstone. KUVP 129714 is identified as a juvenile by the unfused neural arches and vertebral centra. The skull and cervical vertebrae 1–11 are absent. Cervical vertebrae 12 through dorsal 4 are articulated and inverted with dorsal vertebrae 5–7 scattered to the west. One posterior dorsal vertebra is above the right ilium and a second is at the base of the slope below the anterior dorsal vertebrae. The dorsosacral vertebra, sacrum, and 6 anterior caudal vertebrae are articulated and lay on their left sides at the top of the slope. Three medial caudal vertebrae are scattered below and west of the anterior dorsal vertebrae. A series of 7 articulated caudal vertebrae were found in the bottom of the slope. Cervical ribs, dorsal ribs, and chevrons are scattered throughout the slope. The articulated right scapula and coracoid are ~1 m south of the slope. The right and left ilia were separated from the sacrum and lay on the slope. The distal end of an ischium was found above the left ilium. A small *Camarasaurus* tooth was found on the southwestern edge of the skeleton. The excavation was expanded to the south in 1998 and 2004 but failed to recover the rest of the skeleton.

KUVP 129716 is a partially articulated *Camarasaurus* (Fig. 9B). The front half of the skeleton is mostly disarticulated. The rear half of the skeleton containing the pelvic girdle, hindlimbs, and tail ranges from articulated to closely associated but disarticulated. Weathering likely destroyed the skull and anterior portion of the neck

based on the relationship of the skeleton to the land surface. Cervical vertebrae 4–11 are articulated, lay on their left sides, and are arched backwards to maximum retraction. Cervical vertebra 12 through dorsal vertebra 4 are disarticulated. The fifth and sixth dorsal vertebrae are articulated and lay on their right sides facing the posterior portion of the skeleton. Dorsal vertebrae 7–11 are articulated and lay on their right sides. The ribs are scattered throughout the east half of the excavation. The proximal caudal vertebrae are loosely articulated and lay on their left sides. The distal caudal vertebrae and chevrons are scattered on the west side of the excavation. The right and left scapulae are inverted and crossed. The right arm is disarticulated and the left arm is articulated with the anterior surfaces rotated down. The left ulna, radius, and carpals are articulated. The pelvic girdle is rotated onto its left side with the right ilium disarticulated. The left hind leg is folded underneath the pelvic girdle near anatomical position. The right hind limb is shifted left of anatomical position.

An unidentified small diplodocid (KUVP 129717; Fig. 9C) was collected at the eastern edge of the quarry. The skeleton was scattered and less than 30% of the bones were recovered. The pelvic girdle and anterior six caudal vertebrae were loosely articulated. The right scapula and coracoid are fused. The right humerus, radius, ulna, and femur, plus two dorsal vertebrae, three cervical vertebrae, and four ribs were found near the pelvic girdle. The right fibula, phalanges, metapodials, one distal caudal vertebra, and a cervical vertebra were found scattered throughout the excavation.

The brachiosaur (KUVP 129724) consists of all five metatarsals from the left pes, three phalanges, and one claw. The metatarsals were found scattered underneath the tail of KUVP 129716 and the phalanges and claw were scattered around the same skeleton

(Fig. 9B). A distal phalanx from metatarsal five and one astragulus collected in 1997 from around KUVP 129713 is also referred to this specimen (A. Maltese, personal communication, 2004). The landowner collected an articulated right manus of a large brachiosaur in 2005. The specimen was deposited palm-side up and the phalanges were missing (Fig. 9D).

METHODS

After preparation, the surface of every sauropod bone was examined for traces. The position and morphology of the individual traces on the skeletons were recorded. The length, width, and depth of each trace were measured using digital calipers. For elliptical traces, the length is the greatest diameter and the width is perpendicular to the length. A 1-cm-wide transect was taken along the entire length of limb bones, ribs, pubis, and ischia to determine the density of traces. Each transect was divided into proximal, medial, and distal zones. Bone modification was quantified in each zone by the percentage of modified bone surface (Fig. 10). The amount of disarticulation and fluvial transport of the sauropod skeletons was evaluated using Voorhies groups (Table 4). Voorhies groups originally were designed for use with medium-sized mammal skeletons without connective tissue that were transported in a fluvial environment. Concepts in the method, however, can be generally applied to dinosaur skeletons. Behrensmeyer bone weathering stages were used to determine the length of subaerial exposure of bones independently from the trace fossils (Table 4).

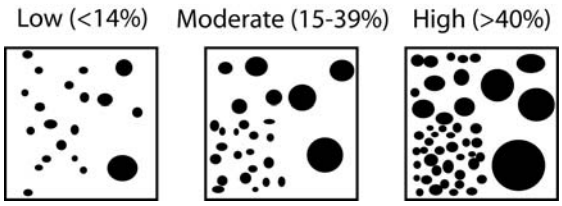

Figure 10. Charts used for determining the density of borings, based on percentage composition charts in the Munsel color chart.

Voorhies Groups		Behrensmeyer Stages	
Group 1	Immediately removed	Stage 0	Fresh, without cracking or flaking Soft tissue present
	Ribs, vertebrae, sternum, scapula, phalanges	Stage 1	Cracks parallel to the long axis of bones Soft tissue may be present
Group 2	Gradually removed		
		Stage 2	Outermost bone flaking
	Limb bones, pelvis		Remnants of soft tissue present
Group 3	Lag deposit	Stage 3	Outer 1.5 cm of bone has fibrous texture No soft tissue present
	Skull, mandible		
		Stage 4	Weathering penetrates to inner cavities of bone
		Stage 5	Bone is falling apart

Table 4. Bone modification stages and groups.

Some of the traces were replicated with silicon peels and plastic casts for analysis with scanning electron microscopy (SEM). Traces prepared using air abrasion were avoided for casting because air abrasion might erase fine details of the trace fossil. Vinac® was removed from surfaces containing any traces by washing with acetone. GI-1000® silicon was poured over the surface of the traces. The silicon cured overnight and then peeled off the bone surface. Dyna-cast® plastic was brushed onto the surface of the peel and pressurized to 70 psi to remove air bubbles. The resulting casts were removed

from the silicon mold after curing. The casts were examined and photographed with an SEM.

Traces on the dinosaur bones were compared to variety of traces on modern and ancient bone (Table 2–3). The Jurassic traces were also compared to a variety of borings in wood produced by modern insects (e.g., Furniss and Carolin, 1977). Comparisons were used to infer the (1) tracemaker, (2) the behavior that produced the trace, and (3) paleoenvironmental significance of the trace.

RESULTS

Trace Fossils

More than 927 traces were measured from the four sauropod skeletons. Shallow pits (633), rosettes (103), hemispherical pits (65), thin, curvilinear, branching grooves (>100), and U- to V-shaped linear grooves (26) comprise the trace-fossil morphologies found on sauropod skeletons at KU-WY-121. The traces on the bones were not found in association with trace fossils originating from the surrounding matrix. No sediment was found lining or coating the bone or any surface of the traces. Bone chips were not found in the matrix or associated with the traces.

Shallow pits.—Shallow pits are roughly circular to elliptical in plan view (Fig. 11A–E). They range from 0.48–8.36 mm in diameter and average 2.80 mm. The pits are less than 0.50 mm deep. The width-to-depth ratio of shallow pits ranges from 3.13–26.27, with an average ratio of 12.07. The wall of the pit forms an ~ 90^{o} angle with the floor of the pit. The walls of most pits are smooth. Some walls, however, are scalloped

(Fig. 11B–C), where each scallop in plan view is ~0.4 mm across—linear distance from the tips of a scallop—and forms an arc 0.1 mm at its greatest width.

Shallow pits are found as isolated traces or low to high-density clusters on limb bones, ribs, gastralia, chevrons, and occasionally vertebral centra. The dimensions of each shallow pit in a cluster of shallow pits are similar compared to shallow pits on other parts of a skeleton. For any given bone, shallow pits have similar dimensions for that particular bone.

The highest concentrations of shallow pits are on the proximal sector of ribs—the rib head and upper portion of the shaft. Shallow pits overlap (Fig. 11D) and coalesce (Fig. 11E) to form irregular patches of modified bone surface < 1 mm deep and can cover up to ~ 54 cm^2. This type of damage is only found on the ribs, scapula, and limb bones of the large *Camarasaurus* (KUVP 129713). Shallow pits are found in moderate concentrations on lateral surfaces of ribs, chevrons, caudal vertebrae, and limb bones. Moderate to high densities of shallow pits were also found on surfaces where two bones lie against each other; for example, overlap of the pubis onto the right femur on KUVP 129716 (Fig. 9B). Low concentrations of shallow pits are found on bone surfaces in between articulated bones; for instance, between metacarpals in the articulated brachiosaur manus and the metatarsals of the pes).

Rosettes.—Rosettes are circular rings of modified bone surrounding a region of unmodified bone (Fig. 12A–E). Outside and inside walls of a rosette are scalloped and are undercut into the unmodified bone (Fig. 12B–C). Rosettes have an outside diameter averaging 2.00–6.00 mm, and an inside diameter of 0.33–3.92 mm. The width-to-depth

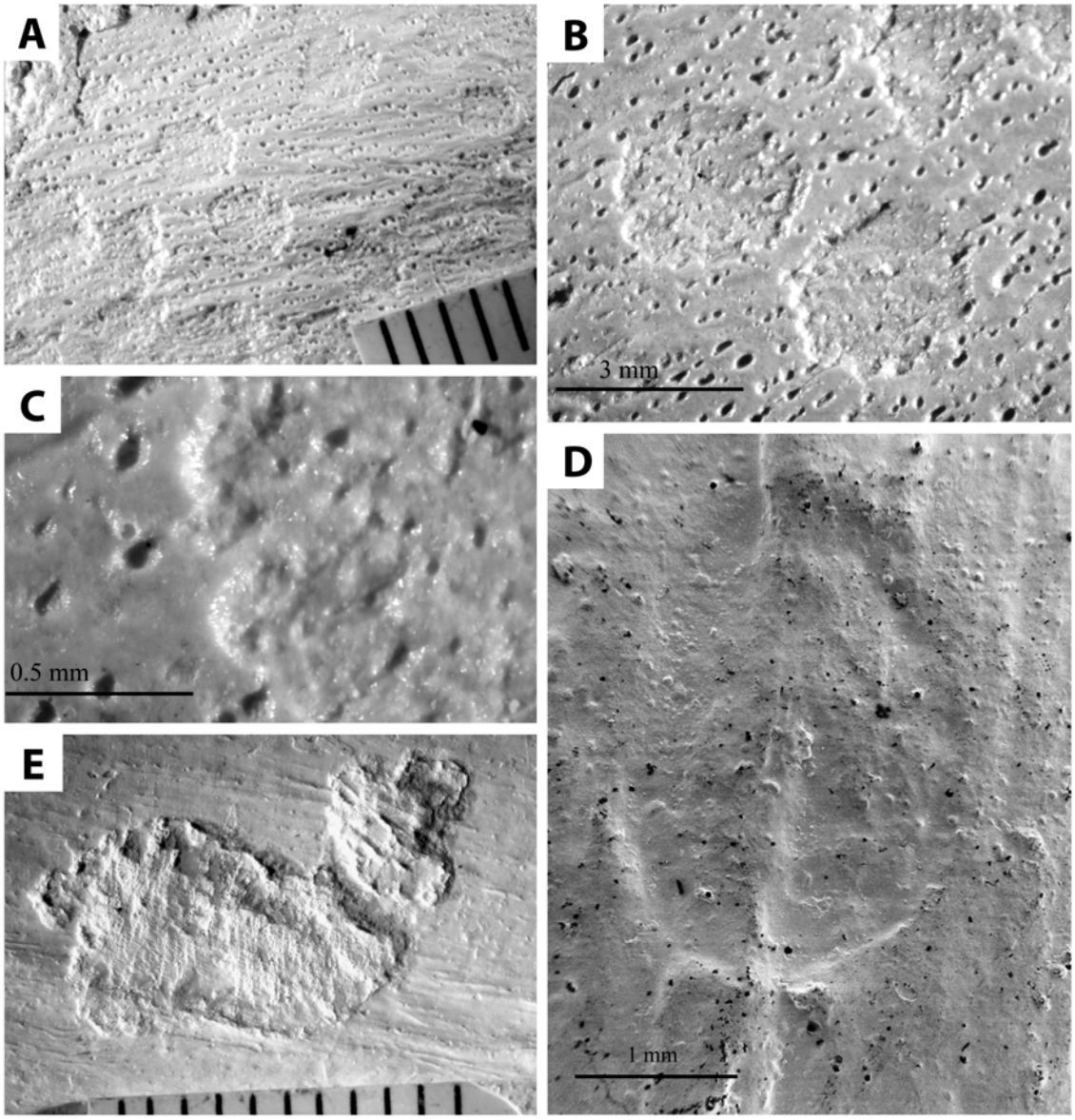

Figure 11. Shallow pits. A) Cluster of shallow pits from metatarsal IV of the brachiosaur (KUVP 129724). B) Close up of shallow pits in center of photograph A. C) Scalloped edges of the left side of the upper left shallow pit in B. D) SEM photograph of overlapping shallow pits on a rib head from the large *Camarasaurus* (KUVP 129713). E) Overlapping and expanded shallow pits on the scapula of the large *Camarasaurus* (KUVP 129713).

ratio of rosettes is 6.56–16.21, with an average ratio of 11.14. Scallops in rosettes share the same dimensions with scallops in shallow pits. Rosettes up to 13.25 mm in diameter on the left scapula of *Camarasaurus* (KUVP 129713) probably resulted from overlapping and coalescing rosettes. The rosette depth typically is less than 0.5 mm. The diameter of the unmodified pedestal does not vary in proportion to the outer diameter of the rosette (Fig. 12B, D).

Rosettes are almost exclusively found on the large *Camarasaurus* (KUVP 129713). High densities of separate and overlapping rosettes (Fig. 12E) are found on the ribs and scapula of KUVP 129713. The rib heads consistently have the highest densities of rosettes, the rib shafts varied from low to high densities. Single rosettes were found on the scapula of the diplodocid (KUVP 129717) and a rib from the second adult *Camarasaurus* (KUVP 129716). Single rosettes are also found in clusters of shallow pits on all three sauropod skeletons, however, single shallow pits are not found in clusters of rosettes on KUVP 129713.

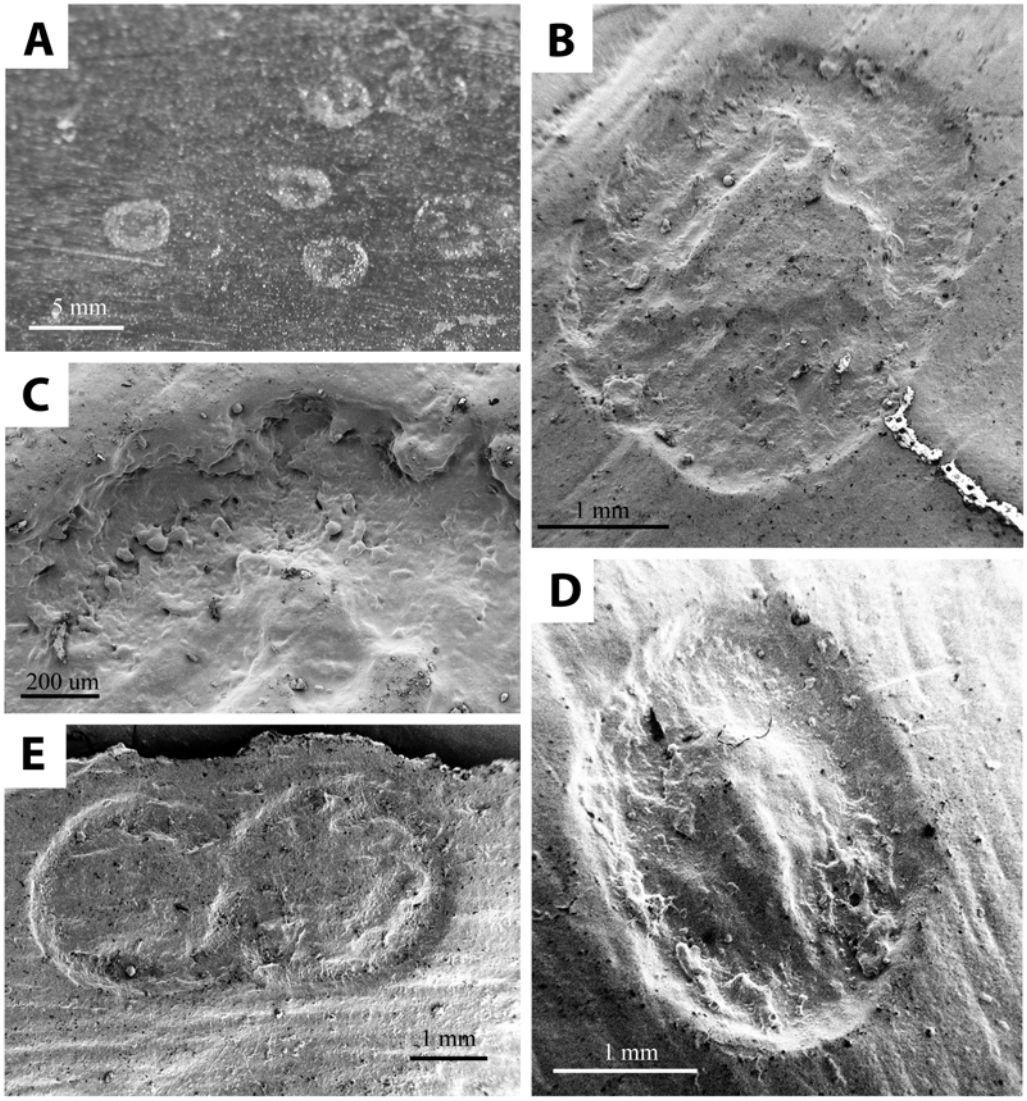

Figure 12. Rosettes from KUVP 129713. A) Cluster of rosettes. B) SEM of a typical rosette with a scalloped pedestal and outer wall. C) Close-up of upper margin of the rosette in B showing the undercut wall. D) Rosette with a smaller unmodified pedestal and few scallops. E) Two overlapping rosettes with thin rings of modified bone.

Hemispherical pits.—Hemispherical pits are circular in plan view with a U-shaped cross section and a diameter of 1.98–5.63 mm (Fig. 13A–D). The average diameter of hemispherical pits on KUVP 129713 (4.19 mm) is larger than KUVP 129716 (3.19 mm). Hemispherical pits are 0.62–1.74 mm in depth, averaging 0.96 mm. The width-to-depth ratio of hemispherical pits is 1.92–4.52 with an average of 3.52. The walls of hemispherical pits are smooth (Fig. 13A–B); scallops are not present. Only two hemispherical pits, found on a rib head of KUVP 129713, have central columns of unmodified bone. Each central column is smooth walled and 57% the diameter of the surrounding hemispherical pit.

Hemispherical pits were found in low-density clusters (Fig. 13C–D) on the centra of dorsal vertebrae 4–6 on KUVP 129716 and the lateral surfaces of a sternal plate and one rib head of KUVP 129713. On KUVP 129716, hemispherical pits are not associated with other traces. On KUVP 129713, hemispherical pits are associated with shallow pits on the sternal plates and both shallow pits and rosettes on a rib head. Hemispherical pits do not overlap other traces.

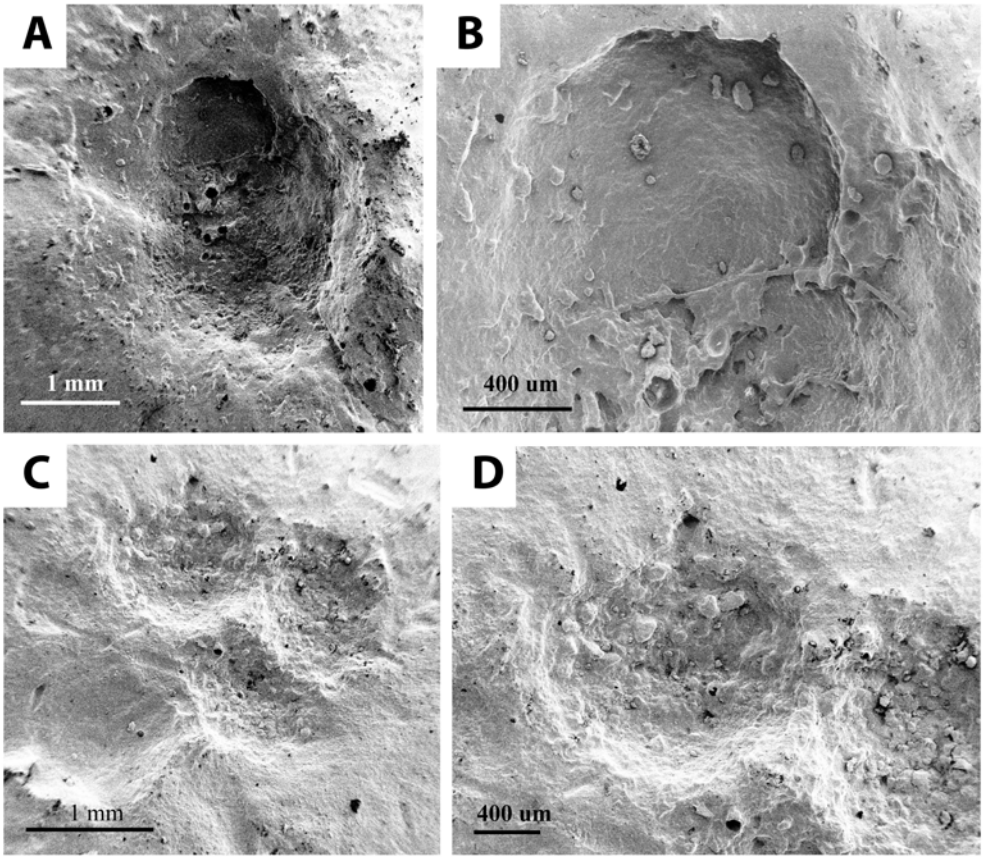

Figure 13. Hemispherical pits. A) SEM of a hemispherical pit from a dorsal vertebra from KUVP 129716. B) The bottom of the hemispherical pit in 8A. C) Cluster of hemispherical pits from the sternal plate of KUVP 129713. D) Close-up of uppermost pit in the cluster. The spheres are quartz sand grains.

Thin, curvilinear, branching grooves.—Branching grooves (Fig. 14A–F) have an irregular dendritic or looping pattern, smooth walls, and are semicircular in cross section. Grooves are found in parallel-running, rarely branching pairs or groups on a posterior cervical rib (KUVP 129714) and a rib head (KUVP 129716). The width of branching grooves is variable, but always less than 1 mm. The length of branching is variable; the

shortest grooves are ~1.5 mm long. Branching grooves on bones collected at or near the modern soil surface are discolored white or associated with oxidized bone (Fig. 14E–F).

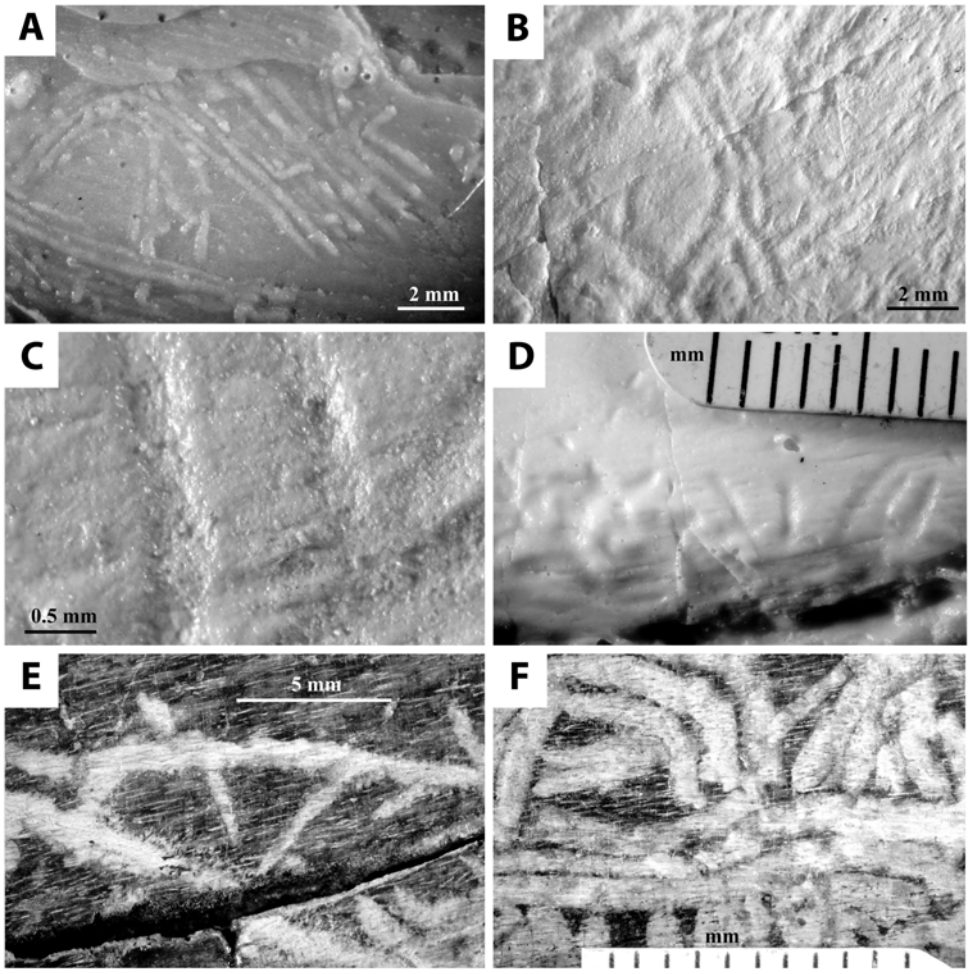

Figure 14. Thin, curvilinear, branching grooves. A) Grooves on a rib head from KUVP 129716. B) Grooves on a cervical rib from KUVP 129714. C) Close up of grooves in B; note shallow U-shape form. D) Grooves on a rib from KUVP 129717; note discontinuous pattern near the left edge of the mm scale. E–F) Example of modern root etching on a scapula from a *Miasaurus*, Late Cretaceous of Montana; note branching pattern, high density of coverage, and bleaching on the bone surface.

Branching grooves are found on all skeletons, but are not present on all bones. These grooves may be present in low to high densities, often covering almost 100% of the bone surface. Branching grooves are occasionally found overlapping shallow pits and rosettes.

U- to V-shaped linear grooves.—Linear grooves are 0.56–9.86 mm across and 0.28–4.69 mm deep with a U- or V-shaped cross section (Fig. 15). The longest groove is 64.7 mm and cuts across a slightly curved surface. Wide grooves penetrate deeper into the bone surface than thin grooves. A linear groove cut across a flat or slightly curved surface is widest at one end, and the margins gradually converge at the other end of the trace. The sides of a groove cut through the edge of a bone are parallel. The internal surface of a linear groove is rough.

Linear grooves are found on small diameter bones—metacarpals, gastralia, and chevrons. Grooves usually are oriented perpendicular to the long axis of the bone. On the right manus of KUVP 129713, numerous parallel linear grooves run subparallel to the long axis of the metacarpals (Fig. 15). Linear grooves are associated with shallow pits on the brachiosaur manus and a single gastralia from KUVP 129716. On metacarpal V of the brachiosaur manus, a deep linear groove crosses the anterior surface of the proximal end. This groove is parallel to the U- to V-shaped linear grooves on the lateral edge.

Figure 15. Linear, U- to V-shaped grooves on the first and second metacarpals from the right manus of a *Camarasaurus* (KUVP 129713).

Distribution of Traces on the Skeletons

Traces are most abundant on the large *Camarasaurus* skeleton (KUVP 129713, Fig. 9A). A high density of overlapping rosettes and shallow pits are present on all surfaces of the limb bones and ribs of KUVP 129713 (Fig. 9A). Hemispherical pits are found only on the sternal plates and rib heads; they have a lower density on the rib heads. Linear grooves are present on the right metacarpals. Branching grooves are on the underside of the left scapula.

Traces are rare on the juvenile *Camarasaurus* (KUVP 129714, Fig. 9A). Shallow pits are present on the underside of two rib heads and a neural arch at the top of the slope and one rib head just below the crest of the slope. Shallow pits, rosettes, and

hemispherical pits are absent from the rest of the skeleton. V-shaped linear grooves are present on the coracoid, ribs, and chevrons. Branching grooves decrease in density from highest to lowest on the skeleton from the margin to the base of the slope, where grooves are absent.

Traces are abundant on the limb bones and ribs of *Camarasaurus* KUVP 129716 (Fig. 9B). Shallow pits, which rarely overlap, are found at low to high densities on the undersides or all surfaces of ribs, on all surfaces of chevrons, mostly on all surfaces of limb bones, and on the top or bottom of the caudal vertebrae of KUVP 129716. One rosette was found on a right rib head. Hemispherical pits were found on the underside of the neural arches of dorsal vertebrae 4–6.

Traces are abundant on the limb bones and ribs of the diplodocid (KUVP 129717; Fig. 9C). Branching grooves modified the entire surface of the limb bones. Shallow pits and rosettes were found on undersides of three bones with low-density curvilinear branching grooves. A single rib head contained two rosettes and 29 shallow pits. Shallow pits were found on the lateral surface of the right scapula and the medial surface of the right fibula. Hemispherical pits and linear grooves are not present on the diplodocid skeleton.

Shallow pits are abundant on the underside of metatarsals IV and V of the brachiosaur pes (KUVP 129724; Fig. 9B), and on the underside of the metacarpals (anterior surface) on the brachiosaur manus (Fig. 9D). Three rosettes were found on metacarpal IV and five on metacarpal V. Hemispherical pits were not found on the manus or pes. Along the lateral edge of both metacarpals are linear grooves that run perpendicular to the shafts. Two shallow linear grooves on the proximal end of

metacarpal IV cross at an acute angle. Branching grooves are present on the brachiosaur pes, but are absent from the brachiosaur manus.

Biostratinomy of the Sauropod Skeletons

The dinosaur skeletons did not fit into any of the Voorhies groups although they range from partially disarticulated to fully disarticulated, because of the lack of evidence for water transport. The sauropod bones, when not associated with a skeleton, appear to be scattered randomly in the quarry. The long bones from the disarticulated diplodocid skeleton (KUVP 129717) do not share common alignment and are not associated with any fluvial cross-bedding.

Nearly all the sauropod bones are cracked but not splintered prior to burial based on the relationship between the cracks and the host matrix. The cracks on many bones cut through shallow pits and rosettes but do not offset them vertically or horizontally. Some of the bones upon preparation exhibited exfoliation, which may be due to the drying of the bones resulting from their removal from the fine-grained matrix or from the tectonic activity in the area. No splintering associated with weathering prior to burial was observed on any of the skeletons. This pattern of bone cracking is categorized as Behrensmeyer stage 1 and the earliest part of stage of 2 (Table 4).

DISCUSSION

Rosettes, Shallow pits, Hemispherical Pits

The rosettes, shallow pits, and hemispherical pits (Fig. 11–13) are interpreted as pupation chambers produced by the larvae of holometabolous insects. Dermestid beetles

or an extinct insect taxon with no body fossil record are the most likely constructors of these traces based on comparisons to modern arthropod traces on bone and in wood (see Table 3 and references therein). Modern dermestid beetle (Coleoptera: Dermestidae) larvae and adults feed on desiccated carcasses, and commonly are used in museums to remove tissue from skeletons (Hinton, 1945; Timm, 1982). Larvae consume bone when other food sources are not available (Hefti et al., 1980). After feeding for approximately four weeks the larvae pupate and bore into any available compact surface, including dry flesh and bone (Hinton, 1945; Gabel, 1955; Timm, 1982). We have observed similar behavior in the University of Kansas dermestid colony. A larva bores a pupation chamber in wood or bone that is circular to oval in plan view with vertical sides and a U-shaped cross section (e.g., Martin and West, 1995; West and Hasiotis, 2007). The larva plugs the entrance of the chamber with its final molt (exuvia) and begins pupation. When pupation is completed, an adult dermestid beetle exits to begin the life cycle again (Hinton, 1945). The rosettes, shallow pits, and hemispherical pits are interpreted to have been constructed as pupation chambers (1) in dried flesh and in contact with the bone (i.e., rosettes, shallow pits), and (2) almost entirely within the bone (i.e., hemispherical pits), based on the morphology of the traces fossils and comparisons to such modern bone-modifying arthropods as dermestid beetles.

Rosettes and Shallow pits.—Rosettes (Fig. 12A–E) appear to be an early stage in the production of shallow pits (Fig. 11A–E) based on a series of rosettes showing a pattern of reduction in the diameter of unmodified pedestals (Fig. 16). The tracemaker chewed the bone surface using an inward spiral pattern. A rosette morphology resulted if the chewing process was discontinued or interrupted, leaving behind a central,

unmodified pedestal. If the process continued until the central pedestal was removed, the rosette morphology was transformed into a shallow pit. Very large shallow pits with diameters of 5.00–8.36 mm, averaging 5.66 mm, are likely the result of overlapping pit construction.

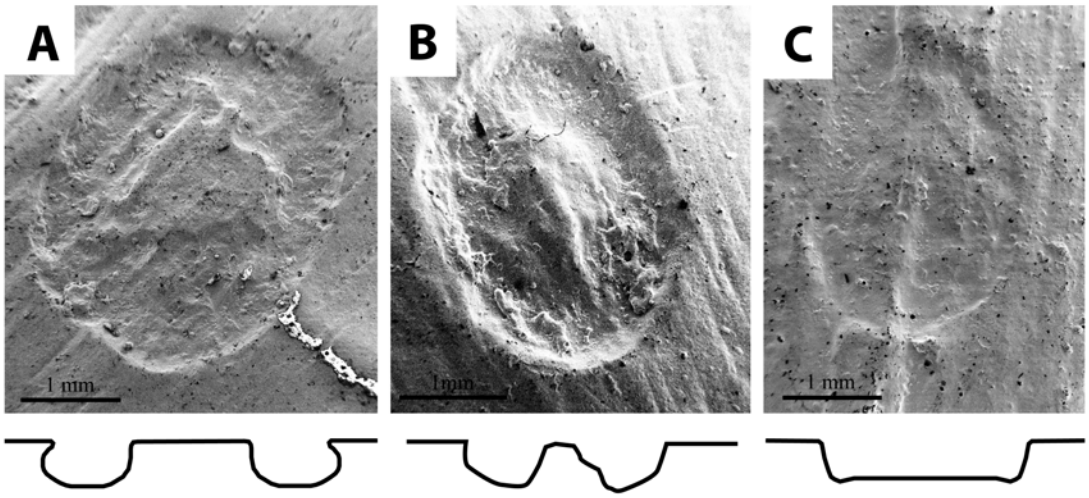

Figure 16. Transition from rosette to shallow pit.

Rosettes and shallow pits likely represent pupation chambers constructed in dried flesh that were in contact with sauropod bone. We hypothesize that a tracemaker chewed through the flesh until it reached the bone surface, which at this point, the pupation chamber was complete. The larva sealed the opening of the chamber, with its final molt (exuvia) to plug the entrance and begin pupation.

We infer that dermestid larvae constructed these traces and may have pupated within the dried flesh of a carcass while in contact with the bone and emerged as an adult when pupation was complete. This particular behavior by dermestids has not been observed directly in modern carcasses; however, we have observed a similar behavior in

association with wood, cardboard, and tight spaces between bones. Dermestid larvae have been observed to bore shallowly into wood and remain mostly outside of the wood to pupate. They bore into tight spaces between bones or within small foramina—blood vessel and nerve passages into bone—and pupate without completing a deep pit. We envision that a similar behavior was used on the sauropod carcasses where only a rosette or shallow pit was produced on the bone surface such that the majority of the chamber remained in the dried flesh, forming a tight space in which pupation could be completed.

Shallow pits, alternatively, could have been produced by another type of arthropod that has not been identified as being osteophagous in its feeding behavior. This behavior would have been similar to that of extant dermestids. These trace fossils could also represent an organism that left no fossil record and is extinct.

Hemispherical pits.—Hemispherical pits (Fig. 13A–D) are interpreted as pupation chambers constructed almost entirely within sauropod bone. The tracemaker chewed downward in a spiral pattern, producing a smooth-walled, relatively deep pit. Central columns of unmodified bone in two of the hemispherical pits (rib head of KUVP 129713) attest to the boring pattern similar to the one used to construct shallow pits. There is no evidence, however, of any transitional forms between shallow pits and hemispherical pits.

We interpret the hemispherical pits to represent pupation chambers of dermestid beetles constructed within sauropod bone likely after the flesh was removed from the bone surface. There is no way to know, however, if any flesh actually remained on the bone when the hemispherical pit was constructed. When the chamber (i.e., hemispherical pit) was complete, the larva likely sealed the opening with its final molt and began pupation. The larva remained in the chamber until pupation was complete and emerged

as an adult. Borings with a similar size, shape, and width-to-depth ratio have been attributed to the activity and pupation of dermestid beetles in Jurassic and Neogene bones (Kitching, 1980; Martin and West, 1995; Hasiotis et al., 1999; West and Hasiotis, 2007).

Ongoing laboratory experiments with *Dermestes maculatus* in the University of Kansas dermestid colony have produced shallow and spherical pits in wood (Fig. 17) similar to those found on the sauropod bones (Bader and Hasiotis, in preparation). The pits in wood are ~2–5 mm in diameter and 0.5–2.0 mm deep. The width-to-depth ratio ranges from 0.93–9.97, with an average ratio of 5.13. The walls are vertical or have a gentle slope, producing a wide U-shaped cross section. The base is flat against a layer of dense late wood and may lie at an acute or perpendicular angle to the walls. Pits with an inclined base are undercut into the wall adjacent to the deepest point. One shallow pit contained a small central pedestal of unmodified wood resembling a rosette. Shallow pits often coalesce into large patches of surface-modified wood. These experiments demonstrate that dermestids can produce borings similar to borings found in the Jurassic sauropod bones, although the wood used in the experiments is softer than bone. Current experiments have dermestids boring into hardened blocks of dental plaster, producing traces similar in morphology to the hemispherical pits found on the sauropod bones. `

Alternatively, hemispherical pits may have been constructed by another type of arthropod that feed on bone or used it for pupation. This behavior would have been similar to that of extant dermestids.

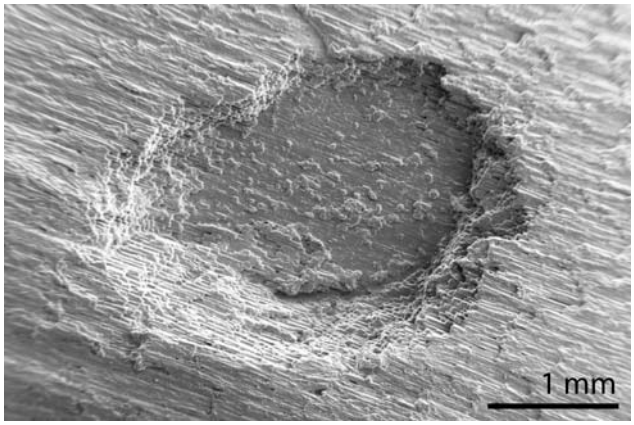

Figure 17. SEM of dermestid boring in pine from ongoing experiments with the dermestid beetle colony at the University of Kansas.

Thin, curvilinear, branching grooves

Thin, curvilinear, branching grooves are interpreted as mining behavior that took advantage of sauropod bone surfaces (Fig. 14A–D). These shallow, closely spaced and branching structures are evidence for the removal of minerals from the bone surface by chemical etching because only smooth surfaces were observed within the grooves. All the grooves appeared to remain open, with no evidence of backfilling or early cementation.

We interpret these shallow branching groove patterns as the chemical etching activity of roots on bone surfaces based on comparisons to similar morphologies ascribed to roots (e.g., Binford, 1981; Ehrenreich, 1995; West and Hasiotis, 2007); herein these are referred to as rhizoetchings. Modern roots chemically etch bone to obtain calcium, iron, and phosphorous—nutrients that are necessary for plant growth (Fig. 14E–F). Phosphorous is an essential macronutrient for plant growth and is often a limiting nutrient in many terrestrial environments (Aber and Melillo, 1991). The shallow branching

grooves where likely produced after the carcasses where buried and during pedogenesis of the sediments encasing the sauropod skeletons. The abundance and density of these rhizoetchings modified the entire surface bones and likely destroyed evidence of rosettes, shallow pits, or hemispherical pits if any were originally present.

Modern root traces can be distinguished from etched patterns produced on bones by ancient roots (i.e., rhizoetchings) associated with those bones at the time of burial. Modern etching patterns on fossil bone produce haloes of chemical activity that appear as white, yellow, or gray discolorations on the bone surface (e.g., Warren, 1975; Stewart, 1979). If this continues, shallow grooves are produced on the surface of the bone (Binford, 1981; Ehrenreich, 1995). Sometimes roots are associated with these types of grooves (S. T. Hasiotis personal observation, 2004). Root damage can include linear arrangements of pits and multiple sinuous, branching grooves with a U-shaped cross section. Extensive root etching can entirely remove cortical bone without leaving identifiable root traces (Andrews, 1990). The activity of roots during the Jurassic produced similar patterns to the modern; however, the surface haloes associated with the ancient roots were obliterated by burial diagenesis and the grooves were filled post burial with matrix that was removed by preparation. No modern roots where found directly associated with the shallow branching grooves on the bones.

Fungal hyphae produce damage similar to root modification (Davis, 1997). Tunnels and grooves with U-shaped cross sections from hyphae range in diameter from 1–100 μm (Sognnaes, 1955; Hackett, 1981; Piepenbrink, 1986; Davis, 1997). These kinds of grooves, however, are much smaller in diameter compared to grooves found on the sauropod skeletons.

Modern and ancient root traces can be distinguished from grooves produced by scolytid and buprestid beetles underneath the bark of dead trees and logs by their smaller diameter (<1 mm), smooth walls, and semicircular cross section. Beetles etch branching grooves with rough walls up to 3 mm wide (e.g., Furniss and Carolin, 1977). The branching pattern of beetle grooves in wood results from one groove crossing an older groove. The cross section of grooves produced by beetles is semicircular in small grooves (<1.3 mm) and gradually becomes a shallow U-shape in larger grooves.

Deep U- to V-shaped Linear Grooves

Deep U- to V-shaped linear grooves (Fig. 15) are interpreted as bite marks from a large theropod, such as *Allosaurus* or *Torvosaurus*, or a large crocodilian. The grooves were found on bones of the manus and pes, gastralia, and chevrons. There are a relatively large number of grooves on the brachiosaur manus and the right manus of KUVP 129713. A carnivore feeding on these distal limb bones could have produced the grooves found on the manus, since it takes a great amount of force to pull a limb off a carcass compared to pulling flesh off of a bone. Orientation of the grooves parallel to the metacarpal shafts on the *Camarasaurus* (KUVP 129713) indicates that the carnivore tried to pull the manus off the skeleton. Grooves perpendicular to the metacarpal shafts of the brachiosaur manus indicate the carnivore twisted the manus off the carcass. Grooves on the gastralia likely resulted from the opening of the abdominal cavity by carnivores. Grooves on the chevrons likely resulted from carnivore teeth scraping the bones to remove muscle from the base of the tail.

Modern studies demonstrate clearly that vertebrate predators and scavengers modify bones (e.g., Behrensmeyer, 1978; Hill, 1987; Weigelt, 1989; Njau and Blumenschine, 2006). Such grooves found on bone in the rock record can best be attributed to damage by a carnivore since there is no reliable method to differentiate feeding during predation vs. scavenging. The only exception is evidence of healed bite marks on potential prey that had escaped and later died of other causes (Carpenter, 2000). The distribution of bite marks on the sauropod skeletons indicates that the marks were likely produced while the carnivore was feeding on the carcass rather than from predation.

Bone modification by modern crocodiles is an appropriate model for bite marks produced by large theropods and Jurassic crocodilians (e.g., Hasiotis, 2004). Crocodiles, for example, produce marks with U- to V-shaped cross sections with rounded pits and punctures in bone with their teeth while capturing prey or feeding on carcasses (Njau and Blumenschine, 2006). The marks are J-shaped when the crocodile is head-shaking or death-rolling while attempting to break apart a carcass.

Other Insects that Modify Bone—Unlikely Tracemakers

Circular to oval pits in bone are often attributed to holometabolous insect pupation chambers (Table 2). Holometabolous insects undergo a complete metamorphosis from egg to larva to pupa to adult (Daly, 1998). Beetles (Coleoptera), moths and butterflies (Lepidoptera), and the wood wasps and sawflies (Hymenoptera) are the only modern holometabolous larvae with chewing mouthparts capable of modifying bone (e.g., Daly, 1988). These insects, with the exception of the dermestid beetles, can

be excluded as the tracemakers of the rosettes, shallow pits, and hemispherical pits on the sauropod bones, based on the trace morphology or behavior exhibited by their extant representatives.

Non-dermestid Beetles (Coleoptera: Histeridae, Silphidae, Scarabaeidae).—Histerid and silphid beetles are unlikely tracemakers of the sauropod bone traces because extant species have not ever been observed to modify bone. Histerids and silphids primarily are predaceous, feeding on fly maggots and occasionally on carrion during the early stages of decay (e.g., Payne and King, 1970; Smith, 1986). Histerids disappear when a carcass reaches the dry stage. Silphids will sometimes feed on dried carrion; however, they will die if they are only provided carrion (Steel, 1927; Smith, 1986). Haglund (1976) showed an illustration of bone damage to buried human skeletons in Australia attributed to *Anoplognathus* (Coleoptera: Scarabaeidae). The irregularly shaped and spaced pitting of cancellous bone appears to be morphologically most similar to pitting produced by acid etching (e.g., Andrews, 1990). This damage, however, also does not match that found on the sauropod skeletons.

Tineid moths (Lepidoptera: Tineidae).—Tineid moths are the only other holometabolous insect known to modify bone (Table 3). They are primarily keratinophagous, feeding on horns, feathers, hair, and skin of desiccated carcasses (McCorquodale, 1898; Busck, 1910; Bornemissza, 1957; Coe, 1978; Deyrup et al., 2005). *Ceratophaga vastella* and *Tinea deperdella* construct tubes composed of silk, earth, and keratin that extend from the underside of horn or bone into the soil (Busck, 1910; Behrensmeyer, 1975, plate 3b). These reinforced tubes are used as temporary shelters during molting (Robinson and Nielsen, 1993). *Tinea deperdella* etch ~2-mm-wide

grooves into horn cores while feeding on the keratin sheath (Behrensmeyer, 1978). Hill (1987) reported that *Ceratophaga* bore straight-sided, cylindrical pupation chambers into the astragali of African bovids. Borings of tineid moths are common in the modern African savanna; they have not yet been recognized in the fossil record.

The morphology of tineid moth damage does not match that of the rosettes, shallow pits, or hemispherical pits on the sauropod bones. The pupation chambers of tineid moth larvae are closely associated with keratin—their food source (Behrensmeyer, 1978; Hill, 1980; Robinson, 1993). The main sources of keratin on a sauropod would have been the skin and the claws and pads of the manus and pes. If tineids or insects with tineid-like behavior fed on sauropod skin and feet, the pupation chambers would have been restricted to bone surfaces in contact with the skin—bones of the manus and pes, skull, and gastralia. Traces are also absent from the sauropod phalanges where tineid moth larva or larva with tineid-like behavior would have been expected to feed on the claws and pads of the feet. These larvae, alternatively, may have been present and fed on the keratin associated with the distal portion of the sauropod limbs but their activity did not penetrate to the bone surface.

Termites (Insecta: Isoptera).—Modern termites are known occasionally to damage or destroy bone (Table 3). Termites build walls of stercoral (Noirot, 1970; Hasiotis, 2003) up from the soil surface to cover the underside of bone (Derry, 1911). Underneath the stercoral, termites incise small round pits along linear trails (Tappen, 1994). The pits are expanded until the bone surface is completely removed. Bones that are not covered by stercoral remain intact (Thorne and Kimsey, 1983). Laboratory experiments by Watson and Abbey (1986) and by Kaiser and Katterwe (2001) indicate

that *Mastotermes*, an Australian termite, can produce paired mandible marks on bone. These traces are characterized by paired grooves with a steep U- to V-shaped cross section and a ridge structure where the two grooves meet. Mandible marks are single or repeat along the edge of a bone or a crack in the bone. Little or no unmodified surface bone remains where the marks coalesce. Shallow star-shaped pits found on Pliocene bones in Africa and in the Oligocene of Europe have been attributed to termite activity (Kaiser, 2000; Fejfar and Kaiser, 2005). These traces are interpreted to have been produced by the repeated subparallel mandible marks focused into one area or by the rotation of the insect over a central axis that results in a star-shaped boring; the construction of these features have not been directly observed. Workers of the termite *Nasutitermes carnarvonesis* destroyed Aboriginal skeletons at a burial site but left the bark-covered burial cylinders intact (Wylie et al., 1987). Small bones from the skeleton were the first to be destroyed completely by termites—the particular type of destruction was not described. The damage was attributed to long-term occupation of the skeleton by termites. Thorne and Kimsey (1983) and Watson and Abbey (1986) suggested that termites scavenge the bones of carcasses for nitrogen (e.g., Prestwich et al., 1980) and other nutrients; this relationship has not yet been demonstrated.

Termites, though present in the Jurassic based on trace fossils of nests (e.g., Hasiotis, 2002, 2003, 2004), likely did not produce the bone damage observed on the sauropod skeletons. The shallow pits, rosettes, and hemispherical pits do not fit the morphology of bone modification observed from modern termites (Table 3). No trace fossils of termite nests or galleries were found during excavation of the quarry. If termites were present, small bones associated with the sauropod skeleton should have

likely been destroyed or at least have shown evidence of termite-related bone modification. No abnormal fill or sediment similar to stercoral was found covering the rosettes, shallow pits, or hemispherical pits. Any postburial modification by termites would be indicated by the presence of lined tunnels around the bone traces, bone chips in the tunnels, or modification of cracks produced by weathering prior to burial.

Britt et al. (2005) and Dangerfield et al. (2005) suggested that termites produced the borings on dinosaur bones in the Morrison Formation described previously by Laws et al. (1997), Hasiotis et al. (1999), and Hasiotis (2004). This interpretation is unlikely for the borings on sauropod bones from KU-WY-121 as well as for previously described material from the Morrison Formation (Hasiotis et al., 1999; Hasiotis, 2004) because of the lack of consistency with the morphologies of known termite bone modification (Watson and Abbey 1986; Haynes, 1991; Tappen, 1994; Kaiser, 2000; Fejfar and Kaiser, 2005). Termites in the Jurassic may have had ability to modify bone; however, we have not seen any evidence of such bone modification in any of the material worked with in this or previous studies.

Other Bone-Modifying Activity

The shallow pits, rosettes, hemispherical pits, curvilinear branching grooves, and linear grooves on the dinosaur bones were not created during excavation or preparation of the fossils. Mechanical excavation and preparation tools (e.g., shovel, pick axe, pry bar, knife, dental tools, and pneumatic tools) leave marks that are smooth sided with shiny surfaces (e.g., West and Hasiotis, 2007). Air abrasion erodes an irregular, elliptical patch into bone surface and obscures fine details of the bone, but rarely penetrates to 1 mm in

depth (K. S. Bader, personal observation, 2007). All traces found on the sauropod bones contained matrix before preparation. Matrix is still present inside many of the deeper traces (Fig. 15).

Bone-Cracking Pattern.—Bone cracking patterns observed on the sauropod skeletons indicate that weathering cracked and flaked but did not splinter the bone surfaces (Behrensmeyer 1978; stages 1–2). This pattern indicates that the sauropod skeletons were subaerially exposed for up to 2–3 years. Cracks that cut through shallow pits and rosettes support the interpretation that bone modification by arthropods occurred before bone weathering. The fine scale of cracking and high degree of skeleton articulation, however, indicates that the majority of the carcasses were exposed from 9 weeks to no more than 24 weeks (6 months). If the carcasses remained on the surface for a longer period of time—1 to 4 years—they would have been disarticulated and widely scattered by scavengers (e.g., Behrensmeyer, 1978; Coe, 1978; Behrensmeyer and Boaz, 1980). Only the diplodocid skeleton (KUVP 129717) does not correspond well to the 9–24 week window because of the highly disarticulated and poorly preserved nature of the skeleton and the high degree of cracking.

TAPHONOMIC IMPLICATIONS

As in modern crime scene investigations or forensic science, the condition and preservation of skeletons are studied to understand how an organism died (necrology), the postmortem changes the organism experienced (biostratinomy), and how the organism was buried and preserved (burial and early diagenesis). Entomology plays a major role in forensic science in that various successions of arthropods on carcasses are

used to establish the time since death, as well as to understand how an organism died when multiple traumas have been inflicted on its body (Byrd and Castner, 2001).

In order to understand the significance of bone modification preserved on the Jurassic sauropod skeletons with respect to the depositional history of the quarry, it is necessary to review the founding principles of forensic entomology and how they are used to understand the changes a carcass goes through after death. Carcasses decay in a series of stages (Table 5), each stage attracting a different group of arthropods (e.g., Bornemissza, 1957; Payne, 1965; Payne and King, 1970). The rate of decay and types of arthropods present in each stage varies depending on the temperature, humidity, exposure to sun or wind, scavenging by vertebrates, moisture concentration (wetness) of the environment, and if the carcass is buried. For example, a buried carcass does not desiccate, the rate of decomposition is slowed, and a different group of arthropods is attracted compared to those arthropods attracted to a carcass on the surface (e.g., Payne et al., 1968). A carcass submerged in water also decomposes at a different rate and attracts a different group of arthropods, dominated by aquatic insects and crustaceans (e.g., Payne and King, 1972; Byrd and Castner, 2001). Most necrophagous arthropods feed exclusively on soft tissues, whereas very few arthropods modify bone.

Shortly after death, a carcass becomes inflated by gases produced by internal decomposition (Payne, 1965; Weigelt, 1989; Lyman, 1994). The skeleton collapses onto the ground when the gases are released. Desiccation of soft tissue and ligaments of the limbs maintains the articulation of joints (Weigelt, 1989). As soft tissue decomposes, bones slowly rotate and disarticulate until reaching a stable position (Lyman, 1994). Moveable joints in the limbs separate first, followed by the articulations of vertebrae and

ribs, and finally sutures between bones of the skull (Lyman, 1994). The skin holds the flattened carcass together until removal by necrophagous arthropods or by decomposition during the dry stage of decay. In extremely dry environments skin may remain and be mummified.

Bornemissza, 1957	**Payne, 1965**	**Coe, 1978**
Mediterranean	Warm Temperate Forest	Tropical Wet-Dry
	Fresh	
Initial Decay	Bloated	Bloat
Putrefaction	Active Decay	Wet or Collapse
Black Putrefaction	Advanced Decay	
Butyric Fermentation		
Dry Decay	Dry	Dry
	Remains	

Table 5. Stages of decomposition.

Climate and the time of death also play a role in the postmortem changes to a body after death. Coe (1978) studied the decomposition of elephant carcasses during a drought in Tsavo (East) National Park in Kenya. The average annual temperature in Tsavo is 27.9^{o}C, but varied between 45 and 50^{o}C during the study. The bloat phase and the wet phase, together, lasted ~20 days; however, the dry phase can last up to 20 years in large carcasses (Table 5). The first dermestid beetles appeared on day 4 and were located on the elevated limbs—parts of the carcass that were not covered in putrefaction fluid and were drier compared to the rest of the carcass. At the onset of the dry phase ~21 days after death there was a great increase in dermestid beetles and tineid moths. Dermestid beetles consumed the skin, whereas the tineid moths fed on the thick keratinized soles of the elephant's feet. After the carcass was skeletonized, termites covered bones with

foraging tunnels and removed dried cartilage and ligaments from bones up to two years after death.

The fundamental principles summarized here (Table 5) are used to reconstruct the taphonomic history of the sauropod skeletons in quarry KU-WY-121. We hypothesize the cause of death, time of death, postmortem modification, and burial of the sauropod skeletons based on the condition and preservation of skeletons.

Necrology

Cause of death.—The cause of death for the sauropods from KU-WY-121 is unknown. Death could have been caused by predation, drowning in a flood, disease, or dehydration and starvation associated with drought. Predation is an unlikely cause of death for all the sauropods because one sauropod would have provided food for several carnivores, eliminating the need to kill multiple prey items at one time. A location where predators repeatedly kill animals one at a time should contain skeletons ranging from articulated fresh kills to widely disarticulated skeletal remains (Behrensmeyer and Boaz, 1983). Carnivores typically destroy or remove such small bones as phalanges and caudal vertebrae (Behrensmeyer and Boaz, 1980); this pattern is not observed in the skeletal remains. The smell or presence of a predator(s) at a recent kill site may also cause potential prey species to avoid the area (Werner, 1994).

Drought and disease commonly are invoked to explain the occurrence of multiple skeletons in fluvial or lacustrine deposits (e.g., Hasiotis et al., 1999). Disease is nearly impossible to prove without the presence soft tissue or the preservation of a chronic pathology within bones (Rothschild and Martin, 1993).

Circumstantial evidence is presented in the next sections that suggest drought was the most likely cause of death for the sauropods at KU-WY-121. The occurrence of dinosaurs in the quarry—comprised of three different sauropod species, two theropod species, and two ornithopods for a total of 12 dinosaur skeletons and other fragmentary dinosaur material—was likely concentrated at the same time based on the association of the skeletons and the sedimentology of the unit. This skeletal concentration may have resulted from these animals originally gathering at a known watering hole, particularly during a drought when all other water sources had been exhausted (Behrensmeyer and Boaz, 1980). The mostly articulated condition of the skeletons suggests that they where not transported far from where they had died. The close association of articulated limbs separated from the bodies likely indicates that the carcasses may have been desiccated before burial such that the drying process tightened the connective tissues of the limbs, vertebrae, and ribs. This process would have allowed the limbs to separate from the body as an articulated unit, whereas the ribs and vertebrae remained articulated (KUVP 129713).

There is no evidence to suggest that all the sauropods died and were buried in a catastrophic flood. It is unlikely that a *Camarasaurus* killed in such a high-energy event could be deposited with the hindlimbs folded underneath the body as if the animal laid down (KUVP 129716, Fig. 9B). The large *Camarasaurus* (KUVP 129113) could have been killed and overturned by a flash flood separate from the flooding event that later buried the other sauropods, however, there is no sedimentologic or paleontologic evidence to support this scenario. Cretaceous dinosaur assemblages interpreted to have resulted from flood-induced mass drowning during river crossing, which are highly

monospecific and the bones typically have fresh fractures that resulted during trampling and deposition (i.e., perimortem and postmortem) (Eberth and Getty, 2005). The skeletons from these types of bone bed assemblages remained wet, the carcass decomposed, and the remains were hydraulically sorted, with long bones—often with their ends missing—oriented with hydrologic flow. At the other end of the spectrum, skeletons associated with flood deposition may be disarticulated and the bones sorted into different Voorhies groups (e.g., Voorhies, 1969). The skeletons removed from KU-WY-121 do not fit either of these patterns.

Time of death.—The sauropods probably died during the dry season at or near their burial site based on (1) the amount of articulation of the sauropod skeletons and (2) the presence of traces on the sauropod bones similar to those produced by modern necrophagous insects associated with dry carcasses. The wet season is excluded as a time of death because rainfall and flooding would have prevented the desiccation of the carcasses and, therefore, excluded the bone modifying arthropods. In modern wet settings, mold growing on moist flesh rapidly kills dermestid beetles (Timm, 1982) as well as many other insects (Daly et al., 1998). Carcasses submerged in water would not have been accessible to terrestrial necrophagous arthropods, including those that modify bone (Payne and King, 1972; Byrd and Castner, 2001).

Biostratinomy

The sauropod skeletons likely went through the first three stages of decomposition (Table 5) because the fourth and final stage—dry stage—is represented by the shallow pits, rosettes, and hemispherical pits interpreted as dermestid-type bone

modification traces. Vertebrate scavengers and necrophagous arthropods likely fed on the carcass during all stages of decomposition. The vertebrate carnivores were likely overwhelmed by the surplus of carcasses and did not consume all of the available flesh nor would it have been necessary to tear apart and scatter the remains to obtain flesh (e.g., Behrensmeyer and Boaz, 1980). The initial moisture levels of the carcasses would have been high enough for such necrophagous insects as flies (Diptera—members of the Brachycera and possibly primitive members of the Eremoneura; Rasnitsyn and Quicke, 2002; Grimaldi and Engel, 2005) and beetles (Coleoptera—members of the Scarabaeoidea and Staphylinoidea; Rasnitsyn and Quicke, 2002; Grimaldi and Engel, 2005) to consume much of the flesh early after death—the fresh stage. Different groups of arthropod successions occupied the sauropod carcasses from the bloated stage to the advanced decay stage as the carcasses varied in moisture, gas content, and fermentation of the flesh (e.g., Smith, 1986).

Sauropod bones with borings on all sides were covered by skin and flesh and were either upright and off the ground due to bloating (e.g., Coe, 1978; West and Hasiotis, 2007) or propped up on other bones above the ground surface (e.g., Weigelt, 1989). Bones with borings found only on the upper surface were likely covered with skin and flesh, while the underside laid directly on the ground surface. Bones with borings found on the underside of bones where likely propped up on other bones above the ground surface or were rolled over onto the side with bone modification by other animals before or during the burial process.

The absence of insect traces on the bones from the juvenile *Camarasaurus* (KUVP 129714) deposited on the slope might be explained by one or more scenarios: (1)

vertebrate scavengers removed the limb bones and most of the soft tissue from the remainder of the carcass, restricting the distribution of necrophagous insects to dried flesh around the vertebrae or (2) the lower portion of the carcass was briefly covered by water that either killed the necrophagous insect larvae or forced the larvae to migrate to other portions of the carcass. Bite marks on the coracoid, ribs, and chevrons of juvenile *Camarasaurus* support the interpretation that carcass was scavenged; however, there is no evidence to support the scenario of partial submergence in water. Results of studies on vertebrate scavenging of carcasses also support scavenging of the juvenile *Camarasaurus*. Hill (1980) described the order of bone removal from medium- to large-sized mammal carcasses by vertebrate scavengers. The first bones removed were the forelimbs, followed by the mandibles, skull, hind limbs, and cervical vertebrae. The remaining vertebrae, sacrum, and ribs may be partially or fully articulated. The juvenile *Camarasaurus* skeleton likely represents the final stages in disarticulation by scavengers. If the soft tissue connecting the vertebrae, pelvic girdle, and ribs had decomposed before burial, then these bones would have also been disarticulated and scattered (e.g., Lyman, 1994).

The bone modification traces observed on the skeletons of KU-WY-121 suggest that the sauropod carcasses were likely subaerially exposed for ~7–14 weeks based on the modern study of arthropod successions on an elephant carcass in a tropical wet-dry climate (Coe, 1978). Approximately three weeks after the death of the sauropods, dermestids (or an arthropod with a similar behavior) colonized the dry carcasses and laid eggs that quickly hatched into necrophagous larvae. The larvae bored pupation chambers into the remaining dried flesh and bone approximately four weeks after hatching. Most

of the larvae pupated into adults approximately one week later, suggesting a total of about 8 weeks (56 days). One skeleton (KUVP 129713), however, has evidence for at least one other colonization of bone-modifying arthropods based on the presence of overlapping shallow pits and rosettes. This second set of borings suggests that an additional one to five weeks had passed in order for the next generation to construct pupation chambers. The range depends on when the next colonization event took place, which could have been shortly after the first, associated with the pupation period of the first group of colonizers, or much later. This assumes that enough flesh was still present on KUVP 129713 or that it remained attractive to the dermestids. A longer overall amount of time, closer to or slightly longer than 14 weeks, for the arthropod successions, however, is more likely because the cannibalistic behavior of dermestid larvae (as well as other necrophagous insects) would have prohibited development of eggs and larvae in the presence of larger, more mature larvae (e.g., Hinton, 1945; Timm, 1982).

An alternative and viable scenario to the simultaneous death of the sauropods and their arthropod successions is that KUVP 129713 perished first and began the stages of decomposition and arthropod successions. As the last stage was reached, the other animals arrived at this locality and died shortly afterward. As this next group of individuals went through the stages of decomposition and reached the dry stage and its arthropod succession, KUVP 129713 was colonized a second time.

A third and equally viable scenario to the sauropod death assemblage is that the diplodocid (skeleton KUVP 129717) perished first and well before the other sauropods, and that the others died in one or two closely related time periods. Most of the skeletal elements are missing from KUVP 129717 and were likely scattered by scavengers. The

pelvic girdle (sacrum, pubis, ischia, and ilia) and anterior caudal vertebrae are closely associated to life position and would have been the most difficult bones for the scavengers to disarticulate. It is also highly possible scavengers moved these bones to this area from nearby. The diplodocid bones also do not show evidence for transport or reworking by water. The diplodocid skeleton shows mostly stage 1 bone weathering characteristics with minor amounts of stage 2 characteristics (Behrensmeyer, 1978); therefore, the skeleton was present anywhere from < 1 to no more than 3 years. After the diplodocid bones were scattered, the other sauropods arrived and died in this locality as well. Either all sauropods died together (scenario 1) or that KUVP 129713 reached this area and died first, followed by the other sauropods that later perished (scenario 2).

This third scenario is likely the most parsimonious explanation for the highly disarticulated and poor condition of the diplodocid skeleton (KUVP 129717), as well as the overlapping bone-modification traces on the large *Camarasaurus* skeleton (KUVP 129713) compared to the non-overlapping traces of the other sauropods. This scenario, overall, suggests that the site contains skeletons that accumulated over approximately no more than 3.5 years, with the bulk of the skeletons contributed during the final 3 to 6 months. The reconstruction of the biostratinomy of KU-WY-121 is as follows: The diplodocid (KUVP 129717) died first, went through all the stages of decomposition, and was scattered over a 1- to 3-year period. After this period time, the large *Camarasaurus* (KUVP 129713) arrived and likely died of dehydration, starvation, a flash flood, or a combination of factors. It went through all the stages of decomposition and was going through bone modification when the other sauropods arrived and all died within a short period of time. As these sauropods went through all the decay stages to reach the dry

stage, both the large *Camarasaurus* (KUVP 129713) and these sauropods (KUVP 129714, -129716, and -129724) were attacked by bone-modifying insects. As a result, the skeleton of the large *Camarasaurus* (KUVP 129713) was modified by two generations of bone-modifying insects and the other sauropod skeletons were modified by only one generation of bone-modifying insects.

Burial and Early Diagenesis

The sauropod carcasses were likely buried by one depositional event or a series of related depositional events that deposited the mud and silt around the skeletons. Due to the limited outcrop exposure (see Fig. 8), it is difficult to determine whether deposition was associated with channel, overbank, crevasse-splay, or avulsive deposition. Nevertheless, the depositing current was not strong enough to move or sort any of the sauropod bones, which remained semiarticuled to weakly disarticulated with respect to their life positions.

After burial, sediments containing the sauropod skeletons were subaerially exposed and underwent pedogenesis for a short time. This is based on the lack of pedogenic features developed in the muddy sandstone encasing the bones (see Fig. 8), suggesting the formation of an entisol or protosol (e.g., Retallack, 2001). Evidence for short duration pedogenesis is in the form of rhizoetchings on the all the skeletons in the quarry and carbonate concretions on the diplodocid skeleton (KUVP 129717). Rhizoetchings were produced on surface of bones closest to the paleosurface, though this surface itself was not clearly evident in the quarry and no evidence of large and deep penetrative rhizoliths were observed in the outcrop. Calcium carbonate precipitated

around the vertebrae of the diplodocid and on the condyles of the femur, humerus, ulna, and radius. The carbonate was massive and grew from several areas on the bone and coalesced into one large concretion. This carbonate was likely deposited while the bones were in the phreatic zone rather than in the vadose zone. The diplodocid skeleton may have been more susceptible to carbonate precipitation because of its longer surface weathering history compared to the other bones in the quarry.

CONCLUSIONS

Quarry KU-WY-121 in the Upper Jurassic Morrison Formation in northeastern Wyoming preserves an assemblage of partially to fully disarticulated sauropod dinosaur skeletons with a complex taphonomic history not evident from the sedimentology or stratigraphy of the enclosing strata. Several lines of evidence were used to reconstruct the death, biostratinomy, and burial history of the quarry.

The sauropod skeletons contained more than 936 traces on bones that were categorized as (1) shallow pits, (2) rosettes, (3) hemispherical pits, (4) thin, curvilinear branching, grooves, and (5) U- to V-shaped linear grooves. Shallow pits, rosettes, and hemispherical pits are interpreted as several kinds of pupation chambers produced by either dermestid beetles (Coleoptera: Dermestidae) or by an unknown arthropod with no body fossil record that exhibited a behavior similar to that of extant dermestid beetles. Despite their origin, these traces likely represent the life cycle of a holometabolous insect. These traces were the most abundant of all traces on the sauropod bone, with hemispherical pits being least abundant of the three. Thin, curvilinear branching, grooves were likely produced by ancient roots chemically etching the bone surface after burial of

the sauropod carcasses, while the carcasses where in the vadose zone. Such etching patterns produced by the activity of ancient roots are referred to as rhizoetchings and are distinguishable from modern root etchings on bone. These traces were most abundant on sauropod bone surfaces closest to an inferred paleosurface. U- to V-shaped linear grooves are interpreted as bite marks produced either by a theropod or a crocodilian while feeding on the carcass. These traces were the least abundant of all the traces found on the sauropod bones.

Rosettes, shallow pits, and hemispherical pits were likely constructed during the dry phase of decomposition while the carcass was subaerially exposed. Rosettes are interpreted as an early stage in the construction of shallow pits. These trace fossils are interpreted as pupation chambers partially constructed in dried flesh and terminated against the sauropod bone. Hemispherical pits are interpreted to represent pupation chambers constructed entirely within sauropod bone. Both types of pupation chambers were likely sealed by the final molt of the larva prior to pupation, after which time an adult emerged to begin the lifecycle. Borings with similar size, shape, and width-to-depth ratios have been attributed to dermestid beetle activity in Jurassic and Neogene bones (Kitching, 1980; Martin and West, 1995; Hasiotis et al., 1999; West and Hasiotis, 2007).

If rosettes, shallow pits, and hemispherical pits represent the work of dermestid beetles, they would be further evidence of Dermestidae having a trace fossil record that is 50–60 million years (Ma) older than its body fossil record (e.g., Crowson, 1981; Laws et al., 1996; Hasiotis et al., 1999; Hasiotis, 2004; Grimaldi and Engel, 2005). The oldest body fossil record of dermestid beetles is in 90–100 Ma amber from Burma (Grimaldi

and Engel, 2005), which is the latest Early Cretaceous to earliest Late Cretaceous (Albian to lower Turonian). Identification of dermestid pupation chambers in the sauropod bones strongly suggests that these coleopterans were present in ecosystems by the Late Jurassic and played an important role in the detritivore nutrient cycling system (Aber and Melillo, 1991).

The application of forensics to taphonomic studies of a vertebrate skeleton was used to produce a detailed timeline for the time of death, modification of the carcasses by scavengers and detritivores, and final burial of the sauropod carcasses. The dinosaur skeletons, although partially disarticulated to fully disarticulated, could not be placed into any of the Voorhies groups because of the lack of evidence for water transport. The type, occurrence, and distribution of bone modification trace fossils and their association with the different sauropod skeletons suggests that the quarry represents several events. The diplodocid (KUVP 129717) died first and its remains were scattered over a 1- to 3-year period. Its bones were bored during that time period. After this event, the large *Camarasaurus* (KUVP 129713) died at this locality before the other sauropods arrived and died. This series of events is based on two generations of bone-modification traces that overlap on skeletal elements of the large *Camarasaurus* (KUVP 129713). The other sauropod skeletons (KUVP 129714, -129716, and -129724) contain only one generation of bone-modification traces, and hence, do not overlap. The sauropod skeletons were buried shortly afterward so that the sediments and skeletons underwent pedogenesis of short duration that produced an entisol or protosol. During this time the bones closest to the soil surface were etched by root activity. Calcium carbonate precipitated around

some of the diplodocid (KUVP 129717) skeletal elements while they were in the phreatic zone. The area was further buried underneath sediment by overbank deposition.

These events were initiated during the dry season, and were likely part of a prolonged drought based on our interpretation of the levels of articulation for each of the sauropod skeletons, bone modification features found on those skeletons, and previous interpretations of the Late Jurassic paleoclimate recorded by the Morrison Formation (Demko et al., 2004; Hasiotis, 2004; Turner and Peterson, 2004). The evidence suggests that sauropods were drawn to this area for its water availability over an extended period of time. Fossils of turtles, fish, crocodiles, snails, and bivalves support the notion of a relatively permanent body of water. A prolonged drought is thought to have occurred based on the different conditions of the sauropod skeletons, which suggest that the area was not resubmerged with differential burial of the skeletons. Only after all the sauropod skeletons accumulated, the soft tissue decomposed, and the bones were bored, did the drought end and the accumulation of skeletons was buried. A short duration of pedogenesis took place before additional sediments covered the area of the skeletons likely through a period of regular succession of wet-dry seasonal climates.

CHAPTER 3. ICHNOTAXONOMY OF INSECT TRACES AT KU-WY-121

Currently in review as:

BADER, K. S., and HASIOTIS, S. T., Insect borings in dinosaur bones from fluvial deposits in the Upper Jurassic Morrison Formation of northeastern Wyoming. *Journal of Paleontology*.

ABSTRACT

Two new ichnogenera and three new ichnospecies are described from sauropod bones collected from fluvial deposits in the Upper Jurassic Morrison Formation of northeastern Wyoming. *Osteogronos* n. igen. includes two ichnospecies, *O. hyposkytos* and *O. nyssa*, of circular to elliptical pits with a depth <0.5 mm bored into the outer surfaces of cortical bone. *Osteogronos nyssa* is distinguished from *O. hyposkytos* by the presence of an unmodified pedestal of bone in the center of the pit. A series of *O. nyssa* showing reduction in the diameter of the unmodified pedestals suggests that *O. nyssa* is an early stage in the construction of *O. hyposkytos*. The two ichnospecies of *Osteogronos* represent end members, each of which are abundant compared to the much rarer intermediate forms. *Osteokryptos entaphiopoles* n. igen. and isp. is a circular pit with a U-shaped cross section bored deeper than 0.5 mm into cortical bone. Transitional forms between *Ok. entaphiopoles* and *Osteogronos* have not been found. Similar trace fossils from the Plio-Pleistocene of North America and Africa are transferred to the ichnogenera *Cubiculum* to *Osteokryptos*. *Osteogronos* is interpreted as a pupation chamber

constructed primarily in dried flesh that surrounded the modified bone. The tracemaker bored through the flesh, reached the bone surface, and chewed into the bone in an inward spiral pattern until a shallow pit was completed. *Osteokryptos* is interpreted as a pupation chamber constructed completely within cortical bone. Body fossils of the tracemakers were not preserved; we interpret that the organisms were likely holometabolous insects with behaviors similar to modern dermestid beetles. Perhaps these borings represent the presence of the Dermestidae in the Late Jurassic, ~50–60 million years earlier than dermestid body fossils preserved in Burmese amber. [The ichnotaxonomic paper that defines these new ichnotaxa is currently under review; therefore, the names used here are unofficial and are used here informally].

INTRODUCTION

Trace fossils produced by necrophagous insects on bone are important tools for the investigation of the timing of death and the nature of postmortem modifications of a vertebrate carcass before burial (Martin and West, 1995; Hasiotis et al, 1999; West and Hasiotis, 2007). After death a carcass is recycled by arthropods, vertebrate scavengers, bacteria, and fungi. Forensic entomology studies the changes in the necrophagous arthropod community as a carcass decomposes (Payne, 1965). Rare components of modern and ancient necrophagous organism communities modify bone and leave a record of distinct traces (Table 1, 2). The presence of arthropod trace fossils on bone usually indicates that the vertebrate carcass desiccated and was subaerially exposed with intact soft tissue for an extended period of time before burial (Bader et al., in review). In this paper, we describe and name two new ichnogenera and three new ichnospecies from the

Upper Jurassic Morrison Formation that are interpreted as bone modification features produced by necrophagous insects on vertebrate carcasses.

Tracemaker	Description	Behavior	Reference
Coleoptera: Dermestidae: *Dermestes vulpinus* and *D. maculatus*	Damage to bone, wood, and metal., including pupation chambers and the focal destruction of cancellous bone from the condyles of limb bones.	Feeding and pupation	Gabel, 1955; Hefti et al., 1980; Timm, 1982; Bader, personal observation.
Coleoptera: Scarabaeidae: *Anoplognathus*	Damage to buried skeletons.	Unknown	Haglund, 1976
Isoptera: Termitidae: *Nasutitermes*, *Mastotermes*, and possibly other species.	Paired scratches and pits on bone surfaces. Enlargement of foramina and excavation of marrow cavities. All modifications occur in a stercoral-covered gallery. Ultimately, all bone covered in stercoral is completely destroyed.	Unknown, possibly dwelling	Wood, 1976; Thorne and Kimsey, 1983; Watson and Abbey, 1986; Wylie et al., 1987; Haynes, 1991; Tappen, 1994; Kaiser and Katterwee, 2001
Lepidoptera: Tineidae	Etch 2 mm-wide grooves in horn cores and straight-sided, cylindrical borings in bovid limb bones.	Dwelling and possibly pupation	McCorquodale, 1898; Behrensmeyer, 1975, 1978; Hill, 1987; Gautier, 1993
Insects, likely Isoptera, Coleoptera, or Lepidoptera	Cylindrical holes in bone.	Unknown	Newman, 1993
Unidentified insects; possibly Hymenoptera: Formicidae	Cylindrical pits and trails on bone surfaces	Pupation and feeding	Gautier, 1993
Nile Crocodile (*Crocodylus niloticus*)	Straight or J-shaped marks with U- to V-shaped cross sections, rounded pits and punctures	Feeding	Njau and Blumenschine, 2006
Roots	Sinuous branching grooves with U-shaped cross section, linear arrangements of pits	Extraction of nutrients	e.g. Binford, 1987; Ehrenreich, 1995
Fungi	Tunnels and grooves with U-shaped cross sections 1-100um in diameter	Extraction of Nutrients	e.g. Davis, 1997

Table 6. Review of modern traces etched into bone from continental environments.

Study	Time Interval	Description	Behavior	Interpretation
Tobien, 1965	Pliocene and Pleistocene	Grooves running parallel to bone surface (possibly *Cubiculum*)	Pupation	Coleoptera
Kitching, 1980	Plio-Pleistocene	Cylindrical burrows in long bones	Pupation	Coleoptera: Dermestidae
Watson and Abbey, 1986	Pleistocene	Paired scratch marks	Unknown	Isoptera: *Mastotermes*
Jodry and Stanford, 1992	Pleistocene	Enlargement of foramina, excavation of marrow cavities	Unknown	Insects, probably Coleoptera
Rogers, 1992	Late Cretaceous	Perforated bones.	Tunneling in soil	Coleoptera
Martin and West, 1995	Pleistocene	Test-tube shaped borings in horn core.	Pupation	Coleoptera: Dermestidae
Hasiotis et al., 1999; Hasiotis, 2004	Late Jurassic	Pits in bone surface.	Pupation	Coleoptera: Dermestidae
Paik, 2000	Cretaceous	Perforated bones and bone-chip filled burrows.	Tunneling in soil	Coleoptera
Kaiser, 2000	Plio-Pleistocene	Star-shaped scratches, grooves, and surface erosion	Unknown	Insects, possibly Isoptera
Kaiser and Katterwee, 2001	Plio-Pleistocene	Paired scratch marks	Unknown	Insects, possibly Isoptera
Fejfar and Kaiser, 2005	Oligocene	Star-shaped scratches, grooves, and surface erosion	Unknown	Isoptera
Roberts et al.., 2007	Late Cretaceous	*Cubiculum ornatus*: shallow, ellipsoidal hollows in bone covered with narrow grooves	Pupation	Necrophagous Insect
Roberts et al.., 2007	Late Cretaceous	*Osteocallis mandibulus*: shallow trail of narrow grooves	Feeding	Necrophagous Insect
Roberts et al.., 2007	Late Cretaceous	Tunnels in bone	Unknown	Necrophagous Insect
West and Hasiotis, 2007	Pleistocene	Oval pits	Pupation	Dermestid beetles
West and Hasiotis, 2007	Pleistocene	Scratches and scallops	Unknown	Insects, possibly Coleoptera
West and Hasiotis, 2007	Pleistocene	Tunnels, notches, channels	Tunneling in soil	Insects, possibly Coleoptera
Kirkland and Bader, 2007	Late Cretaceous	Destruction of condyles on limb bones and associated puparia in surrounding matrix	Feeding on buried carcasses	Coleoptera
Kirkland and Bader, 2007	Late Cretaceous	Cylindrical perforations in buried bones	Tunneling in soil	Coleoptera

Table 7. Review of fossil examples of insect-modified bone from continental paleoenvironments.

Roberts et al. (2007) named and described two insect trace fossils, *Osteocallis mandibulus* and *Cubiculum ornatus* from the Upper Cretaceous Kaiparowits Formation in Utah and the Upper Cretaceous Maevarano Formation in Madagascar. *Osteocallis mandibulus* is a shallow surface trail composed of narrow, arcuate grooves in cortical bone and is interpreted as a feeding or chewing trace produced by an insect. *Cubiculum*

ornatus is an ovoid hollow chamber bored into cortical or cancellous bone. The inside surfaces of the chamber are roughened by shallow, arcuate grooves. *Cubiculum* is interpreted as a pupation chamber of an osteophagous or necrophagous insect. Previously described Neogene bone modifications that are circular to elliptical in plan view (Tobien, 1965; Kitching, 1980; Martin and West, 1995) were referred to *Cubiculum* (Roberts et al., 2007). In this paper, we refine the definition of *Cubiculum* to include only the ovoid borings produced in and on dinosaur bones from the Late Cretaceous of Madagascar.

MATERIALS AND METHODS

In 1997, 1998, 2002, and 2004, the University of Kansas Division of Vertebrate Paleontology excavated six sauropod skeletons from a fluvial deposit in the Upper Jurassic Morrison Formation of northeastern Wyoming (KU-WY-121, Fig. 18); four of these skeletons were available for study. The skeletons range from mostly articulated to disarticulated. There is no evidence for fluvial transport of the remains based on the lack of sorting, winnowing, or alignment associated with the different types of Voorhies groups (Bader et al., in review). Preparation of the dinosaur skeletons revealed traces on bones interpreted as rhizoliths, bite marks from a carnivorous vertebrate, and three other distinct types of trace fossils etched into the outside surfaces of cortical bone: shallow pits, rosettes, and hemispherical pits.

The length, width, and depth of shallow pits (633), rosettes (103), and hemispherical pits (65) from four sauropod skeletons (KUVP 129713, 129714, 129716, 129717), the pes of a brachiosaur (KUVP 129724), and a brachiosaur manus were

measured using digital calipers to determine the range of size and variation in morphology of the traces. Examples of these traces were replicated by pouring GI-1000® silicon on the bone surface and using the resulting mold to create a Dyna-cast® plastic cast. The casts were examined and photographed under a LEO 1550 field emission scanning electron microscope (SEM) at the University of Kansas Biomedical Services Laboratory. The trace fossils and their casts are reposited at the University of Kansas Division of Vertebrate Paleontology (KUVP) and the University of Kansas Division of Invertebrate Paleontology (KUIMP).

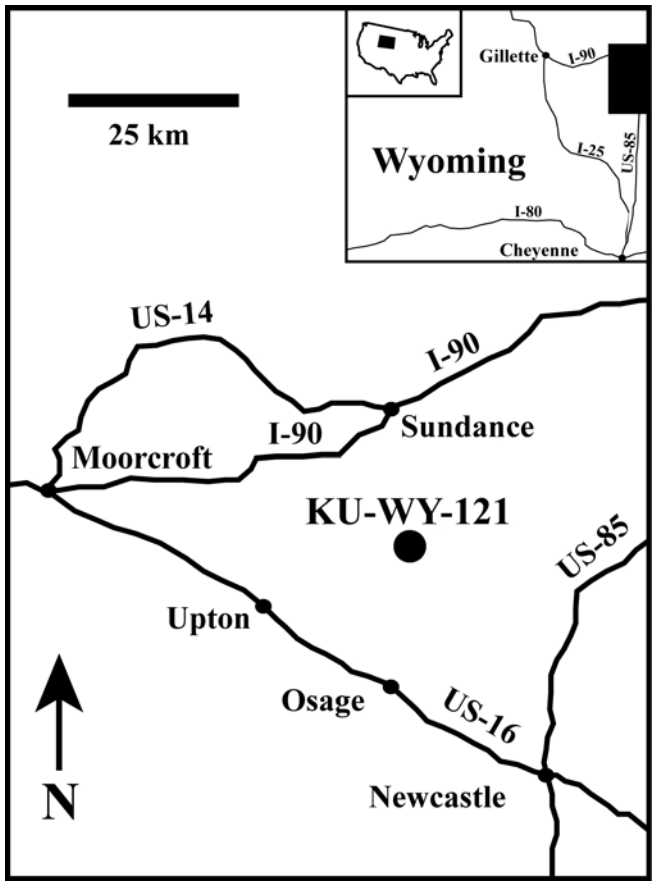

Figure 18. Location of the KU-WY-121 quarry in northeastern Wyoming.

GEOLOGICAL SETTING

The Upper Jurassic Morrison Formation is a 0–300m thick succession of mudstone, siltstone, sandstone, and limestone deposited in eolian, fluvial, lacustrine, and transitional marine environments during the Late Jurassic in the western interior of the United States and southern Canada (Peterson, 1994). The climate during Morrison deposition is interpreted to have ranged from Tropical Wet-Dry in the southern half of the basin to Mediterranean north of central Wyoming and likely alternated between wetter and drier years through the deposition of the Morrison Formation (Demko et al., 2004; Hasiotis, 2004).

In the Black Hills of northeastern Wyoming, the Morrison Formation conformably overlies the marine-deposited Middle Jurassic Sundance Formation and is unconformably overlain by the continental-deposited Lower Cretaceous Lakota Formation (Loomis, 1902; Watson, 1980). The KU-WY-121 quarry is located south of Sundance, Wyoming, in the Morrison Formation approximately 10 m below the contact with the Lakota Formation (Fig. 18–19). The fossil-bearing horizon is a gray mudstone with lenticular beds of sandstone, finely laminated mudstones and siltstones, and clay pebbles at the base. Fossils collected from the mudstone include nearly complete articulated to disarticulated and scattered remains of dinosaur skeletons, turtles, fish, crocodilian teeth, gastropods, bivalves, and plant remains. At the eastern edge of the quarry, the gray mudstone transitions upward into a purple mudstone containing carbonate nodules and rhizoliths ~96 cm above the base of the unit. The gray mudstone overlies a well-cemented gold sandstone bed that contains localized south-facing slopes, depressions, channels, and scours.

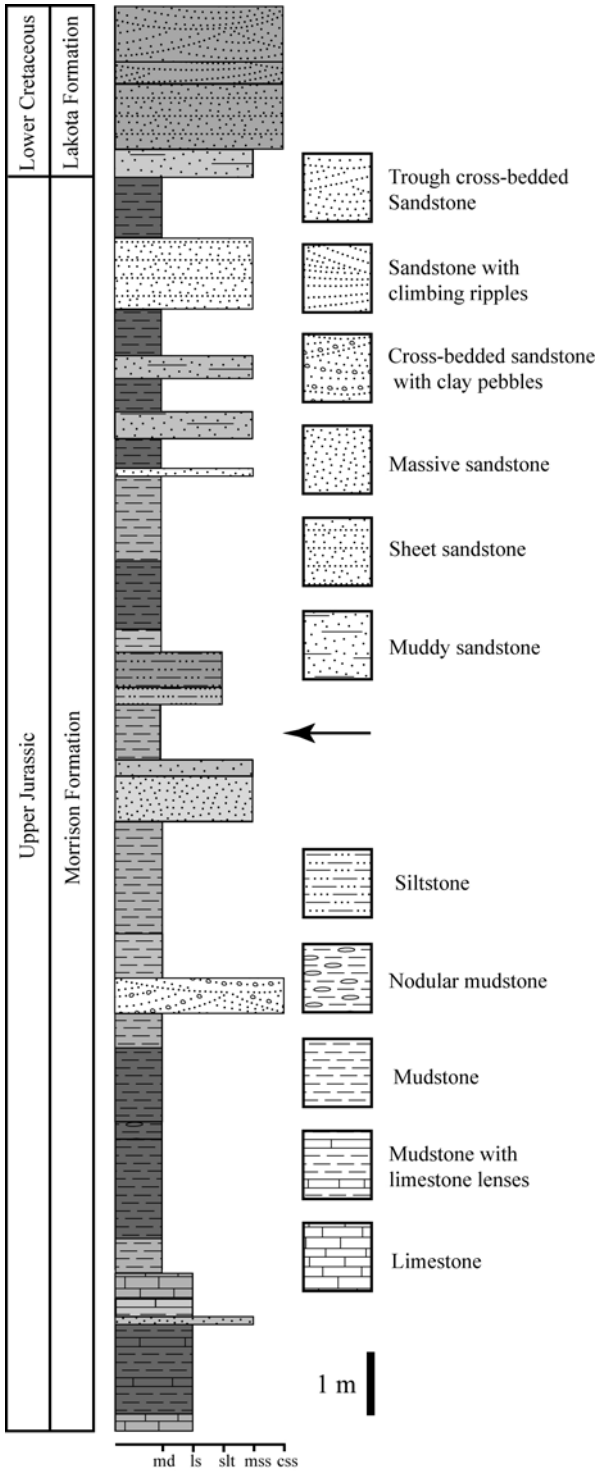

Figure 19. Composite stratigraphic section of the KU-WY-121 quarry. The quarry level is indicated by an arrow.

SYSTEMATIC ICHNOLOGY

Ichnogenus OSTEOGRONOS new ichnogenus

Type ichnospecies.—*Osteogronos hyposkytos* n. isp.

Diagnosis.—Shallow borings into external cortical bone surfaces that are circular to elliptical in plan view and have either smooth or scalloped edges with flat or concave walls that meet the floor of the trace at a 90° angle. The depth is less than 0.5 mm and the width-to-depth ratio ranges from 3.13–26.27. A central pedestal of unmodified bone may be present. These borings may be isolated or can be found in dense clusters with some of the borings overlapping.

Etymology.—*Osteo*- (Greek), bone; *gronos*- (Greek), hollowed out. Refers to the behavior of boring the trace into bone.

Discussion.—*Osteogronos* is clearly differentiated from ichnogenera designated for club-shaped borings in hardgrounds (Kelly and Bromley, 1984) and woodgrounds (Bromley et al., 1984). *Osteogronos* is readily distinguished from borings interpreted as marine organism behavior: *Gastrochaenolites* Leymerie, 1842; Teredolites Leymerie, 1842; *Palaeosabella* Clarke, 1921; *Trypanites* Magdefrau, 1932; *Rogerella* Saint-Seine, 1951; and *Petroxeses* Wilson and Palmer, 1988. *Osteogronos* is easily recognized from borings interpreted as continental organism behavior: *Anobichnium* Linck, 1949; *Cubiculum* Roberts et al., 2007; and *Osteocallis* Roberts et al., 2007. *Anobichnium* are small-diameter, smooth, vertical cylindrical borings that coalesce to form galleries preserved in petrified wood. *Cubiculum* is an ovoid, hollow chamber three to four times longer than wider with internal arcuate grooves. *Osteocallis* is an etched meandering

surface trail on the outer bone surface composed of arcuate grooves. *Osteogronos* is distinguished from *Osteokryptos*, which has a U-shaped cross section and penetrates > 0.5 mm into the cortical bone. *Osteogronos* has not been found associated with any bone chips, lined tunnels, backfilled burrows, and evidence for a stercoral layer covering the bones.

OSTEOGRONOS HYPOSKYTOS new ichnospecies

Fig. 20, Table 8

Diagnosis.—One of two ichnospecies known for this ichnogenus. A shallow pit-like boring in a bone surface that is circular to elliptical in plan view with smooth or scalloped edges and vertical walls oriented at right angles to the bottom of the trace, which is flat with subtle irregularities.

Description.—*Osteogronos hyposkytos* is a circular to elliptical trace in plan view with a depth less than 0.5 mm. The width of the trace ranges from 0.48–8.36 mm in diameter, and averages 2.80 mm (Fig. 20). The width-to-depth ratio ranges from 3.13–26.27, with an average ratio of 12.07. The walls of this trace may be smooth or scalloped and meet the bottom of the pit at an ~ 90^{o} angle. In plan view, each scallop is ~0.4 mm across (linear distance from the tips of a scallop) and forms an arc that is 0.1 mm at its greatest width.

Etymology.—*hypo-* (Greek), under; *skytos-* (Greek), hide or leather. Refers to the interpretation that this trace was bored into bone while dried skin and flesh remained on the carcass.

Type.—KUVP 147901, a copy is reposited in the KUMIP

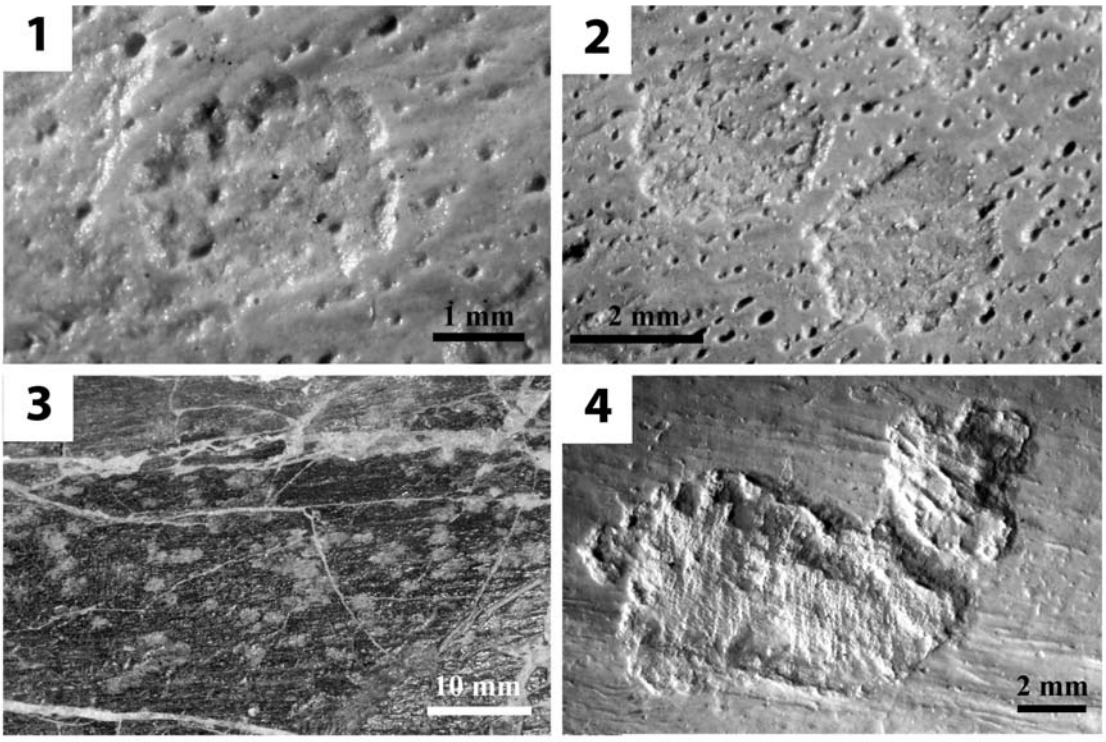

Figure 20. *Osteogronos hyposkytos* n. isp. from KU-WY-121. 1) Plan view of shallow pit from the left metatarsal IV of KUVP 129724. 2) Cluster of shallow pits from KUVP 129724. 3) Large cluster of shallow pits from the left femur of KUVP 129716. 4) Overlapping shallow pits from the scapula of KUVP 129713.

MEASUREMENT	RANGE	MEDIAN	MEAN	STANDARD DEVIATION
Length (mm)	0.92–8.36 mm	2.54 mm	2.80 mm	1.08
Width (mm)	0.48–6.43 mm	2.19 mm	2.34 mm	0.92
Depth (mm)	0.03–0.49 mm	0.26 mm	0.27 mm	0.13
Length/Depth	3.52–26.27 mm	12.1 mm	14.36 mm	7.89

Table 8. Summary of size data for *Osteogronos hyposkytos* from three sauropod skeletons (KUVP 129713, 129716, 129717), the brachiosaur pes (KUVP 129724), and brachiosaur manus from the KU-WY-121 quarry (n=633).

Occurrence.—*Osteogronos hyposkytos* is the most abundant trace fossil found on sauropod skeletons at the KU-WY-121 quarry collected from the upper part of the Morrison Formation. This trace may occur singly, in clusters of up to a hundred or more, or may overlap and form into large patches of modified bone. Single examples of *Osteogronos nyssa* (see description later) may occur in clusters of *O. hyposkytos*. *O. hyposkytos* is common on the ribs, chevrons, and limb bones from two *Camarasaurus* skeletons (KUVP 129713 and 129716) and the brachiosaur pes (KUVP 129724) and brachiosaur manus. This trace was present in low numbers on the ribs of a juvenile *Camarasaurus* (KUVP 129714) and a rib and scapula from the diplodocid skeleton (KUVP 129717).

Discussion.—*Osteogronos hyposkytos* is referred to as a shallow pit in Bader et al. (in review). *O. hyposkytos* has been found in association with *Osteogronos nyssa* and *Osteokryptos entaphiopoles* (see descriptions later) and rhizoetchings on all skeletons at KU-WY-121. It is also associated with a bite mark from a vertebrate scavenger on a gastralia from KUVP 129716.

This trace is distinguished from *Osteogronos nyssa* (see description later) by the absence of a central unmodified pedestal of bone. *O. hyposkytos* is also distinguished from *Osteokryptos* (see description later), which has a U-shaped cross section and penetrates to a greater depth into the cortical bone. *Cubiculum* is much larger in all dimensions and is elliptical in plan view with arcuate grooves inside the trace.

OSTEOGRONOS NYSSA new ichnospecies

Fig. 21, Table 9

Diagnosis.—The second of two ichnospecies known for this ichnogenus. A shallow, circular ring of modified bone surrounding an unmodified pedestal of bone. This trace may be found singly, in clusters, or may overlap and are rarely found on bones with *Osteogronos hyposkytos*, with a few notable exceptions.

Description.—*Osteogronos nyssa* is a shallow ring of modified bone that encompasses a region of unmodified bone referred to as the pedestal. The outer and inner walls of the ring are scalloped and the outer wall is undercut into the surrounding bone. The outside diameter of *O. nyssa* averages 2.00–6.00 mm in width and the pedestal diameter averages 0.33–3.92 mm. The depth of the trace is less than 0.5 mm. The width-to-depth ratio is 6.56–16.21, with an average ratio of 11.14. The scallops have the same dimensions as scallops of *O. hyposkytos*. The diameter of the pedestal does not vary in proportion to the outside diameter of the trace.

Etymology.—*nyssa*- (Greek), turning post. Refers to the central unmodified pedestal of bone around which the insect chewed in a spiral pattern.

Type.—KUVP 147902, a copy is reposited in the KUMIP

Occurrence.—All examples of *Osteogronos nyssa* are found on sauropod skeletons at the KU-WY-121 quarry in the upper part of the Morrison Formation. *O. nyssa* is abundant on the ribs, scapulae, sternal plates, and limb bones of a *Camarasaurus* (KUVP 129713). This ichnofossil is usually found in large clusters with individual traces that overlap rarely.

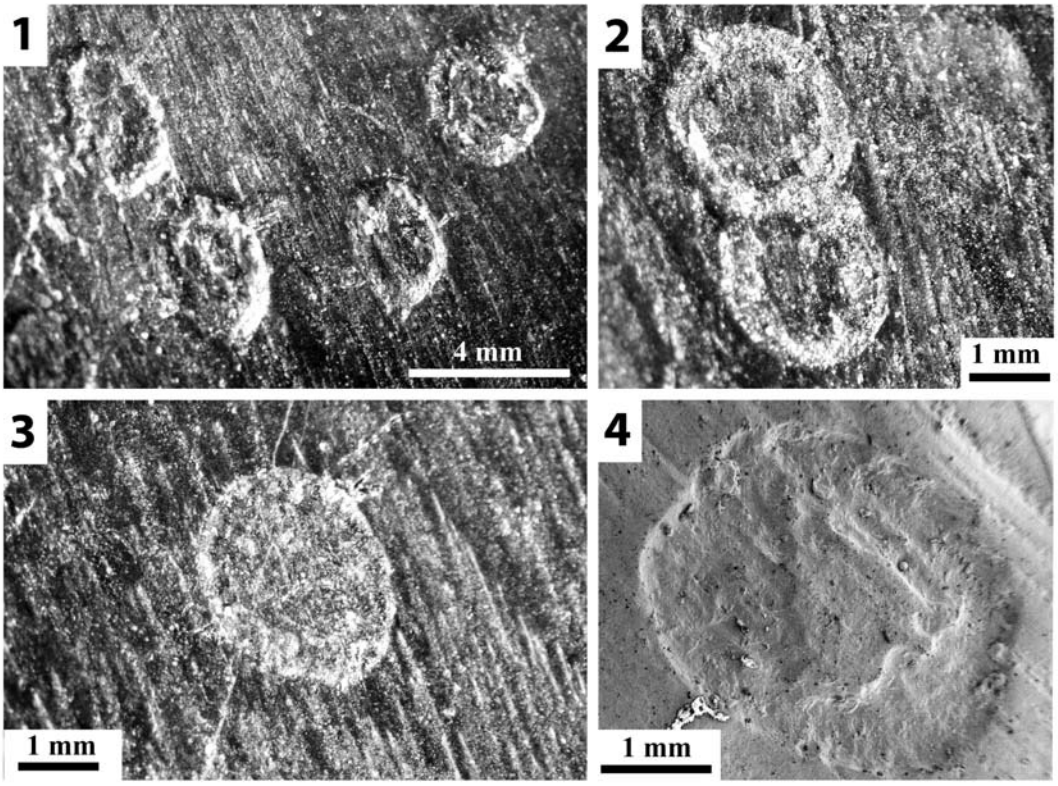

Figure 21. *Osteogronos nyssa* n. isp. from KU-WY-121. 1) Cluster of rosettes from a rib head of KUVP 129713. 2) Overlapping rosettes from the same bone as 1. 3) Rosette cut by a crack from KUVP 129713. 4) SEM or the type of *Osteogronos nyssa*, from a rib head of KUVP 129713.

MEASUREMENT	RANGE	MEDIAN	MEAN	STANDARD DEVIATION
Outer Length (mm)	1.56–8.38 mm	3.61 mm	3.95 mm	1.49
Outer Width (mm)	1.51–7.66 mm	3.08 mm	3.39 mm	1.41
Inner Length (mm)	0.33–6.76 mm	2.43 mm	2.61 mm	1.26
Inner Width (mm)	0.6–6.27 mm	1.87 mm	2.19 mm	1.22
Depth (mm)	0.04–0.49 mm	0.3 mm	0.29 mm	0.16
Length/Depth	6.56–16.21	13.68	10.69	23.32

Table 9. Summary of size data for *Osteogronos nyssa* from two *Camarasaurus* skeletons (KUVP 129713, 199716) and the diplodocid skeleton (KUVP 129717) at the KU-WY-121 quarry (n=103).

Discussion.—*Osteogronos nyssa* is referred to as a rosette in Bader et al. (in review). This trace is found in association with *Osteogronos hyposkytos* and *Osteokryptos entaphiopoles* n. isp. (see description later) on the ribs of KUVP 129713. Single examples of *O. nyssa* have been found within clusters of *O. hyposkytos* on the ribs from a second *Camarasaurus* (KUVP 129716) and diplodocid (KUVP 129717).

This trace is distinguished from *O. hyposkytos* by the presence of an unmodified central pedestal of bone. There are only two examples of *Osteokryptos entaphiopoles* that contain thin, remnants of bone superficially similar to pedestals in *O. nyssa*. These features may have been pedestals at one time; however, there are no intermediate forms to show a progression in the excavation of shallow pits with pedestals to deep U-shaped pits without pedestals.

Osteogronos nyssa is interpreted as an early stage in the construction of shallow pits assigned to *O. hyposkytos*. The two ichnospecies of *Osteogronos* represent two dominant morphologies, each of which are very abundant compared to the much rarer intermediate forms. For this reason, each is assigned to two different ichnospecies. If there were equal numbers of intermediate forms between *O. nyssa* and *O. hyposkytos*, then only one ichnotaxon would have been used to describe the range of morphologies.

Borings characterized as very shallow hemispherical pits and those with remnants of unmodified bone within pits found on a variety of sauropod, *Stegosaurus*, and *Allosaurus* bones in the Carnegie Quarry at Dinosaur National Monument (DNM), Utah (Hasiotis 2004; fig. 13C, F), can be placed into *Osteogronos nyssa* and *O. hyposkytos*. These borings are circular and very shallow; however, some preserve very fine striations

parallel to the curvature of the boring or have slightly deeper groove in the base of the boring.

Ichnogenus *OSTEOKRYPTOS* new ichnogenus

Type ichnospecies.—*Osteokryptos entaphiopoles* n. isp.

Diagnosis.—A vertically oriented, hemispherical or U-shaped pit greater than 0.5 mm in depth that is circular to slightly elliptical in plan view and has smooth walls. This trace occurs in clusters or as isolated individuals in cortical bone.

Etymology.—*Osteo*- (Greek), bone; *kryptos*- (Greek), hiding place or lair. Refers to the interpretation that an organism constructed the trace for protection from predators while it pupated.

Discussion.—*Osteokryptos* has only been identified in continental deposits and is easily distinguished from traces produced in hard materials in marine environments: *Gastrochaenolites* Leymerie, 1842; Teredolites Leymerie, 1842; *Palaeosabella* Clarke, 1921; *Trypanites* Magdefrau, 1932; *Rogerella* Saint-Seine, 1951; and *Petroxeses* Wilson and Palmer, 1988. *Osteokryptos* is distinguished from other continental insect traces in bone, including *Cubiculum*, by its vertically oriented, U-shaped or hemispherical morphology that lacks shallow, arcuate grooves. *Osteokryptos* differs from *Osteogronos*, which does not penetrate as deep into the cortical bone surface and has vertical walls that meet the flat base at a 90° angle. Transitional forms between *Osteogronos* and *Osteokryptos* have not been found on the dinosaur skeletons at KU-WY-121. *Osteokryptos* has not been found associated with any bone chips, lined tunnels, backfilled burrows, and evidence for a stercoral layer covering the bones.

OSTEOKRYPTOS ENTAPHIOPOLES new ichnospecies

Fig. 22, Table 10

Diagnosis.—Same as for the ichnogenus.

Description.—*Osteokryptos* is circular to elliptical in plan view and has a U-shaped cross section. The diameter is 1.98–5.63 mm, averaging 4.19 mm on KUVP 129713 and 3.19 mm on KUVP 129716. The depth is 0.62–1.74 mm, averaging 0.96 mm, and the width-to-depth ratio is 1.92–4.52 with an average of 3.52. The walls are smooth, without scallops or arcuate grooves. Two examples from a rib head of a *Camarasaurus* (KUVP 129713) contain thin columns of unmodified bone, each 57% of the total diameter of the trace.

Etymology.—*Entaphiopoles* (Greek), undertaker. Refers to the inferred necrophagous behavior of the insect that constructed this trace.

Type.—KUVP 147903, a copy is reposited in the KUMIP

Occurrence.—The holotype was collected from the KU-WY-121 quarry in the Morrison Formation. This trace is present in small clusters on the rib heads and sternal plate of one large *Camarasaurus* (KUVP 129713) and the dorsal vertebrae of a second *Camarasaurus* (KUVP 129716).

Discussion.—*Osteokryptos entaphiopoles* is referred to as a hemispherical pit in Bader et al. (in review). *Osteokryptos entaphiopoles* is associated with shallow pits on the sternal plates and both shallow pits and rosettes on a rib head from KUVP 129713. The hemispherical pits do not overlap other traces. *Osteokryptos entaphiopoles* is not associated with any other traces on the dorsal vertebrae of KUVP 129716.

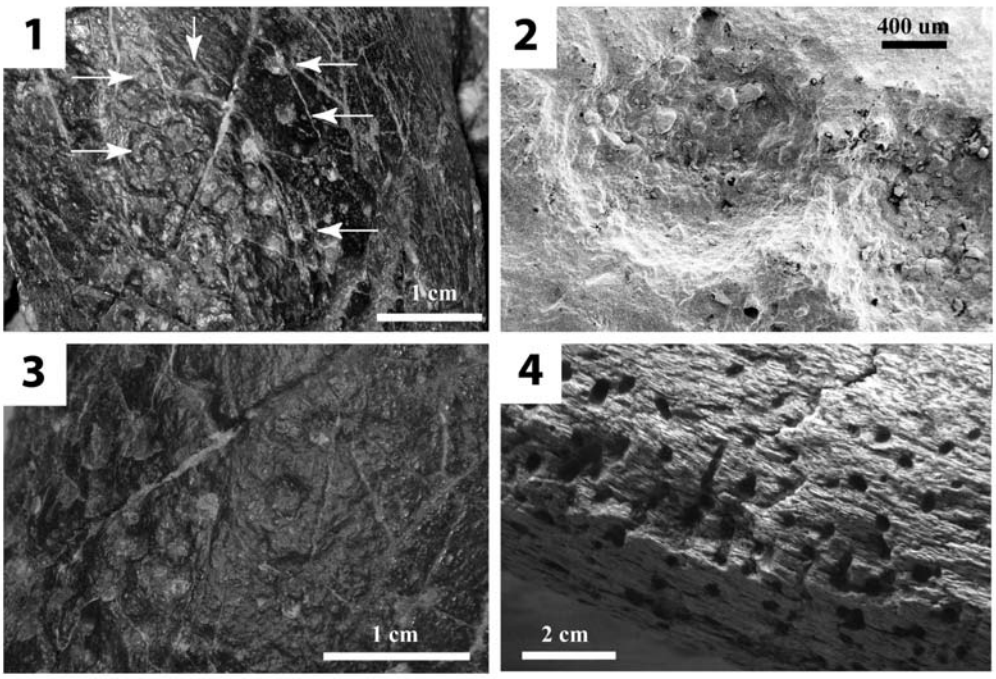

Figure 22. *Osteokryptos entaphiopoles* n. isp. 1) Cluster of hemispherical pits from dorsal 6 of KUVP 129716. 2) SEM of hemispherical pit from the sternal plate of KUVP 129713. 3) Hemispherical pit from dorsal 6 of KUVP 129716. 4) Cluster of dermestid borings in the horn core of a *Bison latifrons*, KUVP 201.

MEASUREMENT	RANGE	MEDIAN	MEAN	STANDARD DEVIATION
Length (mm)	2.51–5.63 mm	3.66 mm	3.88 mm	1.18
Width (mm)	1.98–4.97 mm	3.13 mm	3.48 mm	1.19
Depth (mm)	0.62–1.74 mm	1.02 mm	0.96 mm	0.32
Length/Depth	1.92–4.52 mm	3.63	3.52	1.17

Table 10. Summary of size data for *Osteokryptos entaphiopoles* from two *Camarasaurus* skeletons (KUVP 129713, 199716) at the KU-WY-121 quarry (n=65).

Roberts et al. (2007) referred hemispherical traces in bone from the Neogene of the United States, Africa, and Europe (Tobien, 1965; Kitching, 1980; Martin and West, 1995) to the ichnogenus *Cubiculum*. Unlike the ellipsoidal *Cubiculum*, traces described by Kitching (1980) and Martin and West (1995) are hemispherical with U-shaped cross sections and the surfaces are not covered by shallow, arcuate grooves. These traces are morphologically identical to *Osteokryptos* and should, instead, be referred to this ichnogenus. Traces found on the right horn core of a *Bison latifrons* (Fig.22; Martin and West, 1995) were bored into cancellous bone, not cortical bones as with the other occurrences of *Osteokryptos*. Ellipsoidal traces described by Tobien (1965) are oriented parallel to the bone surface may represent a Neogene example of *Cubiculum*–like behavior, but lack the characteristic arcuate grooves seen in *C. ornatus*.

Some of the borings in dinosaur bones reported by Hasiotis et al. (1999) and Hasiotis (2004) from a variety of bones of sauropods, *Stegosaurus*, and *Allosaurus* in the Carnegie Quarry at Dinosaur National Monument (DNM), Utah, can be placed into *Osteokryptos entaphiopoles* based on the hemispherical morphology of pits. The majority of these types of borings at DNM are relatively smooth walled.

INTERPRETATION OF THE TRACEMAKERS

Osteogronos and *Osteokryptos* are interpreted as pupation chambers bored into bone by the larva of a necrophagous insect (Bader et al., in review). The most likely tracemaker is a dermestid beetle larva (Coleoptera: Dermestidae) based on comparisons with modern examples of arthropod borings in bone and wood (Table 6 and references therein). Some other arthropod, however, may have produced these traces with a

behavior similar to that of modern dermestids but left no body fossil record of its existence. Dermestids are the primary candidate for the tracemakers because their larvae are known to feed on the dried flesh and bone of subaerially exposed carcasses during the dry stage of decomposition (Payne et al, 1968; Payne and King, 1970; Payne and King, 1972) and to bore pupation chambers into any available compact material, including dried flesh and bone (Hinton, 1945; Gabel, 1955; Timm, 1982; West and Hasiotis, 2007). Dermestids are not attracted to carcasses that are submerged in water or buried (Payne et al., 1968; Payne and King, 1972), and do not feed on moist carcasses (Timm, 1982; Byrd and Castner, 2001). High moisture levels in a carcass promote fungal growth, which is lethal to many insects including dermestid beetles (Timm, 1982; Daly et al., 1998). After approximately four weeks of feeding during the dry stage of carcass decomposition (Payne, 1965), a dermestid larva bores a pupation chamber that is circular in plan view with a U-shaped cross section (Martin and West, 1995; West and Hasiotis, 2007). Pupation is completed after about one week and an adult emerges to begin the life cycle again (Hinton, 1945).

Osteogronos is interpreted as a pupation chamber constructed in dried flesh and partially in cortical bone. A larva likely bored a hole into the dried flesh of a carcass until it reached bone. It chewed an inward spiral pattern into the bone surface until a shallow pit was produced; this morphology of boring is assigned to *O. hyposkytos*. If the chewing process was interrupted or discontinued, a pedestal of unmodified bone remained in the center of the boring; this morphology of boring is assigned to *O. nyssa*. Overlapping borings are interpreted as the result of pupation chambers constructed by multiple generations of insects while dried flesh covered the bone surface.

Osteokryptos entaphiopoles is interpreted as a pupation chamber constructed almost entirely within cortical bone. The tracemaker chewed a downward spiral pattern into bone, producing a smooth-walled, U-shaped hemispherical pit. The thin column of bone found in only two examples of *Osteokryptos* is likely an artifact from the construction of each boring, analogous to the unmodified pedestal of bone found in *O. nyssa*.

Other necrophagous or osteophagous arthropods were also considered as possible tracemakers of these bone borings, however, they were rejected based on their extant association with carcasses as well as the differences in their trace morphologies in or associated with bone. Silphid and histerid beetles (Coleoptera: Silphidae and Histeridae) feed primarily on the larvae of such necrophagous insects as fly maggots (Steele, 1927; Payne and King, 1970; Smith, 1986), and have not been observed to feed on or damage bone. Scarab beetle larva (Coleoptera: Scarabaeidae) may damage the cancellous bone of buried skeletons (Haglund, 1976); no actual bone modification was observed—these beetles were found with the skeletons, including the damage portions. Such damage as illustrated in Haglund (1976) is morphologically distinct from the boring morphologies of *Osteogronos* and *Osteokryptos*.

Tineid moth larvae (Lepidoptera: Tineidae) are known to feed on the keratin sheaths of horns and hooves. The larvae modify bone to construct dwelling spaces near their food resources or to construct pupation chambers (McCorquodale, 1898; Behrensmeyer, 1978; Hill, 1987). Trace fossils on dinosaur bones from KU-WY-121 do not match the morphology of tineid larval borings, nor are the borings restricted to areas

that would have been covered by thick layers of keratin, such as bones near the skin surface and the phalanges (Bader et al., in review).

Termites (Isoptera) have been reported to damage bone surfaces long after carcasses were completely stripped of flesh and disarticulated (Derry, 1911; Wood, 1976; Behrensmeyer, 1978; Thorne and Kimsey, 1983; Wylie et al, 1987; Haynes, 1991; Tappen, 1994). Termites build walls of stercoral (e.g. Hasiotis, 2003) to cover the bone surface being modified (Derry, 1911). Under the protection of the stercoral, termites destroy the bone surface by incising small round pits in a linear pattern (Tappen, 1994); these pits are expanded to remove the cortical as well as cancellous bone (Haynes, 1991). Only the portion of the bone covered by stercoral is destroyed (Thorne and Kimsey, 1983). Such patterns of damage are dissimilar in morphology to that represented by *Osteogronos* and *Osteokryptos*.

Britt et al. (2005) and Dangerfield et al. (2005) have suggested that termites produced the borings assigned to *Osteogronos* and *Osteokryptos* on Late Jurassic dinosaur bones in the Morrison Formation described by Laws et al. (1996), Hasiotis et al. 1999), and Hasiotis (2004). *Osteogronos* and *Osteokryptos* have not been found associated with any evidence of stercoral on the dinosaur bones, nor have the borings been found with bone chips, or lined tunnels.

The surficial boring patterns assigned to *Osteocallis mandibulus* Roberts et al. 2007 from the Upper Cretaceous Kaiparowits Formation (Utah, U.S.A.) and Maevarano Formation (Madagascar), however, are very similar to the bone modification patterns produced by termites in laboratory experiments reported in Watson and Abbey (1986) and in Kaiser and Katterwe (2001). Termites produced trails of shallow borings on bone

surfaces characterized by paired grooves, each with a steep U- to V-shaped cross section, with a ridge structure where the two grooves met. Similar patterns of modification have also been observed underneath tunnels of stercoral on concrete building walls in Tanzania (Fig. 23; Hasiotis, personal observation, 2004). *Osteocallis mandibulus* Roberts et al. 2007, therefore, is attributed to damage by foraging termites based on the evidence presented here, observed in the field, and presented in Watson and Abbey (1986) and in Kaiser and Katterwe (2001).

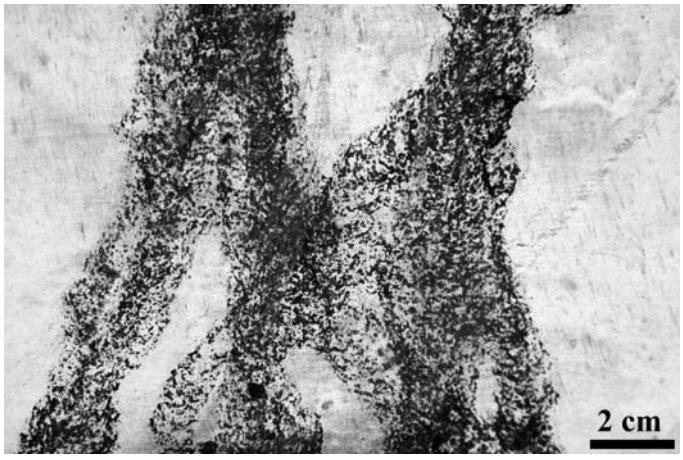

Figure 23. Exposed termite damage to a concrete wall in Tanzania after the associated stercoral covering was removed.

CONCLUSION

Two new ichnogenera and three new ichnospecies of borings represent bone-modification features in preserved on sauropod skeletons collected from fluvial deposits in the Upper Jurassic Morrison Formation of northeastern Wyoming. *Osteogronos* has two ichnospecies, *O. hyposkytos* and *O. nyssa*. Both are shallow (<0.5 mm) pits that are

circular to slightly elliptical in plan view. The two species are distinguished by the presence of an unmodified pedestal of bone in the center of *O. nyssa* and the absence of this structure in *O. hyposkytos*. *O. nyssa* appears to be an early stage in the production of *O. hyposkytos*, based on a series of *O. nyssa* showing reduction in the diameter of unmodified pedestals. Both borings occur as isolated individuals or in dense clusters, and form two distinct morphologic end members with very few intermediates. *Osteokryptos entaphiopoles* is a deep (>0.5 mm) hemispherical pit with a U-shaped cross section. Rare specimens may have a thin, unmodified pedestal of bone. *Osteokryptos entaphiopoles* is found usually in loose clusters, but may be found as isolated specimens. Transitional forms between *Osteokryptos entaphiopoles* and the ichnospecies of *Osteogronos* have not been found.

Osteogronos, *Osteokryptos*, and morphologically similar borings found on other Jurassic dinosaur bones (Laws et al., 1996; Hasiotis et al., 1999; Hasiotis, 2004) as well as on Neogene bones from Africa and North America (Kitching, 1980; Martin and West, 1995) are distinct morphologically from other traces on bone, including *Cubiculum ornatus* Roberts et al. 2007 and *Osteocallis mandibulus* Roberts et al 2007. The Neogene trace fossils are transferred from the ichnogenus *Cubiculum* to *Osteokryptos entaphiopoles*.

Osteogronos and *Osteokryptos entaphiopoles* are interpreted as pupation chambers constructed within desiccated and subaerially exposed carcasses by dermestid beetle larvae (Coleoptera: Dermestidae) or by some other arthropods with a similar necrophagous behavior to that exhibited by modern dermestids. Such an arthropod does not have a fossil record to date. We favor the interpretation *Osteogronos* and *Ok*.

entaphiopoles as borings by dermestid beetle larvae because their excavation of pupation chambers has clearly been linked to the destruction of various hard materials, including concrete, hardwood, metal, and bone (Gabel, 1955; Timm, 1982; West and Hasiotis, 2007). Regardless of the identification of the tracemaker, the borings likely overall represent the pupation chamber of holometabolous insects, because tineid moths and some scarab beetles have life stages associated with bone modification as larvae. Such an interpretation is parsimonious with the holometabolous life cycle because the pupation requires a place that is secluded, protected, and provides support (e.g., Smith, 1986; Daley et al., 1998; Byrd and Castner, 2001).

If constructed by dermestid beetles, *Osteogronos* and *Osteokryptos entaphiopoles* represent the extension of the fossil record of the Dermestidae by 50–60 million years (Ma). The earliest known body fossil of a dermestid is a larva preserved in 90–100 million-year-old amber from Burma (Grimaldi and Engel, 2005). The extension of the fossil record of the Dermestidae (Insecta: Coleoptera) based on the Late Jurassic borings in dinosaur bone is plausible since the earliest known body fossil is nearly identical to extant dermestid larva, which are exclusively necrophagous in their feeding and reproductive behavior (Hinton, 1945; Timm, 1982).

Identification of these borings in sauropod bones, as well as in other dinosaur bones, strongly suggests that arthropods fed on desiccated, subaerially exposed dinosaur carcasses and pupated either in dried flesh (*Osteogronos hyposkytos* and *O. nyssa*) or in cortical bone (*Osteokryptos entaphiopoles*) during the Late Jurassic. Regardless if the bone-modifying organisms were members of the Dermestidae or some unknown group of holometabolous insect, these organisms played an important role detritivore nutrient

cycling system (e.g., Aber and Melillo, 1991; Byrd and Castner, 2001) in the Late Jurassic (Hasiotis et al., 1999; Hasiotis, 2004; Bader et al., in review).

Osteocallis mandibulus Roberts et al. 2007 described from dinosaur bones in the Upper Cretaceous Kaiparowits Formation (Utah, U.S.A.) and Maevarano Formation (Madagascar) are reinterpreted as bone damage by foraging termites. Reinterpretation is based on evidence of extant termite activity associated with bones and other calcareous-based material (Watson and Abbey, 1986; Kaiser and Katterwe, 2001; Hasiotis, personal observations, 2004). *Osteocallis mandibulus* likely represents the removal of bone for nitrogen (e.g., Prestwich et al., 1980) and other nutrients. This specific relationship between termites and carcasses, however, has not yet been demonstrated in modern ecosystems though it has been proposed by Thorne and Kimsey (1983) and Watson and Abbey (1986). This reinterpretation is significant because it is the first to recognize the ancient association between termites and bone, and documents the role of ancient termites in the detritivore nutrient cycle. The termite-bone interaction preserved in the Late Cretaceous deposits likely took place well after flesh was removed from the carcasses (e.g., Coe, 1978; Watson and Abbey, 1986) and either while the bones were still at the surface or after shallow burial (e.g., Smith, 1986).

CHAPTER 4. CONCLUSION

The application of the study of forensic entomology to taphonomic studies greatly improves the ability to determine the season of death and the relative amount of time that had passed between death and final burial. Most necrophagous insects feed on soft tissue, which restricts the study of forensic entomology in paleontology to rare examples of insect-modified bones (Table 2–3). A series of sauropods, ranging from partially to mostly disarticulated were collected at the KU-WY-121 quarry in the Upper Jurassic Morrison Formation. Preparation revealed five distinct types of trace fossils—shallow pits, rosettes, hemispherical pits, bite marks, and rhizoetchings. Shallow pits, rosettes, and hemispherical pits are identified as pupation chambers constructed in dried flesh and bone by a holometabolous insect. These traces are morphologically similar to traces found on dinosaur bones from Dinosaur National Monument (Hasiotis et al., 1999; Hasiotis, 2004).

Two new ichnogenera and three new ichnospecies are described for the insect traces from KU-WY-121 (Chapter 3). *Osteogronos hyposkytos* is assigned to the shallow pits and *O. nyssa* is assigned to the rosettes. *Osteokryptos entaphiopoles* is assigned to the hemispherical pits. Identical pits from the Neogene of Africa and North America are transferred from *Cubiculum* to *Ok. entaphiopoles*. [The ichnotaxonomic paper that defines these new ichnotaxa is currently under review; therefore, the names used here are unofficial and are used here informally].

The carcasses were likely in the dry stage of decay and were subaerially exposed when the shallow pits, rosettes, and hemispherical pits were constructed. Shallow pits and rosettes are the remnants of pupation chambers that were constructed in dried flesh and

terminated against bone. Rosettes are interpreted as an early stage in the production of shallow pits. Hemispherical pits are pupation chambers that were constructed entirely within bone. Each necrophagous insect larva likely bored a downward spiral pattern until the pupation chamber was complete and sealed the entrance with its final larval molt before beginning pupation. After the pupation period, an adult insect emerged, reproduced, and laid eggs. If enough dried flesh was still available, a second generation of larvae fed on the carcass and bored pupation chambers into the remaining flesh and bone.

The most likely tracemaker of the pupation chambers is a dermestid beetle (Coleoptera: Dermestidae), based on comparisons with trace constructed by modern bone-modifying insects, or they were constructed by a holometabolous insect with a necrophagous behavior similar to that of modern dermestids. Dermestid larvae feed on subaerially exposed dry flesh and bone during the dry stage of carcass decomposition (Hinton, 1945; Payne, 1965). After ~4 weeks of feeding, the larvae bore pupation chambers into dried flesh, bone, wood, or any other available compact material (Gabel, 1955; Timm, 1982). The oldest body fossil of a dermestid beetle is that of a modern-appearing larva in 90–100 Ma Burmese amber (Grimaldi and Engel, 2005). If the insect traces in bone represent dermestid beetle pupation chambers, the fossil record of the Dermestidae would be extended by 50–60 million years (Crowson, 1981; Grimaldi and Engel, 2005).

Arthropod traces are found on every type of bone at KU-WY-121; however, they are most common on the ribs, chevrons, and limb bones. The arthropod traces are restricted in distribution on the diplodocid (KUVP 129717) and the juvenile *Camarasaurus* (KUVP 129714). It is likely that the arthropod traces on the diplodocid

were destroyed by rhizoetching after the skeleton was buried. The unique absence of arthropod traces from portions of the juvenile *Camarasaurus* skeleton (KUVP 129714) that are on and below the slope and the presence of shallow pits on bones at the top of the slope could represent a permanent or temporary water level. This phenomenon will be addressed after preparation commences on the brachiosaur and the final *Camarasaurus* skeletons.

Forensic entomology and taphonomic studies are combined to create a timeline for the death, subaerial exposure, and burial of the sauropod skeletons (Chapter 2). The diplodocid (KUVP 129717) died first, desiccated, and its skeleton was scattered approximately 1 to 3 years before the other dinosaurs. Necrophagous arthropod bored into its bones during this period of time. The large *Camarasaurus* (KUVP 129713) died second, probably early in the dry season. Its carcass desiccated and was bored by the first generation of arthropod before the other *Camarasaurus* (KUVP 129714 and 129716) arrived at the locality and died. The carcasses of these two *Camarasaurus* desiccated and were bored by necrophagous arthropod while the large *Camarasaurus* carcass was bored by a second generation of insects. This timeline is based on the presence of overlapping pits on KUVP 12913 and the absence of overlapping pits on the other skeletons. Approximately 14 weeks after the large *Camarasaurus* died, the skeletons were buried by a flooding event that did not have a strong enough current to transport the sauropod bones. The enclosing sediment underwent pedogenesis and bones closest to the surface (KUVP 129717) were etched by roots and encased in calcium carbonate concretions.

It is likely that the sauropods died after accumulating around a permanent or semipermanent body of water during an extended dry season or drought. An exact cause

of death is unknown; it is possible that the sauropods died from starvation, dehydration, or disease. It is also likely that the large *Camarasaurus* died at the end of the previous wet season and was deposited upside-down by a flash flood. The interpretation of seasonal precipitation and flooding is consistent with previous interpretations of a Tropical Wet-Dry to Mediterranean climate during Morrison deposition (Demko, et al, 2004; Hasiotis, 2004; Turner and Peterson, 2004). Three to four months of dry weather are required for the carcasses to desiccate and for at least two generations of bone-modifying insects to bore pupation chambers into the sauropod bones. The dry season ended after pupation of the second generation of insects when the locality was flooded and the skeletons were buried.

FUTURE INVESTIGATIONS

Insect-bone interaction studies should be expanded to investigate the effect of such other potential tracemakers as carrion and scarab beetles (Coleoptera: Silphidae and Scarabaeidae). Arthropod-damaged dinosaur skeletons from the Upper Cretaceous of Mongolia should be described in detail for the type and distribution of damage to the skeletal elements, as well as their relationship with the sedimentary succession to determine the timing of bone-modification (Kirkland and Bader, 2007).

REFERENCES

ABER, J.D., and MELILLO, J.M., 1991. *Terrestrial Ecosystems*. Saunders College Publishing, Philadelphia, 430 pp.

ANDREWS, P., 1990, Owls, Caves, and Fossils. The University of Chicago Press, 231 p.

BEHRENSMEYER, A.K., 1975, The Taphonomy and paleoecology of the Plio-Pleistocene vertebrate assemblages of Lake Rudolf, Kenya: Bulletin of the Museum of Comparative Zoology, v. 146, p. 473–578.

BEHRENSMEYER, A. K., 1978, Taphonomic and ecologic information from bone weathering: Paleobiology, v. 4 (2), p. 150–162.

BEHRENSMEYER, A. K., and BOAZ, D. E. D., 1980, Recent Bones of Amboseli National Park, Kenya: *in* Behrensmeyer, A. K., and Hill, A. P. eds., Fossils in the Making: Vertebrate Taphonomy and Paleoecology: University of Chicago Press, Chicago, p. 72–92.

BINFORD, L. R., 1981, Bones: Ancient Men and Modern Myths, Academic Press: New York, 320 p.

BORNEMISSZA, G. F., 1957, An analysis of arthropod succession in carrion and the effect of its decomposition on the soil fauna: Australia Journal of Zoology, v. 5, p. 1–12.

BRITT, B. B., SCHEETZ, R. D., and DANGERFIELD, A., 2005, Insect burrows and borings on Upper Jurassic (Morrison Formation) dinosaur bones: Geological Society of America Abstracts with Programs, v. 37(7), p. 443.

BUSCK, A., 1910, Notes on a horn-feeding lepidopterous larva from Africa: Smithsonian Miscellaneous Collections, v. 56(8), p. 1–2.

BYRD, J. H. and CASTNER, J. L. (eds.), 2001. Forensic Entomology—The Utility of Arthropods in Legal Investigations. CRC Press, Boca Raton, 418 p.

CARPENTER, K., 2000, Evidence of predatory behavior by carnivorous dinosaurs: Gaia, v. 15, p. 135–144.

COE, M., 1978, The decomposition of elephant carcasses in the Tsavo (East) National Park, Kenya: Journal of Arid Environments, v. 1, p. 71–86.

CROWSON, R. A., 1981, The Biology of the Coleoptera: Academic Press, New York. 802 p.

DALY, H. V., DOYEN, J. T., and PURCELL, A. H., 1998, Introduction to insect biology and diversity: Oxford University Press, Oxford, 675 p.

DANGERFIELD, A., BRITT, B., SCHEETZ, R., and PICKARD, M., 2005, Jurassic dinosaurs and insects: the paleoecological role of termites as carrion feeders: Geological Society of America Abstracts with Programs, v. 37 (7), p. 443.

DAVIS, P. G., 1997, The bioerosion of bird bones: International Journal of Osteoarchaeology, v. 7, p. 388-401.

DEMKO, T.M., CURRIE, B.S., and NICOLL, K.A., 2004, Regional paleoclimatic and stratigraphic implications of paleosols and fluvial-overbank architecture in the Morrison Formation (Upper Jurassic), Western Interior, USA.: Sedimentary Geology, v. 167, p. 115-136.

DERRY, D. E., 1911, Damage done to skulls and bones by termites: Nature, v. 86(2164), p. 245-246.

DEYRUP, M., DEYRUP, N. E., EISNER, M., AND EISNER, T., 2005, A caterpillar that eats tortoise shells: American Entomologist, 51(4), p. 245–248.

EBERTH, D.A, and GETTY, M.A., 2005, Ceratopsian bonebeds: occurrence, origins, and significance, *in* Currie, P.J. and Koppelhus, E.B., eds., Dinosaur Provincial Park. Indiana University Press, Bloomington, 648 p.

EHRENREICH, R. M, 1995, Archaeometry into Archaeology: Journal of Archaeological Method and Theory, v. 2(1), p. 43–44.

FEJFAR, O., and KAISER, T. M., 2005, Insect bone-modification and paleoecology of Oligocene mammal-bearing sites in the Doupov Mountains, northwestern Bohemia: Palaeontologia Electronica, v. 8(1).

FURNISS, R. L., and CAROLIN, V. M., 1977, Western Forest Insects: U.S. Department of Agriculture Forest Service, Miscellaneous Publication No. 1339.

GABEL, H. H., 1955, Beitrag zur Kenntnis der Biologie des Speckkafers *Dermestes vulpinus* F: Zeitschrift fur Angewandte Entomologie, v. 37, p. 153–191.

GAUTIER, A., 1993, Trace fossils in archaeozoology: Journal of Archaeological Science, v. 20, p. 511–523.

GRIMALDI, D., and ENGEL, M. S., 2005, Evolution of the Insects: Cambridge University Press, Cambridge, 755 p.

HACKETT, C. J., 1981, Microscopical focal destruction (tunnels) in exhumed human bones: Medicine, Science and the Law, v. 21, p. 243–265.

HAGLUND, L., 1976, An archaeological analysis of the Broadbeach Aboriginal burial ground: University of Queensland Press, St. Lucia, Queensland, 118 p.

HASIOTIS, S. T., 2002. *Continental Trace Fossils*. SEPM, Short Course Notes Number 51, Tulsa, Oklahoma, 132 p.

HASIOTIS, S. T., 2003. Complex ichnofossils of solitary to social soil organisms: understanding their evolution and roles in terrestrial paleoecosystems. Palaeogeography, Palaeoclimatology, Palaeoecology, v. 192, p. 259-320.

HASIOTIS, S.T., 2004, Reconnaissance of Upper Jurassic Morrison Formation ichnofossils, Rocky Mountain Region, USA: paleoenvironmental, stratigraphic, and paleoclimatic significance of terrestrial and freshwater ichnocoenoses: Sedimentary Geology, v. 167, p. 177–268.

HASIOTIS, S.T., FIORILLO, A. R., and HANNA, R. R., 1999, Preliminary report on borings in Jurassic dinosaur bones: Evidence for invertebrate-vertebrate interactions, *in* Gillette, D. G., ed., Vertebrate paleontology in Utah: Miscellaneous Publication – Utah Geological Survey, 99-1; p. 193–200.

HAYNES, G., 1991, Mammoths, mastodonts, and elephants: Biology, behavior, and the fossil record: Cambridge University Press, Cambridge 427 p.

HEFTI, E., TRECHSEL, U., RUFENACHT, H., and FLEISCH, H., 1980, Use of dermestid beetles for cleaning bones: Calcified Tissue International, v. 31, p. 45–47.

HILL, A. P., 1980, Early postmortem damage to the remains of some contemporary east African mammals, *in* Behrensmeyer, A. K., and Hill, A. P., eds., Fossils in the Making: Vertebrate Taphonomy and Paleoecology: Chicago, University of Chicago Press, p. 131–152.

HILL, A. P., 1987, Damage to some fossil bones from Laetoli, *in* Leakey, M. D., and Harris, J. M., eds., Laetoli: A Pliocene Site in Northern Tanzania: Oxford, Clarendon Press, p. 543–545.

HINTON, H. E., 1963, A monograph of the beetles associated with stored products: British Museum of Natural History, p. 234–401.

JODRY, M. A., and STANFORD D. J., 1992, Stewart's Cattle Guard site: an analysis of bison remains in a Folsom kill-butchery campsite, *in* Stanford, D. J., and Day, J. S. eds., Ice Age Hunters of the Rockies: University Press of Colorado, Niwot, p. 101–168.

KAISER, T. M., 2000, Proposed fossil insect modification to fossil mammalian bone from Plio-Pleistocene hominid-bearing deposits of Laetoli (Northern Tanzania): Annals of the Entomological Society of America, v. 93(4), p. 693–700.

KAISER, T. M., and KATTERWE, H., 2001, The application of 3D-Microprofilometry as a tool in the surface diagnosis of fossil and sub-fossil vertebrate hard tissue: an example from the Pliocene Upper Laetolil Beds, Tanzania: International Journal of Osteoarchaeology, v. 11, p. 350–356.

KIRKLAND, J. I., AND BADER, K., 2007, Insect scavenging of a Protoceratops carcass preserved in the Upper Cretaceous Djadoktha Formation, Tugrikin Shireh, Mongolia: Ceratopsian Symposium, p. 83–89.

KITCHING, J. W., 1980, On some Arthropoda from the Limeworks, Makapansgat, Potgietersrus: Palaeontologia Africana, v. 23, p. 63–68.

LAWS, G. R., HASIOTIS, S. T., FIORILLO, A., CHURE, D., BREITHAUPT, B. H., and HORNER, J. 1996. The demise of a Jurassic dinosaur after death - three cheers for the dermestid beetle. Geological Society of America National Meeting, Denver, Colorado, v. 28(7), p. 299.

LOOMIS, F. B., 1902, On Jurassic Stratigraphy on the west side of the Black Hills, Second paper on American Jurassic Stratigraphy: Bulletin of the American Museum of Natural History, v. 16(31), p. 401–407.

LYMAN, R. L., 1994, Vertebrate Taphonomy: Cambridge University Press, Cambridge, 550 p.

MARTIN, L. D., and WEST, D. L., 1995, The recognition and use of dermestid (Insecta: Coleoptera) pupation chambers in paleoecology: Paleogeography, Paleoclimatology, Paleoecology, v. 113. p. 303-310.

MCCORQUODALE, W. H., 1898, Horn-feeding larvae: Nature, London, v. 58(1493), p. 140–141.

NICHOLS, G., 1999, Sedimentology and Stratigraphy: Blackwell Science Ltd., Oxford, 355 p.

NEWMAN, R. A., 1993, The incidence of damage marks on Swartkrans fossil bones from the 1978-1986 excavations, *in* Brain, C. K., ed., Swartkrans: A Caves Chronicle of Early Man: Transvaal Museum Monograph, p. 217–228.

NJAU, J. K., and BLUMENSCHINE, R. J., 2006, A diagnosis of crocodile feeding traces on larger mammal bone, with fossil examples from the Plio-Pleistocene Olduvai Basin, Tanzania: Journal of Human Evolution, v. 50, p. 142–162.

PAIK, I. S., 2000, Bone chip-filled burrows associated with bored dinosaur bone in floodplain paleosols of the Cretaceous Hasandong Formation, Korea: Palaeogeography, Palaeoclimatology, Palaeoecology, v. 157, p. 213–225.

PAYNE, J. A., 1965, A summer carrion study of the baby pig *Sus scrofa* Linnaeus: Ecology, v. 46(5), p. 592–602.

PAYNE, J. A., KING, E. W., and BEINHART, G., 1968, Arthropod succession and decomposition of buried pigs: Nature, v. 219, p. 1180–1181.

PAYNE, J. A., and KING, E. W., 1970, Coleoptera associated with pig carrion: Entomologist's Monthly Magazine, v. 105, p. 224–232.

PAYNE, J. A., and KING, E. W., 1972, Insect succession and decomposition of pig carcasses in water: Journal of the Georgia Entomological Society, v. 7(3), p. 153–162.

PETERSON, F., 1994, Sand dunes, sabkhas, streams, and shallow seas: Jurassic paleogeography in the southern part of the Western Interior Basin, *in* Caputo M.V., Peterson, J.A., and Franczyk, K.J. eds., Mesozoic Systems of the Rocky Mountain Region, USA: Rocky Mountain Section, Society for Sedimentary Geology (SEPM), Denver, CO, p. 233–272.

PIEPENBRINK, H., 1986, Two examples of biogenous dead bone decomposition and their consequences for taphonomic interpretation: Journal of Archaeological Science, v. 13, p. 417–430.

PRESTWICH, G. D., BENTLEY, B. L., and CARPENTER, E. J., 1980, Nitrogen sources for Neotropical Nasute termites: fixation and selective foraging: Oecologicia, v. 46, p. 397–401.

RASNITSYN, A.P. and QUICKE, D.L.J., 2002, History of Insects: Kluwer Academic Publishers, Dordrecht, 517 p.

RETALLACK, G.J., 2001. Soils of the Past, 2nd edition, Blackwell Science, Oxford, 404 pp.

ROBERTS, E. M., ROGERS, R. R., and FOREMAN, B. Z., 2007, Continental insect borings in dinosaur bone: examples from the Late Cretaceous of Madagascar and Utah: Journal of Paleontology, v. 81(1), p. 201–208.

ROGERS, R. R., 1992, Non-marine borings in dinosaur bones from the Upper Cretaceous Two Medicine Formation, northwestern Montana: Journal of Vertebrate Paleontology, v. 12(4), p. 528–531.

ROBINSON, G. S., and NIELSEN, E. S., 1993, Tineid genera of Australia (Lepidoptera): Monographs of Australian Lepidoptera, v. 2, East Melbourne, Victoria, Australia 344 p.

ROTHSCHILD, B.M. and MARTIN, L.D. 1993. *Paleopathology: Disease in the Fossil Record*. CRC Press, London, 386 p.

SMITH, K.G. V., 1986. A Manual of Forensic Entomology. Cornell University Press, Ithaca New York, 205 p.

SOGNNAES, R. F., 1955, Postmortem microscopic defects in the teeth of ancient man: AMA Archives of Pathology, 59, p. 559–570.

STEELE, B. F., 1927, Notes on the feeding habits of carrion beetles. Journal of the New York Entomological Society, v. 35, p. 77–81.

TAPPEN, M., 1994, Bone weathering in the tropical rain forest: Journal of Archaeological Science, v. 21, p. 667–673.

THORNE, B. L., and KIMSEY, R. B., 1983, Attraction of neotropical *Nasutitermes* termites to carrion: Biotropica, v. 15(4), p. 295–296.

TIMM, R. M., 1982, Dermestids: Field Museum of Natural History Bulletin, v. 53, p. 14–18.

TOBIEN, H., 1965, Insekten-FraBspuren an tertiaren und pleistozanen Saugetier-Knochen: Senckenbergiana lethaea, v. 46a, p. 441–451.

TURNER, C.E., and PETERSON, F., 2004. Reconstruction of the Upper Jurassic Morrison Formation extinct ecosystem—a synthesis: Sedimentary Geology, v. 167, p. 309-355.

VOORHIES, M. R., 1969, Taphonomy and population dynamics of an Early Pliocene vertebrate fauna, Knox County, Nebraska: Contributions to Geology, Special Paper No. 1, University of Wyoming, 69 p.

WATSON, J. A. L., and ABBEY, H. M., 1986, The effects of termites (Isoptera) on bone: some archeological implications: Sociobiology, v. 11(3), p. 245–254.

WATSON, J. E., ed., 1980, Catalog of Wyoming Stratigraphy: Tooke Engineering Co, Inc. 350 p.

WEIGELT, J., 1989, Recent vertebrate carcasses and their paleobiological implications: University of Chicago Press, Chicago, 187 p.

WERNER, E. E., 1994, Individual behavior and higher-order species interactions: in Real, L. A., ed., Behavioral Mechanisms in Evolutionary Ecology: The University of Chicago Press, Chicago, p. 297–326.

WEST, D. J. and HASIOTIS, S. T., 2007, Trace Fossils in an Archaeological Context: Examples from Bison Skeletons, Lipscomb County, Texas, U.S.A. The trace-fossil record of vertebrates: *in* Miller, W., III ed., Trace Fossils—Concepts, Problems, Prospects: Elsevier Press, p. 545–561.

WEST, D. L., and MARTIN, L. D., 2002, Insect trace fossils as environmental/taphonomic indicators in archaeology and paleoecology, *in* Dort, W., ed., TER-QUA Symposium, 3, p. 163–173.

WOOD, W. B., 1976, The skeletal material from the Brooloo Range and Rocky Hole Creek burial sites: Archaeology and Physical Anthropology in Oceania, v. 11(3), p. 175-185.

WYLIE, F. R., WALSH, G. L., and YULE, R. A., 1987, Insect damage to aboriginal relics at burial and rock-art sites near Carnarvon in central Queensland: Journal of the Australian Entomological Society, v. 26, p. 335–345.

APPENDIX

TABLES OF TRACE FOSSIL MEASUREMENTS FROM KU-WY-121

Approximately 803 traces (635 shallow pits, 103 rosettes, and 65 hemispherical pits) were measured using digital calipers. The length of a trace is defined as the greatest diameter of a trace in plan view. The width of a trace is measured perpendicular to the length.

Key to Tables—All measurements were taken in millimeters. Length[1] and Width[1] refer to the outside diameter of shallow pits and rosettes. Length[2] and Width[2] refer to the diameter of the unmodified pedestal of bone in rosettes. The length/depth ratio is measured using the outside diameter of the trace. Deep, hemispherical pits are designated as Deep Pits. Abbreviations: Ant.=Anterior, Cau.=Caudal, Dis.= Distal, Dor.=Dorsal, D-L=Dorsolateral surface, D-M= Dorsomedial surface, L.=Left, Lat.=Lateral, Med.=Medial, Pos.=Posterior, Pro.=Proximal, R.=Right, Sec.=Section, Sur.=Surface, Ven.=Ventral, Ver.=Vertebra, L=Ventral/lateral surface.

KUVP 129713—Examination of the large adult *Camarasaurus* was restricted to surfaces that had been prepared at Science City in 2006 and 2007 and resulted in the discovery of 328 traces: 92 rosettes, 16 hemispherical pits, and 220 shallow pits. Unfortunately, individual ribs were not assigned field numbers and were collected in ~30 cm sections that were poorly labeled. An attempt has been made to identify these ribs before preparation is completed and the fragments are reassembled. Two deep pits from

the lateral surface of a rib head contain thin, unmodified columns of bone. These deep pits are indicated by: Deep Pit*.

Element	Morphology	Length[1]	Width[1]	Length[2]	Width[2]	Depth	Length/Depth Ratio
Rib Head	Rosette	5.76	4.01	2.3	1.28	0.3	19.2
	Rosette	4.27	2.65	3.22	1.47	0.39	10.95
	Rosette	3.78	1.51	3.02	0.96	0.48	7.88
	Rosette	3.42	1.68	2.92	0.97	0.32	10.69
	Rosette	3.35	1.73	2.57	0.78	0.39	8.59
	Rosette	3.64	1.63	3.27	1.17	0.27	13.48
	Rosette	3.08	2.07	2.78	1.93	0.19	16.21
	Rosette	5.83	4.16	4.1	2.8	0.42	13.88
	Rosette	2.9	2.17	2.82	1.95	0.34	8.53
	Rosette	2.58	1.67	2.18	1.75	0.4	6.56
	Rosette	3.15	2.08	3.06	1.96	0.48	6.56
	Rosette	2.75	2.02	2.79	1.62	0.4	6.88
	Rosette	4.38	2.38	3.41	1.71	0.48	9.13
	Rosette	3.98	1.9	2.95	1.25	0.26	15.31
	Rosette	3.9	2.53	2.88	1.87	0.34	11.47
R. Rib, Prox. Shaft, Lat. Surface	Rosette	3.57	2.78	1.88	1.4		
	Rosette	2.63	2.62	1.42	1.04		
	Rosette	3.12	2.84	2.43	1.42		
	Rosette	5.51	3.67	3.92	2.34		
	Rosette	3.42	3.06	2.2	1.67		
	Rosette	3.93	2.86	3.23	2.35		
	Rosette	2.71	2.4	2.26	2.16		
	Rosette	2.81	2.52	2.02	1.74		
	Rosette	2.69	2.47	2.3	1.89		
	Rosette	2.77	2.29	2.03	1.35		
	Rosette	2.96	2.1	2.09	1.89		
	Rosette	2.45	2.36	1.92	1.6		
	Rosette	3.57	2.85	2.43	2.08		
	Rosette	4.05	2.66	2.07	1.49		
	Rosette	3.5	3.73	3.23	3.22		
R. Rib, Prox. Shaft, Lat. Surface	Shallow Pit	2.74	2.41				
	Shallow Pit	2.9	2.74				
	Shallow Pit	2.81	2.55				
	Shallow Pit	2.92	3.26				
	Shallow Pit	2.6	2.93				
	Shallow Pit	2.31	2.23				
	Shallow Pit	3.36	2.56				
	Shallow Pit	2.75	2.5				
	Shallow Pit	1.66	1.59				
	Shallow Pit	2.16	2.79				
	Shallow Pit	2.68	2.57				
	Shallow Pit	2.99	2.36				
	Shallow Pit	3.5	2.63				
	Shallow Pit	3.62	3.15				
	Shallow Pit	2.29	1.85				
	Shallow Pit	2.33	2.06				
	Shallow Pit	2.98	2.76				
	Shallow Pit	2.76	2.25				
	Shallow Pit	1.98	2.74				
	Shallow Pit	1.73	2.29				

Element	Morphology	Length[1]	Width[1]	Length[2]	Width[2]	Depth	Length/Depth Ratio
R. Rib, Prox. Shaft, Lat. Surface	Shallow Pit	2.05	2.47				
	Shallow Pit	2.63	1.86				
	Shallow Pit	1.54	2.19				
	Shallow Pit	2.26	2.78				
	Shallow Pit	2.49	2.6				
	Shallow Pit	2.06	2.53				
	Shallow Pit	3.01	2.55				
	Shallow Pit	2.74	3				
	Shallow Pit	3.22	2.64				
	Shallow Pit	2.27	1.77				
R. Rib, Prox.Shaft, Med. Surface	Shallow Pit	4.35	3.81				
	Shallow Pit	1.61	1.62				
	Shallow Pit	3.21	4.48				
	Shallow Pit	1.99	1.99				
	Shallow Pit	1.82	1.74				
	Shallow Pit	2.08	2.07				
	Shallow Pit	2.44	2.44				
	Shallow Pit	2.71	2.23				
	Shallow Pit	1.98	2.22				
	Shallow Pit	1.63	1.43				
Right Rib #6, Lat. Surface	Rosette	5.54	5.18	2.3	2.04	0.7	79.14
	Rosette	2.73	2.34	1.57	1.53		
	Rosette	4.72	4.13	2.1	1.8	0.89	5.30
	Shallow Pit	2.62	2.48				
	Shallow Pit	2.9	2.44				
	Shallow Pit	3.42	3.29				
	Shallow Pit	4.53	3.52				
	Shallow Pit	2.75	2.69				
	Shallow Pit	3.1	2.88				
	Shallow Pit	2.4	1.8				
	Shallow Pit	1.91	1.69				
	Shallow Pit	2.54	2.51				
	Shallow Pit	2.19	2.05				
	Shallow Pit	2.59	1.65				
	Shallow Pit	3.24	2.92				
	Shallow Pit	3.28	2.86				
	Shallow Pit	2.3	2.02				
	Shallow Pit	2.05	1.81				
	Shallow Pit	1.62	1.4				
	Shallow Pit	2.08	2.02				
Right Rib #6, Ant. Surface	Rosette	2.33	1.71	1.38	1.29		
	Shallow Pit	3.37	3.11				
Rib Head, Lat. Surface	Deep Pit*	4.59	5.29	2.74	2.58		
	Deep Pit*	4.31	4.97	2.47	3.13		
	Deep Pit	5.59	5.63				
	Deep Pit	2.33	2.36				
	Deep Pit	3.08	3.57				
	Deep Pit	2.91	3.16				
	Deep Pit	4.66	5.42				
	Deep Pit	3.89	4.62				
	Deep Pit	3.7	4.36				
Rib Head, Ant. Surface	Deep Pit	4.31	4.97				
Rib Head, Med. Surface	Shallow Pit	4.6	3.68				
	Shallow Pit	2.21	2.92				
	Shallow Pit	3.37	3.7				
L. Scapula, D-L Surface	Rosette	5.6	3.8	3.7	3.37		
	Rosette	5.5	4.01	4.45	3.55		

Element	Morphology	Length[1]	Width[1]	Length[2]	Width[2]	Depth	Length/Depth Ratio
L. Scapula, D-L Surface	Rosette	4.74	4.23	2.69	1.82		
	Rosette	7.87	6.55	5.62	4.98		
	Rosette	4.67	4.1	2.78	2.49		
	Rosette	3.58	3.52	1.79	1.72		
	Rosette	6.42	6.3	4.08	4.77		
	Rosette	4.28	3.47	2.86	2.55		
	Rosette	4.62	3.79	3.15	3.08		
	Rosette	4.14	4.16	3.65	3.11		
	Rosette	4.9	4	3.71	3.45		
	Rosette	2.33	2.34	1.46	1.31		
	Rosette	2.53	2.16	1.71	1.43		
	Rosette	8.38	7.47	6.78	6.27		
	Rosette	2.88	2.61	1.83	0.95		
	Rosette	3.47	3.05	2.51	2.38		
	Rosette	2.5	1.88	0.99	0.86		
	Rosette	3.85	3.28	3.62	2.2		
	Rosette	2.73	2.12	0.97	0.6		
	Rosette	2.64	2.16	1.34	1.22		
	Rosette	4.12	3.85	2.61	2.69		
	Rosette	2.61	3.45	1.75	1.86		
	Rosette	3.38	4.92	2.01	2.68		
	Rosette	2.78	2.27	1.18	1.51		
	Rosette	2.99	3.69	1.65	2.1		
	Rosette	2.54	1.81	1.84	1.38		
L. Scapula, V-L. Surface	Rosette	2.97	3.76	1.73	2.5		
	Rosette	3.51	2.61	2.16	1.63		
	Rosette	6.06	5	4.03	3.92		
	Rosette	5.82	4.53	3.68	2.8		
	Rosette	6.73	5.08	4.59	4.68		
	Rosette	7.12	5.78	5.46	4.82		
	Rosette	6.14	4.05	4.02	2.27		
	Rosette	5.16	3.84	2.81	3.03		
	Rosette	8.15	7.66	6.72	5.9		
	Rosette	7.19	5.08	5.84	4.02		
	Rosette	4.01	4.58	3.17	3.17		
	Rosette	6.26	6.98	4.95	6.12		
	Rosette	3.21	2.84	2.44	2.46		
	Rosette	1.56	1.58	0.75	1.18		
	Rosette	3.74	4.02	3.18	3.52		
	Rosette	5.31	6.04	4.18	4.92		
	Rosette	3.66	4.65	2.8	3.57		
	Rosette	4.65	5.25	2.33	1.98		
	Rosette	4.33	5.41	3.35	3.86		
	Rosette	2.61	3.34	1.55	1.38		
Splenial? (Skull)	Rosette	3.42	2.66	2.22	1.86		
L. Nasal (Skull), Med. Surface	Shallow Pit	5.81	5.19				
	Shallow Pit	3.95	2.27				
Occipital (Skull), Dor. Surface	Shallow Pit	2.54	2.02				
	Shallow Pit	2.31	1.92				
L. Surangular (Skull)	Shallow Pit	2.49	2				
R. Sternal Plate, Lat. Surface	Deep Pit	3.35	2.97			0.98	3.41
	Deep Pit	5.46	5.13			1.74	3.13
	Deep Pit	5.12	4.74			1.31	3.91
	Deep Pit	7.37	5.71			1.2	6.14
	Deep Pit	7.27	7.12			1.08	6.73
	Deep Pit	8.36	6.77			1.61	5.19
	Shallow Pit	5.22	4.78			0.1	52.2

Element	Morphology	Length[1]	Width[1]	Length[2]	Width[2]	Depth	Length/Depth Ratio
R. Sternal Plate, Lat. Surface	Shallow Pit	6.41	6.13			0.51	12.57
	Shallow Pit	7.02	4.39			0.38	18.47
	Shallow Pit	2.1	1.43				
	Shallow Pit	2.43	1.94				
	Shallow Pit	1.89	1.65				
	Shallow Pit	3.2	2.74				
	Shallow Pit	3.03	2.72				
	Shallow Pit	2.07	1.62				
	Shallow Pit	3.91	3.95				
	Shallow Pit	2.21	2.05				
	Shallow Pit	1.42	1.25				
	Shallow Pit	1.58	1.13				
	Shallow Pit	1.96	1.29				
	Shallow Pit	1.79	1.78				
	Shallow Pit	2.26	1.91				
	Shallow Pit	2.54	2.3				
	Shallow Pit	5.38	4.47				
	Shallow Pit	6.84	6.43				
	Shallow Pit	6.35	4.16				
	Shallow Pit	5.2	4.6				
	Shallow Pit	5.71	5.65				
	Shallow Pit	2.66	2.37				
	Shallow Pit	6.17	4.12				
	Shallow Pit	5	4.07				
	Shallow Pit	3.79	3.54				
	Shallow Pit	4.22	3.7				
	Shallow Pit	6.76	3.68				
	Shallow Pit	3.8	3.2				
	Shallow Pit	2.55	2.19				
	Shallow Pit	2.47	2.41				
	Shallow Pit	4.78	3.8				
	Shallow Pit	4.64	4.17				
R. Sternal Plate, Med. Surface	Shallow Pit	1.74	1.69				
	Shallow Pit	1.8	1.67				
	Shallow Pit	0.92	0.9				
	Shallow Pit	1.72	1.46				
	Shallow Pit	1.17	0.98				
	Shallow Pit	1.84	1.39				
	Shallow Pit	1.88	1.8				
	Shallow Pit	2.78	2.43				
	Shallow Pit	1.35	1.27				
	Shallow Pit	1.37	1.26				
	Shallow Pit	1.65	1.29				
	Shallow Pit	1.44	1.17				
	Shallow Pit	1.54	1.52				
	Shallow Pit	1.37	1.3				
	Shallow Pit	2.33	1.93				
	Shallow Pit	1.85	1.46				
	Shallow Pit	1.76	1.54				
	Shallow Pit	1.26	1.15				
	Shallow Pit	2.21	1.86				
	Shallow Pit	1.3	1.24				
	Shallow Pit	2.07	2.01				
	Shallow Pit	1.75	1.5				
	Shallow Pit	1.43	1.41				
	Shallow Pit	1.79	1.63				
	Shallow Pit	1.29	1.05				

Element	Morphology	Length[1]	Width[1]	Length[2]	Width[2]	Depth	Length/Depth Ratio
R. Sternal Plate, Med. Surface	Shallow Pit	1.24	1.22				
	Shallow Pit	1.85	1.69				
	Shallow Pit	1.3	1.1				
	Shallow Pit	1.81	1.76				
	Shallow Pit	1.78	1.64				
	Shallow Pit	2.87	2.07				
	Shallow Pit	2.22	1.37				
	Shallow Pit	2.27	1.55				
	Shallow Pit	1.1	1.07				
	Shallow Pit	1.47	1.32				
	Shallow Pit	1.59	1.35				
	Shallow Pit	1.79	1.11				
	Shallow Pit	1.71	1.37				
	Shallow Pit	1.52	1.13				
	Shallow Pit	1.4	1.09				
	Shallow Pit	2.59	1.68				
	Shallow Pit	2.25	2.09				
	Shallow Pit	2.25	2.08				
	Shallow Pit	0.97	0.91				
	Shallow Pit	1.19	1.09				
	Shallow Pit	1.77	1.2				
	Shallow Pit	1.31	1.26				
	Shallow Pit	1.88	1.52				
	Shallow Pit	1.96	1.68				
	Shallow Pit	1.54	1.25				
	Shallow Pit	1.61	1.49				
	Shallow Pit	2.86	2.17				
	Shallow Pit	1.53	0.85				
	Shallow Pit	1.55	1.4				
	Shallow Pit	1.14	1.13				
	Shallow Pit	1.73	1.45				
	Shallow Pit	1.98	1.64				
	Shallow Pit	2.17	2.05				
	Shallow Pit	2.36	2.27				
	Shallow Pit	1.75	1.31				
	Shallow Pit	1.72	1.59				
	Shallow Pit	1.3	1.14				
	Shallow Pit	3.12	2.95				
	Shallow Pit	1.54	1.54				
	Shallow Pit	1.37	1.19				
	Shallow Pit	1.86	1.28				
	Shallow Pit	1.18	1				
	Shallow Pit	1.02	0.68				
	Shallow Pit	2.25	1.98				
	Shallow Pit	1.65	1.33				
	Shallow Pit	1.81	1.33				
L. Fibula, Med. Surface	Shallow Pit	3.21	3.12			0.1	32.1
	Shallow Pit	4.95	3.38			0.41	12.07
	Shallow Pit	3.59	3.05			0.26	13.81
	Shallow Pit	4.38	3.6			0.16	27.36
	Shallow Pit	5.72	4.33			0.72	7.94
	Shallow Pit	4.88	3.88			0.23	21.22
	Shallow Pit	2.57	2.01			0.15	17.13
	Shallow Pit	5.27	4.5			0.36	14.64
	Shallow Pit	2.73	2.23				
	Shallow Pit	2.89	2.52			0.04	72.25
	Shallow Pit	4.99	3.95			0.19	26.26

Element	Morphology	Length[1]	Width[1]	Length[2]	Width[2]	Depth	Length/Depth Ratio
L. Fibula, Lat. Surface	Shallow Pit	4.92	3.57			0.35	14.06
	Shallow Pit	4.65	4.14			0.12	38.75
	Shallow Pit	4.02	3.51			0.17	23.65
	Shallow Pit	2.51	2.68			0.19	13.21
	Shallow Pit	3.01	2.41			0.18	16.72
	Shallow Pit	2.51	2			0.13	19.31
	Shallow Pit	2.86	2.22			0.35	8.17
	Shallow Pit	1.88	1.68			0.08	23.5
	Shallow Pit	3.79	2.78			0.29	13.07
	Shallow Pit	4.16	2.77			0.51	8.16
L. Tibia, Med. Surface	Shallow Pit	3.79	3.33			0.23	16.47
	Shallow Pit	3.56	3.11			0.03	118.67
L. Metacarpal I, Pos. Surface	Rosette	3.93	3.88	1.38	1.64	0.22	17.86
	Shallow Pit	4.44	3.97			0.26	17.08
	Shallow Pit	4.26	3.98			0.39	10.92
	Shallow Pit	4.14	4.28			0.26	15.92
	Shallow Pit	4.41	4.32				
L. Humerus, Med. Surface	Rosette	5.72	5.26	4.2	3.59	0.12	47.67
	Rosette	4.66	4.42	3.57	2.82	0.16	29.13
	Rosette	4.16	3.81	2.6	1.97	0.17	24.47
	Rosette	2.51	2.23	1.23	0.82	0.03	83.67
	Rosette	4.87	5.15	2.71	2.08	0.17	28.65
	Rosette	4.35	4.1	1.84	1.34	0.11	39.55
	Rosette	4.44	4.19	2.55	1.8	0.04	111
	Rosette	4.05	3.47	1.64	1.63	0.49	8.27
	Rosette	4.84	4.33	1.64	1.92	0.27	17.93
	Rosette	3.61	3.95	2.04	1.13	0.28	12.89
	Shallow Pit	5.4	3.55			0.16	33.75
	Shallow Pit	5.37	4.39			0.23	23.35
	Shallow Pit	5.39	5.25			0.19	28.37
	Shallow Pit	7.31	5.89			0.3	24.37
	Shallow Pit	5.26	4.33			0.22	23.91
	Shallow Pit	5.99	4.89			0.28	21.39
	Shallow Pit	3.77	3.08			0.1	37.7
	Shallow Pit	4.36	4.18			0.37	11.78
	Shallow Pit	6.12	5.37			0.44	13.91
	Shallow Pit	5.03	3.69			0.09	55.89
	Shallow Pit	4.09	3.97			0.41	9.98
L. Humerus, Lat. Surface	Shallow Pit	1.79	1.55				
	Shallow Pit	2.91	2.55				
	Shallow Pit	2.8	2.06				
	Shallow Pit	1.94	1.63				
	Shallow Pit	4.03	3.83			0.33	12.21
	Shallow Pit	3.98	3.45			0.19	20.95
	Shallow Pit	2.2	2.12				
	Shallow Pit	2.68	2.26			0.13	20.62
	Shallow Pit	2.89	2.74			0.29	9.97
	Shallow Pit	3.69	3.62			0.11	33.55
	Shallow Pit	2.68	2.58			0.12	22.33
	Shallow Pit	2.92	2.46				

KUVP 129714—Shallow pits are rare on the juvenile *Camarasaurus* and are restricted to bones found at the top of the slope where it was deposited.

Element	Morphology	Length[1]	Width[1]	Length[2]	Width[2]	Depth	Length/Depth Ratio
Rib on top of slope	Shallow Pit	4.58	3.78			0.41	11.17
	Shallow Pit	5.01	3.65			0.37	13.54

KUVP 129716—Shallow pits are the most common traces on this adult *Camarasaurus* and are abundant on the ribs and limb bones: 208 shallow pits, 49 hemispherical pits, and 1 rosette were measured. Bones from the right side of the skeleton were partially buried in foam, limiting their availability for this study.

Element	Morphology	Length[1]	Width[1]	Length[2]	Width[2]	Depth	Length/Depth Ratio
Dor. Ver. 4, R. Pos. Neural Arch	Deep Pit	4	3.45				
	Deep Pit	3.79	2.71				
	Deep Pit	2.93	2.47				
	Deep Pit	3.65	2.72				
	Deep Pit	3.41	2.6				
	Deep Pit	2.95	2.82				
	Deep Pit	2.68	2.62				
	Deep Pit	2.87	2.79				
	Deep Pit	3.27	1.98				
Dor. Ver. 5, R. Pos. Neural Arch	Deep Pit	3.55	3.52				
	Deep Pit	3.75	3.47				
Dor. Ver. 6, R. Postzygomatic	Deep Pit	3.19	2.66				
	Deep Pit	3.71	3.01				
Dor. Ver. 6, R. Pos. Neural Arch	Deep Pit	2.62	2.06			0.72	3.64
	Deep Pit	3.04	2.97			0.94	3.23
	Deep Pit	2.8	2.06			0.62	4.52
	Deep Pit	2.52	2.42			0.96	2.63
	Deep Pit	4.33	4.1			1.2	3.61
	Deep Pit	4.58	4.27			1.15	3.98
	Deep Pit	2.99	2.73			0.86	3.48
	Deep Pit	3.23	2.47			0.99	3.26
	Deep Pit	3.41	2.66			1.04	3.28
	Deep Pit	2.95	2.15			0.69	4.28
	Deep Pit	3.24	2.71			0.74	4.38
	Deep Pit	3.04	2.4			1.58	1.92
Cau. Ver. 1, R. Pos. Neural Arch	Deep Pit	4.63	4.38				
	Deep Pit	4.23	4.12				
	Deep Pit	4.01	3.88				
	Deep Pit	4.01	3.43				
Cau. Ver. 3, R. Side of Centrum	Shallow Pit	6.36	5.29				
	Shallow Pit	5.25	3.68				
	Shallow Pit	4.62	4.51				
	Shallow Pit	4.27	4.14				
	Shallow Pit	5.85	4.26				
	Shallow Pit	5.65	4.8				

Element	Morphology	Length[1]	Width[1]	Length[2]	Width[2]	Depth	Length/Depth Ratio
Cau. Ver. 3, R. Side of Centrum	Shallow Pit	4.32	4.06				
Cau. Ver. 4, R. Side of Centrum	Shallow Pit	3.59	3.07				
	Shallow Pit	4.33	3.16				
	Shallow Pit	4.52	2.92				
	Shallow Pit	3.79	3.09				
	Shallow Pit	3.74	3.41				
	Shallow Pit	4.07	3.62				
Cau. Ver. 5, L. Side of Centrum	Shallow Pit	5.41	5.4				
	Shallow Pit	3.39	3.2				
	Shallow Pit	5.98	5.57				
	Shallow Pit	3.3	2.99				
	Shallow Pit	2.8	2.06				
L. Ilium, M. Surface	Deep Pit	4.71	4.6				
	Deep Pit	4.3	3.44				
	Deep Pit	4.56	3.73				
	Deep Pit	5.51	5.1				
	Deep Pit	4.42	4.05				
L. Pubis, M. Surface (BP50)	Shallow Pit	4.29	3.96				
	Shallow Pit	3.02	2.24				
	Shallow Pit	3.64	2.78				
	Shallow Pit	1.48	1.23				
	Shallow Pit	1.86	1.57				
	Shallow Pit	1.71	1.46				
	Shallow Pit	2.44	1.48				
	Shallow Pit	1.96	1.38				
	Shallow Pit	1.64	1.46				
	Shallow Pit	2.11	1.74				
	Shallow Pit	1.93	1.58				
	Shallow Pit	1.83	1.74				
	Shallow Pit	1.94	1.92				
	Shallow Pit	2.54	2				
	Shallow Pit	2.9	2.05				
	Shallow Pit	2.48	2.18				
	Shallow Pit	2.03	1.83				
	Shallow Pit	3.2	2.86				
	Shallow Pit	2.41	2.13				
	Shallow Pit	2.01	1.85				
R. Ischium, Ven. Surface (BP72)	Deep Pit	3.55	2.82				
	Deep Pit	3.01	2.13				
	Deep Pit	4.31	3.41				
	Deep Pit	2.51	1.91				
	Deep Pit	2.62	1.84				
	Deep Pit	4.16	2.45				
	Deep Pit	3.18	2.67				
	Deep Pit	3.46	3.12				
	Deep Pit	5.93	4.02				
	Deep Pit	3.66	2.69				
	Deep Pit	4.04	3.86				
	Deep Pit	4.14	3.13				
	Deep Pit	2.9	2.79				
	Deep Pit	2.66	2.64				
	Deep Pit	3.18	3.13				
R. Rib head, Pos. Sur. (BP74)	Rosette	6.91	5.33	1.82	1.4		
	Shallow Pit	5.27	4.53				
L. Rib, Med. Sur. (BP121)	Shallow Pit	2.64	2.07				
L. Rib, Pro. Med. Sur. (BP134)	Shallow Pit	2.67	2.64				
	Shallow Pit	4.6	3.29				

Element	Morphology	Length[1]	Width[1]	Length[2]	Width[2]	Depth	Length/Depth Ratio
R. Rib head, Ant. Sur. (BP138)	Shallow Pit	3.52	3.25				
	Shallow Pit	3.66	3.05				
	Shallow Pit	2.51	2.06				
	Shallow Pit	1.9	1.49				
	Shallow Pit	2.92	2.68				
	Shallow Pit	2.14	1.94				
	Shallow Pit	2.23	1.78				
L Rib, Lat Sur Med Sect BP182)	Shallow Pit	3.99	3.52				
	Shallow Pit	2.84	2.08				
	Shallow Pit	2.13	1.87				
	Shallow Pit	2.06	1.66				
	Shallow Pit	2.7	1.81				
	Shallow Pit	2.25	1.92				
	Shallow Pit	2.02	1.94				
	Shallow Pit	2.46	2.41				
	Shallow Pit	2.96	2.85				
	Shallow Pit	2.92	2.03				
	Shallow Pit	2.56	2.5				
	Shallow Pit	2.65	2.62				
Hyoid (BP305)	Shallow Pit	2.12	1.88				
	Shallow Pit	2.45	1.35				
	Shallow Pit	2.27	2.1				
	Shallow Pit	2.3	1.45				
	Shallow Pit	1.92	1.56				
	Shallow Pit	1.18	0.88				
	Shallow Pit	1.65	1.1				
Chevron 4, R. Surface (BP55)	Shallow Pit	4.07	3.56				
	Shallow Pit	3.1	2.7				
	Shallow Pit	3.2	2.79				
	Shallow Pit	2.64	2.33				
	Shallow Pit	2.97	2.7				
	Shallow Pit	2.51	2.36				
	Shallow Pit	2.37	2.2				
	Shallow Pit	2.65	2.06				
	Shallow Pit	4.35	3.34				
	Shallow Pit	2.31	2.03				
	Shallow Pit	2.12	2.1				
	Shallow Pit	2.84	2.65				
	Shallow Pit	2.22	2.17				
	Shallow Pit	2.46	2.35				
	Shallow Pit	1.86	1.74				
	Shallow Pit	1.92	1.57				
	Shallow Pit	3.2	2.58				
	Shallow Pit	2.41	2.34				
	Shallow Pit	2.28	2.16				
	Shallow Pit	3.07	2.93				
	Shallow Pit	1.59	1.56				
	Shallow Pit	2.32	2.03				
	Shallow Pit	1.98	1.85				
	Shallow Pit	2.13	1.96				
	Shallow Pit	3.11	2.62				
	Shallow Pit	4.12	3.47				
	Shallow Pit	2.45	2.21				
	Shallow Pit	3.53	2.82				
	Shallow Pit	3.04	2.23				
	Shallow Pit	3.23	3.13				
	Shallow Pit	2.78	2.44				

Element	Morphology	Length[1]	Width[1]	Length[2]	Width[2]	Depth	Length/Depth Ratio
Chevron 4, R. Surface (BP55)	Shallow Pit	2.75	2.59				
	Shallow Pit	2.98	2.85				
	Shallow Pit	2.57	2.46				
	Shallow Pit	3.31	3.25				
	Shallow Pit	2.3	1.95				
	Shallow Pit	1.4	1.39				
	Shallow Pit	1.68	1.48				
	Shallow Pit	1.78	1.4				
	Shallow Pit	0.99	0.91				
	Shallow Pit	1.62	1.4				
	Shallow Pit	2.62	2.04				
Chevron 5 (BP03)	Shallow Pit	3.01	2.47				
	Shallow Pit	2.54	2.38				
	Shallow Pit	3.55	3.45				
	Shallow Pit	2.56	2.37				
	Shallow Pit	2.9	2.51				
	Shallow Pit	4.25	2.92				
	Shallow Pit	2.41	2.12				
	Shallow Pit	4.45	3.06				
	Shallow Pit	3.92	3.2				
	Shallow Pit	2.86	2.6				
	Shallow Pit	3.4	2.74				
	Shallow Pit	2.92	2.45				
	Shallow Pit	3.01	2.11				
	Shallow Pit	3.85	3.34				
	Shallow Pit	3.85	2.5				
Chevron 6 (BP94)	Shallow Pit	2.88	2.09				
	Shallow Pit	2.46	2.19				
	Shallow Pit	1.38	1.21				
	Shallow Pit	1.37	1.01				
	Shallow Pit	1.53	1.51				
	Shallow Pit	1.5	1.41				
	Shallow Pit	1.63	1.21				
	Shallow Pit	2.75	1.41				
	Shallow Pit	2.32	2.22				
	Shallow Pit	1.52	0.98				
	Shallow Pit	2.67	1.95				
	Shallow Pit	1.76	1.67				
	Shallow Pit	2.9	2.05				
Chevron 7, Dis. Sector (BP96)	Shallow Pit	3.11	2.82				
	Shallow Pit	3.48	2.37				
	Shallow Pit	1.93	1.41				
Chevron 8	Shallow Pit	2.27	1.63				
	Shallow Pit	2.07	1.9				
	Shallow Pit	2.55	1.75				
	Shallow Pit	3.2	2.87				
	Shallow Pit	3.38	2.3				
	Shallow Pit	2.93	2.79				
	Shallow Pit	2.98	2.73				
	Shallow Pit	2.56	2.53				
	Shallow Pit	2.44	2.41				
L. Femur, Lat. Margin (BP45)	Shallow Pit	2.27	1.63				
	Shallow Pit	2.07	1.9				
	Shallow Pit	2.55	1.75				
	Shallow Pit	3.2	2.87				
	Shallow Pit	3.38	2.3				
	Shallow Pit	2.93	2.79				

Element	Morphology	Length[1]	Width[1]	Length[2]	Width[2]	Depth	Length/Depth Ratio
L. Femur, Lat. Margin (BP45)	Shallow Pit	2.98	2.73				
	Shallow Pit	2.56	2.53				
	Shallow Pit	2.44	2.41				
	Shallow Pit	2.27	1.63				
	Shallow Pit	2.07	1.9				
	Shallow Pit	2.55	1.75				
	Shallow Pit	3.2	2.87				
	Shallow Pit	3.38	2.3				
	Shallow Pit	2.93	2.79				
	Shallow Pit	2.98	2.73				
	Shallow Pit	2.56	2.53				
	Shallow Pit	2.44	2.41				
	Shallow Pit	2.27	1.63				
	Shallow Pit	2.07	1.9				
	Shallow Pit	2.55	1.75				
	Shallow Pit	3.2	2.87				
	Shallow Pit	3.38	2.3				
	Shallow Pit	2.93	2.79				
	Shallow Pit	2.98	2.73				
	Shallow Pit	2.56	2.53				
	Shallow Pit	2.44	2.41				
	Shallow Pit	2.27	1.63				
	Shallow Pit	2.07	1.9				
	Shallow Pit	2.55	1.75				
	Shallow Pit	3.2	2.87				
	Shallow Pit	3.38	2.3				
	Shallow Pit	2.93	2.79				
	Shallow Pit	2.98	2.73				
L. Femur, 12” above Dist. End	Shallow Pit	5.11	4.59				
L. Radius, Lat. Surface (BP187)	Shallow Pit	2.65	2.18				
	Shallow Pit	3.71	3.36				
	Shallow Pit	3.21	2.25				
	Shallow Pit	2.15	2.14				
	Shallow Pit	2.62	2.43				
	Shallow Pit	2.27	2.09				
	Shallow Pit	2.53	2.02				
	Shallow Pit	2.73	1.94				
	Shallow Pit	2.74	2.24				
	Shallow Pit	1.99	1.92				
	Shallow Pit	2.62	1.88				
	Shallow Pit	2.71	2.03				
	Shallow Pit	2.47	2.35				
	Shallow Pit	3.17	2.54				
L Metacarpal I, Pos Sur (BP169)	Shallow Pit	2.6	2.39				
	Shallow Pit	2.39	2.22				
	Shallow Pit	2.67	2.4				
	Shallow Pit	3.03	2.02				
	Shallow Pit	2.76	2.57				
	Shallow Pit	1.79	1.39				
	Shallow Pit	1.97	1.37				
	Shallow Pit	2.01	1.84				

KUVP 129717—2 rosettes and 41 shallow pits were measured on the diplodocid skeleton. It is possible that root etching obscured or destroyed rosettes and pits on the other skeletal elements.

Element	Morphology	Length[1]	Width[1]	Length[2]	Width[2]	Depth	Length/Depth Ratio
Rib, Lat. Shaft (EP39)	Shallow Pit	1.95	1.71				
	Shallow Pit	3.41	2.57				
	Shallow Pit	2.9	1.96				
	Shallow Pit	2.54	2.03				
	Shallow Pit	2.27	1.48				
	Shallow Pit	1.39	1.05				
Rib, Med. Shaft (EP39)	Rosette	1.91	1.61	0.33	0.61		
	Shallow Pit	2.08	1.97				
	Shallow Pit	1.3	1.03				
	Shallow Pit	1.53	1.32				
	Shallow Pit	1.38	1.19				
	Shallow Pit	0.98	0.74				
	Shallow Pit	1.93	1.47				
	Shallow Pit	1.48	0.92				
	Shallow Pit	1.61	1.42				
Rib, Ant. Head (EP39)	Rosette	3.07	2.79	2.2	2.2		
	Shallow Pit	2.23	1.97				
	Shallow Pit	2.19	1.98				
	Shallow Pit	2.33	2				
	Shallow Pit	2.31	2.06				
	Shallow Pit	2.79	2.35				
	Shallow Pit	3.29	2.76				
	Shallow Pit	3.36	2.97				
	Shallow Pit	2.61	2.37				
	Shallow Pit	2.43	2.03				
	Shallow Pit	2.13	1.92				
Rib, Pos. Head (EP39)	Shallow Pit	2.39	2.12				
	Shallow Pit	2.59	2.42				
	Shallow Pit	2	1.75				
	Shallow Pit	2.42	1.75				
	Shallow Pit	1.55	1.13				
R. Scapula, Lat. Shaft	Shallow Pit	2.45	1.98				
	Shallow Pit	2.66	2.62				
	Shallow Pit	4.71	3.3				
	Shallow Pit	2.23	1.94				
	Shallow Pit	1.95	1.86				
	Shallow Pit	2.51	1.7				
	Shallow Pit	2.08	2.02				
	Shallow Pit	1.78	1.77				
	Shallow Pit	3.24	3.19				
	Shallow Pit	3.29	2.91				
R. Fibula, Med. Sur. (7-27-04#3)	Shallow Pit	3.43	2.47				
	Shallow Pit	3.08	2.24				

KUVP 129724—Twenty five shallow pits were found on metatarsals IV and V of the partially articulated left pes of a brachiosaur. The brachiosaur manus known as Big Hand might be part of KUVP 129724 and is also covered by shallow pits.

Element	Morphology	Length[1]	Width[1]	Length[2]	Width[2]	Depth	Length/Depth Ratio
L. Metatarsal IV, D-L. Surface	Shallow Pit	2.68	2.08				
	Shallow Pit	2.3	1.89				
	Shallow Pit	2.2	1.95				
	Shallow Pit	2.43	1.65				
	Shallow Pit	3	2.42				
	Shallow Pit	2.21	2.04				
	Shallow Pit	2.4	1.84				
	Shallow Pit	2.95	2.85				
	Shallow Pit	2.21	1.85				
L. Metatarsal IV, D-M. Surface	Shallow Pit	2.3	2.13				
	Shallow Pit	0.91	0.89				
L. Metatarsal IV, Ven. Surface	Shallow Pit	1.44	1.28				
	Shallow Pit	1.45	1.22				
	Shallow Pit	1.14	0.74				
	Shallow Pit	1.86	1.55				
	Shallow Pit	1.9	1.78				
	Shallow Pit	1.8	1.77				
	Shallow Pit	0.8	0.48				
	Shallow Pit	1.54	1.25				
	Shallow Pit	1.44	1.4				
	Shallow Pit	1.74	1.62				
	Shallow Pit	1.55	1.47				
	Shallow Pit	1.59	1.47				
L. Metatarsal V, Med. Surface	Shallow Pit	3.85	2.16				
	Shallow Pit	2.33	2.03				

Big Hand—Eight rosettes and 139 shallow pits were measured from the articulated metacarpals.

Element	Morphology	Length[1]	Width[1]	Length[2]	Width[2]	Depth	Length/Depth Ratio
R. Metacarpal I, Ant. Surface	Shallow Pit	4.13	3.85			0.25	16.52
	Shallow Pit	2.08	1.97			0.05	41.6
	Shallow Pit	2.5	1.86			0.25	10
	Shallow Pit	2.07	1.51				
	Shallow Pit	2.04	2.02				
	Shallow Pit	1.94	1.87				
	Shallow Pit	1.78	1.63				
	Shallow Pit	2.57	2.42				
	Shallow Pit	1.36	1.16				
	Shallow Pit	1.56	1.32				
	Shallow Pit	1.67	1.28				
	Shallow Pit	1.35	0.98				
	Shallow Pit	1.16	0.9				
	Shallow Pit	2.45	2.37			0.1	24.5
	Shallow Pit	3.62	3.05			0.16	22.63

Element	Morphology	Length[1]	Width[1]	Length[2]	Width[2]	Depth	Length/Depth Ratio
R. Metacarpal II, Ant. Surface	Shallow Pit	4.74	4.74			0.2	23.7
	Shallow Pit	3.61	3.49			0.31	11.65
	Shallow Pit	3.51	3.26			0.14	25.07
	Shallow Pit	3.49	3.02			0.15	23.27
	Shallow Pit	3.06	2.9			0.25	12.24
	Shallow Pit	2.71	2.54			0.14	19.36
	Shallow Pit	3.18	2.91			0.17	18.71
	Shallow Pit	4.34	3.5			0.14	31
	Shallow Pit	2.9	2.73			0.05	58
	Shallow Pit	3.76	3.19			0.2	18.8
	Shallow Pit	2.22	2.04				
	Shallow Pit	2.16	1.84				
	Shallow Pit	3.07	2.89			0.21	14.62
	Shallow Pit	3.45	3.08			0.39	8.85
	Shallow Pit	2.65	2.34				
	Shallow Pit	3.84	3.59			0.15	25.6
	Shallow Pit	3.58	2.88			0.06	59.67
	Shallow Pit	3.44	3.06				
	Shallow Pit	3.94	3.57			0.15	26.27
	Shallow Pit	2.98	2.79			0.18	16.56
	Shallow Pit	1.87	1.8				
R. Metacarpal III, Ant. Surface	Shallow Pit	3.31	2.85			0.41	8.07
	Shallow Pit	3.46	3.24			0.22	15.73
	Shallow Pit	3.14	3.09			0.26	12.08
	Shallow Pit	2.99	2.66			0.34	8.79
	Shallow Pit	2.85	2.47			0.35	8.14
	Shallow Pit	3.24	2.61			0.37	8.76
	Shallow Pit	2.69	2.49			0.29	9.28
	Shallow Pit	2.81	2.51			0.61	4.61
	Shallow Pit	2.08	1.49			0.31	6.71
	Shallow Pit	2.18	2.03			0.18	12.11
	Shallow Pit	2.53	2.48			0.43	5.88
	Shallow Pit	3.08	2.72			0.35	8.8
	Shallow Pit	2.99	2.68			0.4	7.48
	Shallow Pit	2.99	2.98			0.57	5.25
	Shallow Pit	3.49	3.13			0.41	8.51
	Shallow Pit	4.42	4.08			0.43	10.28
	Shallow Pit	3.08	2.77			0.38	8.11
	Shallow Pit	3.09	2.33			0.33	9.36
	Shallow Pit	1.89	1.71				
	Shallow Pit	3.19	3.02			0.27	11.81
	Shallow Pit	2	1.34				
	Shallow Pit	1.82	1.64				
	Shallow Pit	1.8	1.64				
	Shallow Pit	1.8	1.6				
	Shallow Pit	1.78	1.67				
	Shallow Pit	2.4	1.87			0.43	5.58
	Shallow Pit	2.68	2.64			0.45	5.96
	Shallow Pit	4.38	3.75			0.33	13.27
	Shallow Pit	1.38	1.24				
	Shallow Pit	1.23	1.04				
	Shallow Pit	3.75	3.25			0.21	17.86
	Shallow Pit	2.69	2.47			0.15	17.93
	Shallow Pit	3.3	2.6			0.45	7.33
	Shallow Pit	2.71	2.25			0.38	7.13
	Shallow Pit	2.38	2.14			0.43	5.53
	Shallow Pit	3.99	3.74			0.49	8.14

Element	Morphology	Length[1]	Width[1]	Length[2]	Width[2]	Depth	Length/Depth Ratio
R. Metacarpal III, Ant. Surface	Shallow Pit	2.75	2.45			0.28	9.82
	Shallow Pit	2.37	2.35			0.38	6.24
	Shallow Pit	1.37	1.05				
	Shallow Pit	3.84	3.09			0.39	9.85
	Shallow Pit	2.09	2.04			0.32	6.53
	Shallow Pit	1.6	1.48				
	Shallow Pit	2.18	2.11				
	Shallow Pit	2.72	2.44			0.15	18.13
	Shallow Pit	2.68	1.86			0.25	10.72
	Shallow Pit	2.58	2.45			0.17	15.18
	Shallow Pit	2.94	2.56			0.46	6.39
	Shallow Pit	2.44	2.36			0.36	6.78
	Shallow Pit	2.75	2.62			0.33	8.33
R. Metacarpal IV, Ant. Surface	Rosette	1.93	1.81	1.08	1.06		
	Rosette	1.79	1.75	1.05	1		
	Rosette	1.99	1.87	1.04	1.02		
	Shallow Pit	3.44	3.04			0.35	9.83
	Shallow Pit	3.08	2.66			0.3	10.27
	Shallow Pit	2.55	2.17			0.26	9.81
	Shallow Pit	3.58	3.33			0.37	9.68
	Shallow Pit	2.49	1.58			0.35	7.11
	Shallow Pit	4.8	3.27			0.24	20
	Shallow Pit	1.6	1.33				
	Shallow Pit	2.53	2.16				
	Shallow Pit	3.15	2.45			0.3	10.5
	Shallow Pit	3.27	2.81			0.42	7.79
	Shallow Pit	3.25	2			0.17	19.12
	Shallow Pit	4.42	3.56			0.48	9.21
	Shallow Pit	1.76	1.73				
	Shallow Pit	2.01	1.68				
	Shallow Pit	1.93	1.49				
	Shallow Pit	2.88	2.2			0.26	11.08
	Shallow Pit	2.21	1.95				
	Shallow Pit	2.79	2.49				
	Shallow Pit	2.37	2.12				
	Shallow Pit	2.94	2.55			0.32	9.19
	Shallow Pit	2.33	1.77				
	Shallow Pit	2.04	1.28				
	Shallow Pit	2.33	2.24				
	Shallow Pit	2.23	1.95				
	Shallow Pit	2.03	1.42				
	Shallow Pit	1.43	1.09				
	Shallow Pit	2	1.64				
	Shallow Pit	1.65	1.49				
	Shallow Pit	2.86	2.38				
	Shallow Pit	2.25	2.1				
	Shallow Pit	1.73	1.53				
	Shallow Pit	1.54	1.35				
	Shallow Pit	1.67	1.32				
	Shallow Pit	2.17	1.6				
	Shallow Pit	1.79	1.43				
R. Metacarpal V, Ant. Surface	Rosette	1.98	1.77	0.75	1.06		
	Shallow Pit	2.36	2.19			0.18	13.11
	Shallow Pit	2.04	1.93			0.58	3.52
	Shallow Pit	2.18	1.87			0.22	9.91
	Shallow Pit	4.24	3.79			0.39	10.87
	Shallow Pit	2.6	2.21				

Element	Morphology	Length[1]	Width[1]	Length[2]	Width[2]	Depth	Length/Depth Ratio
	Shallow Pit	2.33	1.88			0.16	14.56
	Shallow Pit	3.25	2.36			0.31	10.48
	Shallow Pit	2.54	2.03				
	Shallow Pit	3.88	3.09			0.29	13.38
	Shallow Pit	3.87	2.92			0.6	6.45
	Shallow Pit	2.68	2.54				
	Shallow Pit	1.58	2.26				
	Shallow Pit	2.32	2			0.24	9.67
	Shallow Pit	2.54	1.78			0.12	21.17
R. Metacarpal V, Pos. Surface	Rosette	2.39	2.06	0.72	0.68		
	Rosette	3.09	3.08	2.85	2.02		
	Rosette	2.14	2.04	0.72	0.72		
	Rosette	2.62	2.21	0.98	1.13		
	Shallow Pit	3.15	2.84			0.12	26.25
	Shallow Pit	2.37	2.53				
	Shallow Pit	3.09	2.42			0.1	30.9